

UCSF

UC San Francisco Electronic Theses and Dissertations

Title

Cloning, expression and characterization of a human homologue of Drosophila rhomboid

Permalink

<https://escholarship.org/uc/item/9927c3rs>

Author

Rizen, Michael,

Publication Date

1999

Peer reviewed|Thesis/dissertation

Cloning, Expression and Characterization of a Human Homologue
of *Drosophila rhomboid*

by

Michael Rizen

DISSERTATION

Submitted in partial satisfaction of the requirements for the degree of

DOCTOR OF PHILOSOPHY

in

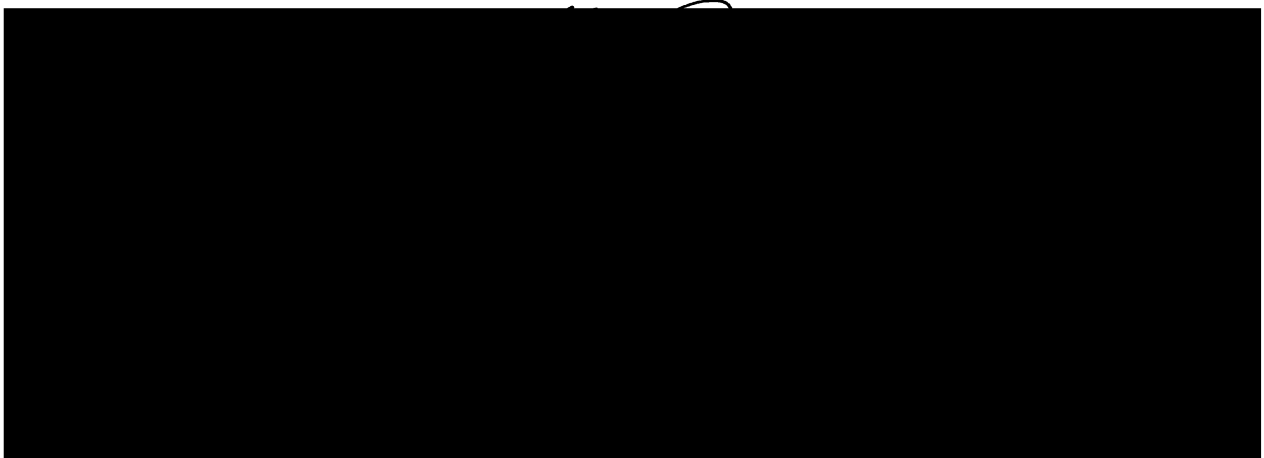
Biochemistry and Biophysics

in the

GRADUATE DIVISION

of the

UNIVERSITY OF CALIFORNIA SAN FRANCISCO



Date

University Librarian

Degree Conferred:

Copyright 1999

by

Michael Rizen

Acknowledgements

As I prepare to leave graduate school and return to medical school, perhaps my most important task is to recognize the many people who have helped me to survive my graduate training and complete this dissertation.

I would first like to thank Professor Doug Hanahan and all of the members of his lab where I conducted my Masters research. Special thanks to Anne Neill for her motherly love and support during my years there. In addition, collaborators Carol Greider, Maria Blasco and Dr. Judah Folkman are gratefully acknowledged.

Professor Rik Derynck has been a most able mentor. I am grateful that he was willing to take me on as a fourth year graduate student to work toward my Doctoral degree. He guided me through a very challenging project with patience, wisdom and friendship. I am indebted to all of the members of the Derynck Lab for their help and support throughout my years there. Special thanks to Dr. Tamara Alliston, Dr. Jeremy Skillington and Dr. Xin-Hua Feng for their critical reading of various parts of my dissertation and, more importantly, for their generosity and friendship. Thanks to Hong-Zhong Zhang, who started the work on human rhomboid and cloned the partial cDNA discussed in Chapter 2 of this dissertation. I have also had the pleasure of collaborating with Annabel Guichard from Ethan Bier's lab at UCSD. She performed the transgenic fly experiments presented in Chapter 4.

I am glad to have known and worked with Dr. Gavin Thurston throughout my graduate school years. He has been a valuable colleague, mentor, and friend. I wish him and his wife Mary much success and happiness.

Other friends at UCSF must be recognized for their contributions both to my work and my sanity. First and foremost is Dr. Sue Jaspersen. I have learned a great deal about science (and life in Nebraska!) from her. More importantly, I have benefited from her love and kindness (not to mention her great recipes!). I know we will remain friends, and I wish her the best of luck in Boulder and beyond.

In addition, I'd like to thank Dr. Hien Tran for afternoon tennis, late night pho runs, and friendship throughout this crazy journey. I hope he finds a good job and a good woman!

Special thanks to my longtime friend Dr. David Bitko for his critical reading of this dissertation. I continue to enjoy our late-night phone calls, which are always a stimulating exchange of advice, political insights and funny stories.

Without a doubt, I would not have come this far without the love of my family.

I could not have asked for more caring, supportive (and patient!) parents. I am as proud of them as they are of me. I have been fortunate to have the additional support of my stepparents, whom I also love very much. I am also blessed to have wonderful grandparents whose love for me seems to know no bounds. It has been a unique pleasure to have my younger sister Liz in San Francisco these past few years. I'm grateful for her support and glad that we have grown closer. Thanks also to her soon-to-be husband Aric for his friendship and generosity. I would also like to thank my older sister Jill. Although geographically distant, she is close to my heart, and I appreciate her love and support.

Recently, my family expanded to include three more sisters: Alex, Hang, and Trinh. They have served as tremendous examples of strength in the face of diversity and of sheer determination. My interactions with them have contributed greatly to my happiness and well-being.

May 23, 1998 was the best day of my life. That was the day I married my beautiful wife Stephanie. Anyone who has ever met her knows that she is the most concentrated source of love and kindness in the universe! She is the love of my life and my best friend. Whenever I felt like quitting, she patiently encouraged me to push onward. Her belief in me was absolutely essential to the completion of this work. Anh yeu em Tuyet-Nga.

Abstract

Cloning, Expression and Characterization of a Human Homologue of *Drosophila rhomboid*

Michael Rizen

The EGF receptor–MAP kinase signaling pathway is highly conserved throughout evolution, reflecting its essential role in the regulation of cell growth and differentiation in both development and the adult organism. In *Drosophila melanogaster*, the single EGF receptor family member DER is activated primarily by the TGF α -like ligand *spitz*. During fly development, the precise localization and level of DER activation is believed to be controlled by the multi-membrane spanning specificity factor *rhomboid*. From genetic studies in *Drosophila*, several hypotheses have been generated to explain the actions of *rhomboid*. These include catalysis of the enzymatic cleavage of the transmembrane *spitz* ligand, enhancement of the *spitz*-DER interaction or modulation of post-receptor signaling events. To determine if a similar specificity factor is involved in the control of mammalian EGFR-MAP kinase signaling, and to establish a biochemical basis for rhomboid function, a cDNA for a human homologue of *rhomboid* was cloned. The human rhomboid cDNA hRho encodes a predicted multi-membrane spanning protein with sequence and structural similarity to *Drosophila rhomboid*. A descriptive characterization of hRho was carried out in mammalian cell culture. The protein was found to localize to both intracellular membranes and the cell surface and to physically associate with both the EGF receptor and transmembrane TGF α . Transient transfection experiments suggested that hRho increased the level of EGFR phosphorylation and c-fos

transcription; however, these effects were not reproduced in a tetracycline regulatable hRho stable cell line. Additional experiments *in vitro* suggested that hRho may modulate intracellular and/or cell surface processing of TM-TGF α . Finally, the sensitive *Drosophila* wing vein assay was used to explore hRho function *in vivo*. The results demonstrated that hRho shared partial functional homology with *rhomboid*, and that its effects were mediated by the EGF receptor. These studies revealed that *rhomboid*-like specificity factors exist in higher organisms and most likely play similar roles in precisely regulating the location and magnitude of growth factor activation of the EGFR-MAP kinase pathway.

A handwritten signature in black ink, appearing to read 'Rh J L', is centered on the page below the main text.

Table of Contents

	<u>Page</u>
Acknowledgements	iii
Abstract	v
List of Tables	viii
List of Figures	ix
Chapter 1 Introduction	1
Chapter 2 Cloning of a Human Homologue of <i>Drosophila rhomboid</i>	47
Chapter 3 Descriptive Characterization of Human Rhomboid	82
Chapter 4 Functional Characterization of Human Rhomboid	122
Chapter 5 Summary and Future Directions	187
Bibliography	199

List of Tables

	<u>Page</u>
Table 1 Principal components of EGFR-MAP kinase signaling in mammals, <i>Drosophila</i> and <i>Caenorhabditis</i>	24

List of Figures

	<u>Page</u>
Chapter 2	
Fig 2.1 Schematic diagram of the various hRho constructs	71
Fig 2.2 IP-Western analysis of Myc tagged partial hRho (pHRM) expression	72
Fig 2.3 <i>In vitro</i> transcription/translation of Flag tagged partial hRho (pHRF)	73
Fig 2.4 IP-Western analysis of pHRF expression	74
Fig 2.5 IP-Western analysis of short hRho (pHRF-short) expression	75
Fig 2.6 Agarose gel electrophoresis of the various hRho constructs	76
Fig 2.7 <i>In vitro</i> transcription/translation of the various hRho constructs	77
Fig 2.8 IP-Western analysis of long hRho (pHRF-long) expression	78
Fig 2.9 cDNA and deduced amino acid sequences of full length hRho	79
Fig 2.10 Hydrophobicity plot of the full length hRho protein	80
Fig 2.11 Amino acid sequence alignment of several rhomboid-like proteins	81
Chapter3	
Fig 3.1 Immunofluorescent staining of full length hRho in COS-1 cells	111
Fig 3.2 IP-Western analysis of N- and C-terminally tagged full length hRho	112
Fig 3.3 Co-localization of hRho and the ER membrane protein mp-30	113
Fig 3.4 Biotinylation of hRho on the surface of COS-1 cells	114
Fig 3.5 RT-PCR analysis of rho expression in various mouse tissues	115
Fig 3.6 RT-PCR analysis of EGFR and TGF α expression in various mouse Tissues	116
Fig 3.7 IP of full length hRho and associated proteins from metabolically labeled HEK-293 or HeLa cells	117

	<u>Page</u>
Fig 3.8 Physical interaction of hrho with EGFR	118
Fig 3.9 Mapping of physical interaction of hrho with EGFR	119
Fig 3.10 Physical interaction of hrho with TM-TGF α	120
Fig 3.11 Physical interaction of hrho, EGFR and TM-TGF α in a tripartite complex.	121
 Chapter 4	
Fig 4.1 Apparent hrho induced c-fos induction in CHO cells	168
Fig 4.2 hrho induced “downregulation” of co-expressed EGFR	169
Fig 4.3 Dose-dependent hrho induced “downregulation” of co-expressed β gal	170
Fig 4.4 Apparent hrho induced increase in EGFR phosphorylation	171
Fig 4.5 Dose-dependent hrho induced increase in EGFR phosphorylation	172
Fig 4.6 Schematic diagram of the pBi5-FHR-long construct used to generate tetracycline regulatable hrho stable cell lines.	173
Fig 4.7 Western blot screen of tetracycline regulatable hrho stable clones	174
Fig 4.8 Tetracycline repressibility of hrho positive stable clones	175
Fig 4.9 Stable hrho expression does not affect endogenous EGFR levels	176
Fig 4.10 Stable hrho expression does not affect soluble TGF α mediated phosphorylation of endogenous EGFR	177
Fig 4.11 Stable hrho expression does not affect TM-TGF α mediated phosphorylation of endogenous EGFR	178
Fig 4.12 Stable hrho expression does not affect basal or EGF stimulated phosphorylation of endogenous p42 or p44 MAP kinase	179
Fig 4.13 Stable hrho expression does not affect basal or TM-TGF α stimulated phosphorylation of endogenous p42 or p44 MAP kinase	180

	<u>Page</u>
Fig 4.14 Apparent effect of stable hrho expression on DNA synthesis	181
Fig 4.15 Effect of tetracycline on DNA synthesis of control stable clones	182
Fig 4.16 Apparent hrho induced alteration of the intracellular processing of TM-TGF α	183
Fig 4.17 Apparent hrho induced inhibition of serum induced proteolysis of TM-TGF α	184
Fig 4.18 Schematic diagram of the constructs used to generate hrho transgenic flies	185
Fig 4.19 Analysis of wing vein development in hrho transgenic flies	186

Chapter 1

Introduction

A fundamental process governing the behavior of all cells is the communication of information from outside the cell into the complex machinery that resides inside. The information is commonly referred to as a “signal” and the transmission of this information is called “signaling.” The cellular events elicited by signals can range from cell division to cell differentiation and even cell death. Signals can originate from several sources and can occur in various forms. A signal can arise from the attachments a cell makes with the extracellular matrix, from contact or adhesion with proteins on neighboring cells, or from distant cells or tissues by way of soluble molecules and proteins. This last group of signaling mediators can be subdivided into two groups: those that have access to the inside of the cell and those that do not. The former group includes ions and other small molecules, which can easily diffuse or be transported through specialized channels in the plasma membrane, and lipophilic molecules, such as steroid hormones, which can diffuse directly across the phospholipid bilayer. The latter group includes larger hydrophilic molecules, such as growth factors, which cannot easily penetrate the plasma membrane. Cells solve the problem of how to receive signals from these larger hydrophilic molecules by way of integral membrane proteins called receptors that span the plasma membrane. A signaling molecule that binds to a receptor is commonly referred to as a ligand. Receptors simultaneously communicate with ligands in the extracellular space and with proteins in the cytoplasm of the cell, thereby providing a crucial conduit for information flow into the cell.

Note that not all receptors are lodged in the plasma membrane. Lipophilic ligands that can diffuse across the plasma membrane utilize intracellular receptors. Although these

receptors then do not bridge a membrane, they still serve as intermediaries between the ligand and the rest of the cellular signaling machinery. The steroid hormone receptors, for example, are part of a large class of DNA binding transcriptional regulatory factors (for reviews see Beato *et al.* 1995, Williams and Franklyn 1994, Evans 1988, Yamamoto 1985).

Among the plasma membrane receptors, there is great diversity in the mechanisms for transmission of the signal brought by the ligand. Glycoprotein hormones, chemokines, and neurotransmitters all transmit their signals through G-protein coupled receptors, which are receptors coupled to GTPase proteins inside the plasma membrane (reviewed in Ji *et al.* 1998, Gether and Kobilka 1998, Bourne 1997, Hepler and Gilman 1992, Bourne *et al.* 1991). Several growth factors such as platelet-derived growth factor (PDGF), fibroblast growth factor (FGF) and epidermal growth factor (EGF) signal through receptors which have either intrinsic or associated kinase activity, the ability to transfer a phosphate from adenosine triphosphate (ATP) to another protein.

Receptors which have intrinsic kinase activity are referred to as receptor kinases. They transmit the signal carried by the ligand to another signaling molecule by means of phosphorylation. This receptor class can be subdivided into two groups, serine/threonine kinases and tyrosine kinases, depending on which amino acid residue the kinase phosphorylates. A prototypical example of a receptor serine/threonine kinase is the Type II Transforming Growth Factor- β receptor (TGF β R-II). An example of a receptor tyrosine kinase is the Platelet Derived Growth Factor Receptor- α (PDGFR- α).

It is important to note that receptors can be involved in signaling via phosphorylation even if they themselves do not possess kinase activity. They do so by recruiting cytoplasmic molecules which themselves possess kinase activity. Immunologic antigens, cytokines such as interleukin-2 (IL-2) and interferon- γ (IFN- γ), and some hormones such as growth hormone (GH) signal in this fashion. For example, upon binding of GH, the Growth Hormone Receptor (GHR) recruits members of the Janus kinase (Jak) family of cytoplasmic kinases. The Jaks, in turn, phosphorylate both themselves and the receptor, thereby regulating the activity of downstream signal transducers (Carter-Su and Smit 1998, Argetsinger *et al.* 1993).

An important feature of receptor tyrosine kinases (RTKs) is that after ligand binding they often must first communicate with themselves via oligomerization (Schlessinger 1988) before they can communicate with downstream signaling molecules. A given receptor kinase typically belongs to a large family of structurally related receptors.

Oligomerization provides a simple mechanism for the generation of greater signaling diversity. For example, to bind dimeric PDGF ligand, PDGFR- α can either homodimerize or heterodimerize with PDGFR- β and this can result in differential signal transmission and elicit distinct responses in the cell (Heldin 1995, Hammacher *et al.* 1989). Ligand induced receptor oligomerization (most often homo- or heterodimerization) permits intermolecular cross-phosphorylation by means of the intrinsic kinase activity of the receptor subunits. This is now well established as a universal mechanism for the activation of a wide variety of cell surface receptors including hormone and growth factor receptors, lymphokine receptors and T and B cell

receptors (Lemmon and Schlessinger 1994). “Activated” receptors can then interact with and/or phosphorylate a variety of downstream signal transducers. Which molecules are recruited depends upon both the structure of the receptor and its subunit composition. The combination of a signal in the form of a ligand, receptor(s), downstream signal transducer(s) and ultimately target gene(s) whose transcription are regulated by the signal constitute an example of what is commonly referred to as a “signaling pathway.” There are many such signaling pathways in the cell and there is frequently “cross-talk” between the various pathways. This provides the cell with a vast array of complicated yet intricately coordinated responses to the various stimuli it may encounter.

EGF Receptor Signaling

Among the best studied signaling pathways are those mediated by the epidermal growth factor family of ligands. Epidermal growth factor (EGF) was first discovered as a potent mitogen of cells from the epidermal layer of the skin (Cohen 1962, Cohen and Elliot 1963, Angeletti *et al.* 1964, Cohen 1965, Hooper and Cohen 1967). The epidermal growth factor receptor (EGFR) was later identified as the receptor for this ligand (Ullrich *et al.* 1984, Hock *et al.* 1979, Carpenter and Cohen 1976). EGFR (also known as HER1, c-ERBB or ERBB1), like most growth factor receptors, is one member of a larger family of structurally related receptors which includes Neu (HER2, ERBB2), ERBB3 (HER3) and ERBB4 (HER4, Tyro 2) (Riese and Stern 1998, Tzahar 1996, Earp 1995, Fantl *et al.* 1993). EGFR is a type I transmembrane protein with its N-terminus outside the cell, followed by a single hydrophobic transmembrane domain, a juxtamembrane region, a

cytoplasmic tyrosine kinase domain and a C-terminal tail. It is a member of RTK Subclass I, which consists of receptors that bind monomeric ligands and contain two cysteine-rich regions in their extracellular ligand binding domains (Yarden and Ullrich 1988).

In mammals, EGFR is widely expressed in cells from epithelial tissues, but not on haematopoietic cells. EGFR is also expressed in the embryo, where it has been implicated in a variety of developmental processes (Paria *et al.* 1993). Perhaps the most dramatic demonstration of the biological importance of EGFR for mammalian development and physiology came from the generation of mice with a targeted disruption of the EGFR gene (Miettinen *et al.* 1995, Sibilio and Wagner 1995, Threadgill *et al.* 1995). These EGFR knockout mice died prematurely and had severe defects in epithelial development in several organs including the skin, lungs and gastrointestinal tract. More recently, defects in craniofacial development and palate closure have been identified (Miettinen *et al.* 1999). Both decreased cell proliferation and defective cell differentiation were evident in the affected organs, suggesting a role for EGFR signaling in both of these cellular processes. The severity of the EGFR null phenotype is not surprising when one considers the wide range of epithelial cells in which EGFR is normally expressed, the fact that several major cellular signaling pathways emanate from EGFR, and the fact that EGFR is the primary receptor for not one, but a whole family of EGF-like ligands. Interestingly, invertebrates such as the fruitfly *Drosophila melanogaster* have an even stricter requirement for EGFR for normal growth and development, since unlike in higher organisms, there is only one member of the EGF receptor tyrosine kinase family in the fly

genome. The many roles of EGFR in fly development will be discussed in greater depth later in this chapter.

As mentioned above, multiple signaling pathways emanate from EGFR. The three best characterized are the phospholipase C-gamma (PLC- γ) pathway, the phosphoinositol-3-kinase (PI-3 kinase) pathway and the the p21^{ras} mitogen activated protein kinase (RAS-MAP kinase) pathway. These three pathways will be reviewed here with particular emphasis on the last. Each of these pathways is quite complex; the full details of which are beyond the scope of this discussion. The discussion will therefore be limited to identifying the key components of these pathways downstream of EGFR and the principal effects that activation of these pathways has on the cell.

The PLC- γ Pathway

The PLC- γ pathway is involved in phospholipid turnover which plays an important role in signal transduction. Upon ligand activation of EGFR, PLC- γ associates with the tyrosine phosphorylated receptor and is then itself tyrosine phosphorylated and activated by the receptor (Margolis *et al.* 1989, Margolis *et al.* 1990). The activated enzyme then hydrolyzes phosphatidylinositol 4,5 bisphosphate (PIP₂) to diacylglycerol (DAG) and inositol 1,4,5 trisphosphate (IP₃). DAG regulates protein kinase C (PKC), a major signaling kinase with at least 11 different isoforms. PKC phosphorylates several downstream targets that affect a wide variety of cellular processes ranging from cell growth to cytoskeletal remodeling and apoptosis (for reviews see Kanashiro and Khalil 1998, Toker 1998, Rhee and Bae 1997, Newton 1997). IP₃, the other product of PIP₂

hydrolysis, also activates PKC. In addition, it promotes the mobilization of intracellular calcium stores, thereby affecting a variety of calcium-regulated cellular processes (for reviews see Clapham 1995, Berridge 1993).

The PI-3 Kinase Pathway

Another important EGFR signaling pathway is the PI-3 kinase pathway. PI-3 kinase is a dimeric enzyme containing an 85 kilodalton regulatory subunit (p85) and a 110 kilodalton catalytic subunit (p110). Upon EGFR activation, PI-3 kinase binds to the receptor through its p85 subunit and this binding enhances its enzymatic activity towards PIP₂ and other downstream substrates (Raffioni and Bradshaw 1992, Hu *et al.* 1992, Skolnik *et al.* 1991, Bjorge *et al.* 1990). PI-3 kinase activity results in the addition of a phosphate to PIP₂ which generates phosphatidylinositol 3,4,5 trisphosphate (PIP₃) (Hawkins *et al.* 1992, Auger *et al.* 1989). More recently PI-3 kinase was found to also be a serine/threonine kinase capable of phosphorylating protein substrates, including its own regulatory 85 kilodalton subunit (Hunter 1995, Dhand *et al.* 1994, Carpenter *et al.* 1993). Several studies have demonstrated a role for PI-3 kinase-generated PIP₃ in the control of cell shape and motility. So-called “membrane ruffling” is believed to be mediated by proteins downstream of PI-3 kinase, including the small G-proteins cdc42, rac and rho (Tapon and Hall 1997, Nobes and Hall 1995, Kotani *et al.* 1994, Wennstrom *et al.* 1994).

The RAS-MAP Kinase pathway

The RAS-MAP Kinase pathway has been implicated as the major transcytoplasmic signaling pathway mediating mitogenic responses from growth factor receptors such as EGFR (for reviews see Widmann *et al.* 1999, Robinson and Cobb 1997, Denhardt 1996, van der Geer *et al.* 1994). It is one of the best studied signaling pathways, and much of what is now known about the mammalian pathway comes from work done in lower organisms such as *C. elegans* and *Drosophila*. Unlike the two pathways discussed above, the RAS-MAP kinase pathway does not begin with the binding of an enzyme to the activated EGFR. Instead, a cytoplasmic protein GRB2 binds to the tyrosine phosphorylated receptor (Lowenstein *et al.* 1992). GRB2 has no enzymatic activity but serves as an adapter protein that provides a crucial link between the activated EGFR and propagation of the signal by the small G-protein p21^{ras} (RAS) (Buday and Downward 1993).

Activation of RAS has been shown to occur in response to proliferative signals from a large number of RTKs (Schlessinger 1993). Like all G-proteins, the function of RAS depends upon its ability to alternate between inactive and active forms and upon its subcellular localization (Boguski and McCormick 1993). The SOS protein exists in a complex with the aforementioned GRB2 protein and serves as the guanine nucleotide exchange factor for RAS, converting it from its inactive (GDP bound) state to an active (GTP bound) state (Buday and Downward 1993, Chardin *et al.* 1993, Egan *et al.* 1993, Li *et al.* 1993, Rozakis-Adcock *et al.* 1993). In both its inactive and active state RAS remains tethered to the cytoplasmic side of the plasma membrane through lipophilic

interactions involving post-translational modification of its C-terminus (reviewed in Wagner and Williams 1994, Lowy and Willumsen 1993).

While several downstream targets of activated RAS exist (reviewed in Campbell *et al.* 1998, Denhardt 1996, McCormick 1995), the most intensely studied is the MAP kinase pathway, most likely because it is the major pathway stimulated by mitogens and growth factors. At the core of the MAP kinase pathway is a module of three sequentially activated kinases that include a MEK kinase (MEKK), a MAPK/ERK kinase (MEK) and a MAPK/ERK. The best characterized RAS regulated MAPK cascade consists of the proteins Raf, MEK1/2 and ERK1/2. Raf normally localizes to the cytoplasm, but upon mitogenic stimulation of EGFR and other RTKs it rapidly binds to activated RAS protein at the plasma membrane (Moodie *et al.* 1993, Vojtek *et al.* 1993, Warne *et al.* 1993, Zhang *et al.* 1993). The localization of Raf to the plasma membrane by RAS is a necessary first step for the activation of Raf. In addition, key amino acid residues are phosphorylated to fully activate Raf. A detailed mechanism of Raf activation has not been established, but it is thought to occur through interactions with members of the Src family of cytoplasmic kinases, the p21 activated kinase Pak3, the CNK protein, the kinase suppressor of ras KSR, and members of the 14-3-3 protein family (Marais *et al.* 1995, King *et al.* 1998, Therrien *et al.* 1998, Therrien *et al.* 1995, Tzivion *et al.* 1998). Phosphorylation induced conformational changes in Raf activate its serine/threonine kinase activity towards its principle downstream targets MEK1 and MEK2 (Dent *et al.* 1992, Howe *et al.* 1992, Kyriakis *et al.* 1992).

MEK1 and MEK2 are members of a group of related proteins that possess unique dual kinase specificity. Upon activation by Raf, MEK1 and MEK2 exhibit kinase activity toward specific threonine and tyrosine residues in their downstream targets, the extracellular signal regulated kinases ERK1 and ERK2 (Zheng and Guan 1993a, Zheng and Guan 1993b, Crews and Erikson 1993, Crews *et al.* 1992).

ERK1 and ERK2 (also known as p44^{MAPK} and p42^{MAPK}) form a subfamily of the MAP kinase family of proteins. They are the principal MAP kinases activated by growth factor stimulation of cells and appear to be essential shared elements of mitogenic signaling pathways. The other MAP kinases are activated by different MEKK/MEKs in response to other types of stimuli such as stress, cytokines, and differentiation factors (for reviews see Widmann *et al.* 1999, Robinson and Cobb 1997). Upon activation by dual phosphorylation (Payne *et al.* 1991), ERK1 and ERK2 are capable of nuclear translocation (Lenormand *et al.* 1993, Chen *et al.* 1992). In the nucleus, these MAP kinases can phosphorylate a variety of targets such as the transcription factor Elk-1, which cooperates with other factors to activate transcription of the so-called early response gene c-fos (Marais *et al.* 1993, Hill *et al.* 1993). More recent studies have demonstrated a connection between the activation and nuclear retention of ERKs and the expression of cyclin D1 and entry into the cell cycle, thereby suggesting mechanisms for MAP kinase mediated stimulation of cell proliferation (Brunet *et al.* 1999, Lavoie *et al.* 1996). In addition, a large pool of activated ERKs has been shown to reside in the cytoplasm (Reszka *et al.* 1995). Cytoplasmic targets of ERK1/2 phosphorylation include microtubule associated proteins, various kinases such as phospholipase A2 and glycogen

synthase kinase-3, and upstream signaling elements such as EGFR, SOS, Raf and MEK (reviewed in Seger and Krebs 1995). This last example demonstrates how the MAP kinases might affect a broad range of cellular processes and also how they can provide feedback regulation on the pathway that activates them.

EGFR Ligands

Even from this simplified discussion of EGFR signaling pathways, it is clear that there is enormous complexity and diversity in the intracellular signaling mechanisms utilized by the cell. However, yet another level of complexity and diversity exists outside the cell in the form of multiple ligands which utilize EGFR as either their only or primary receptor. To date there are 6 known ligands of EGFR: epidermal growth factor (EGF), Transforming Growth Factor- α , (TGF α), amphiregulin (AR), betacellulin (BTC), epiregulin (EPR) and heparin-binding EGF-like growth factor (HB-EGF) (Riese and Stern 1998 and references therein). Differences in signaling properties among these various ligands can be accounted for at least partly by differences in the affinities of the ligand receptor interactions. Moreover, these differences in affinity often correlate with differences in the duration and intensity of MAPK activation and proliferative responses.

All the ligands mentioned above are synthesized as transmembrane proteins that can be proteolytically cleaved to release soluble forms of the protein. In addition, there is evidence that at least some of the ligands can function in their membrane-anchored forms in “juxtacrine” (cell-to-cell) signaling. The region of highest homology among the

various ligands is the “EGF-domain,” the portion of the extracellular domain that is proteolytically released to generate the fully processed soluble form. This domain is a sequence of 45-50 amino acids containing six characteristically spaced cysteines resulting in three disulfide bonds that contribute to a three-looped secondary structure (Gregory 1975, Savage *et al.* 1973). There is no significant homology among the various ligands in the domains that lie outside of the EGF domain; however, this does not preclude a biological importance for these domains. Some of these domains are subject to post-translational modifications such as glycosylation. To date, the contribution of these domains and their modifications to the functions of the ligands has not been thoroughly studied.

TGF α

After EGF itself, the first EGFR ligand to be isolated and biochemically characterized was TGF α (Marquardt *et al.* 1984, Derynck *et al.* 1984, Lee *et al.* 1985). TGF α was initially discovered in the conditioned medium of retrovirus transformed cells. It was found to interact with the same receptor as EGF and to induce the phenotypic transformation of some cell lines (de Larco and Todaro 1978, Todaro *et al.* 1980, Massague 1983, Carpenter *et al.* 1983). Because of the assay in which it was discovered, the concept that TGF α could contribute to tumor development emerged. Indeed, this has made TGF α one of the most intensely studied and well characterized EGFR ligands.

The expression of TGF α and its potential roles in the development of various human cancers have been extensively studied (for reviews see Salomon *et al.* 1995, Derynck

1992). The central theme of these studies is that TGF α and its receptor EGFR are upregulated in a vast array of solid tumors and tumor cell lines (Derynck *et al.* 1987). These observations led to the idea that TGF α acts to drive proliferation in an autocrine fashion during tumorigenesis (Sporn and Todaro 1980, Di Fiore *et al.* 1987, Di Marco *et al.* 1989). In addition, the ability of TGF α to induce neovascularization may also contribute to tumor formation (Schreiber *et al.* 1986). More direct evidence that TGF α expression could contribute to tumorigenesis came with the development of transgenic mice overexpressing TGF α . These animals displayed a variety of hyperplastic and neoplastic lesions depending on the strain of mouse and the promoter used to drive TGF α expression (Sandgren *et al.* 1990, Jhappan *et al.* 1990, Matsui *et al.* 1990). More recently, converse experiments were performed in an attempt to reduce the expression of TGF α in tumor cells using either antisense or antibody neutralization techniques. These experiments showed that reduction of TGF α expression could slow the growth of tumor cells (Laird *et al.* 1994, Walker *et al.* 1995, Seki *et al.* 1997).

Although initially identified and studied in relation to transformation and tumorigenesis, a considerable body of evidence suggests that TGF α plays a role in normal embryonic development and adult physiology (for review see Derynck 1992). A variety of RNA and protein detection methods have demonstrated TGF α expression in several locations in the developing mouse embryo, suggesting a critical role for TGF α in development (Rappolee *et al.* 1988a, Wilcox and Derynck 1988a). However, TGF α knockout mice exhibit a relatively mild phenotype that does not indicate a precise role for the protein during development. These mice are generally healthy and fertile but display abnormal skin

architecture, wavy hair, curly whiskers and corneal inflammation (Luetkeke *et al.* 1993, Mann *et al.* 1993). The most likely explanation for the absence of a severe phenotype, despite fairly ubiquitous expression of TGF α in development, is that the other EGFR ligands can compensate for the deficiency of TGF α in the knockout mouse. Therefore, the EGFR knockout phenotype described earlier in this chapter may provide a better indication of the importance of TGF α in development.

In the normal adult, TGF α is expressed in most if not all epithelial cells including those found in skin (Coffey *et al.* 1987), brain (Wilcox and Derynck 1988b), gastrointestinal mucosa (Carlidge and Elder 1989) and mammary gland (Snedeker *et al.* 1991). The mitogenic activity of TGF α most likely contributes to normal maintenance and proliferation of these tissues. In addition, TGF α expression in skin keratinocytes (Coffey *et al.* 1987) and activated macrophages (Madtes *et al.* 1988, Rappolee *et al.* 1988b) is likely to play a role for in cell migration and neovascularization during normal wound repair (Martin *et al.* 1992, Schultz *et al.* 1991, Schultz *et al.* 1987, Barronden and Green 1987).

In summary, TGF α expression may contribute to the formation of a wide variety of tumors. It is also ubiquitously expressed in normal cells, particularly epithelial cells. It is a normal physiological ligand of the EGFR that contributes to cellular proliferation both in organ and tissue development and in the adult.

Since a substantial area of investigation in later chapters of this thesis centers on studies of TGF α mediated EGFR/MAP kinase signaling, a brief review of the structure and processing of transmembrane TGF α (TM-TGF α) is presented. Human TGF α is synthesized as the 160 amino acid type I transmembrane protein pre-proTM-TGF α (Derynck *et al.* 1984, Lee *et al.* 1985). The 22 residue amino terminal signal peptide is rapidly removed during protein translocation to generate proTM-TGF α . (Brachmann *et al.* 1989). The pro-region, which consists of the 17 residues downstream of the signal peptide cleavage site, is N-glycosylated and also carries O-linked carbohydrates (Bringman *et al.* 1987, Teixido *et al.* 1987). This is followed by the 50 amino acid EGF domain, which corresponds to the fully processed secreted form TGF α . The EGF domain is both preceded and followed by the cleavage site Ala/-Val-Val. Cleavage at the amino-terminal site removes the pro-region to generate TM-TGF α , while cleavage at the carboxy-terminal site results in the release of soluble forms of TGF α from the cell. Finally, the EGF domain is followed by a transmembrane domain and a 39 residue cytoplasmic domain. The cytoplasmic domain is rich in cysteine and is modified by palmitoylation which may mediate its association with the inner surface of the plasma membrane as well as cytoplasmic proteins (Bringman *et al.* 1987, Shum *et al.* 1996).

The post-translational modification of the pro-region mentioned above results in the generation of three predominant forms of transmembrane TGF α . Pulse-chase analysis of the synthesis of cell associated forms of TGF α has shown that the intermediate-sized ~25 kd form is the initial proTM-TGF α precursor (Dempsey and Coffey 1994, Bringman *et al.* 1987). This form contains an N-linked high mannose oligosaccharide in the pro-

region (Kuo 1999, Briley *et al.* 1997). The largest ~30 kd form contains additional complex N- and O- linked carbohydrate modification of the pro-region (Kuo 1999, Teixido and Massague 1988, Bringman *et al.* 1987), and the smallest ~20 kd form is the “mature” TM-TGF α from which the pro-domain has been proteolytically removed (Bringman *et al.* 1987, Teixido *et al.* 1987).

Two predominant forms of soluble TGF α can typically be detected in the conditioned medium of cells overexpressing the growth factor. The larger ~18 kd form contains the complex glycosylated pro-domain and the EGF domain and results from the cleavage of the ~30 kd transmembrane form. The smaller ~6 kd form consists of the EGF domain and results from the cleavage of the ~20 kd mature TM-TGF. This form corresponds to the mature 50 amino acid form of TGF α . (Bringman *et al.* 1987) While very little work has been done to characterize the proteolytic event responsible for the removal of the pro-domain, several studies have attempted to characterize the regulation and localization of the protease(s) responsible for the release of soluble TGF α from cells.

TGF α Proteolysis

The earliest studies demonstrated that TGF α ectodomain cleavage was a regulated process which could be stimulated by multiple signals including serum, PMA (an activator of protein kinase C) and elevated cytosolic calcium (Pandiella and Massague 1991a, Pandiella and Massague 1991b). A later study demonstrated that release of soluble TGF α could occur in the absence of cytosol, suggesting that the protease responsible was plasma membrane anchored (Bosenberg *et al.* 1993). Subsequent studies

suggested that several transmembrane proteins in addition to TGF α might share a common broad specificity proteolytic machinery (Arribas and Massague 1995). Most recently, it has been demonstrated that this cleavage machinery is regulated by at least two distinct MAP-kinase signaling pathways and its activation can occur in the absence of new protein synthesis (Fan and Derynck 1999). The proteolytic activity responsible for release of soluble forms of TGF α was originally thought to be an elastase-like serine protease, based on studies of the effects of various classes of protease inhibitors on ectodomain shedding (Pandiella *et al.* 1992). However, more recent work demonstrated that one or more metalloproteases were responsible for shedding of the ectodomains of diverse cell surface proteins, including TM-TGF α (Arribas *et al.* 1996, Feehan *et al.* 1996, Solomon *et al.* 1997). Finally, the metalloproteinase responsible for most, if not all, of the release of TGF α from the cell surface was identified as TACE, a member of the ADAM family of metalloproteases originally identified as the tumor necrosis factor α converting enzyme (Black *et al.* 1997, Moss *et al.* 1997 and references therein). The most definitive evidence that TACE is a TGF α protease comes from studies of TACE knockout mice. These mice display many of the same anomalies present in the EGFR knockout mice. Furthermore, cell lines derived from these mice release virtually no soluble TGF α upon stimulation with PMA (Peschon *et al.* 1998).

One reason for such a significant amount of research into the process by which a transmembrane growth factor is cleaved from the cell surface is that it represents a unique biological control point for the actions of the ligand. Several growth factors have been shown to be active in their membrane-anchored forms, including TGF α (Brachman *et al.*

1989, Wong *et al.* 1989), EGF (Dobashi and Stern 1991), HB-EGF (Naglich *et al.* 1992) and TNF α (Perez *et al.* 1990). The transmembrane forms of these growth factors are believed to act as juxtacrine regulators of cell-cell signaling (Bosenberg and Massague 1993, Massague and Pandiella 1993). In fact, the transmembrane forms of TGF α are likely to be more prevalent than the soluble forms, since all cells expressing TGF α exhibit transmembrane precursors at their cell surface, yet not all cells release soluble TGF α into the medium (Derynck *et al.* 1987, Brachman *et al.* 1989). Furthermore, TM-TGF α is thought to be the predominant form present in some normal and diseased tissues (Russell *et al.* 1993, Hoffman *et al.* 1997). Therefore, the current paradigm for TGF α signaling is that proteolysis does not serve to “activate” the protein, but rather to convert it from one active form to another.

This “active-to-active” concept has profound biological implications. First, membrane tethered TGF α can act only at a short distance to engage EGF receptors either on the same cell or an immediately neighboring cell. In development, this strict localization might be important for controlling the proliferation or differentiation program of a particular zone of cells or for establishing a particular boundary between groups of cells. In contrast, soluble forms of TGF α can diffuse to act at a distance from the cell that secreted them and can stimulate a much larger number of cells. The concentration of the growth factor would be highest at its source and then decrease with distance from the secreting cell. This might be important in development for establishing a growth factor concentration gradient that can serve as an axis for developmental patterning events. Since TM-TGF α is expressed fairly ubiquitously, more limited expression of factors that

regulate TGF α proteolysis, could then dictate exactly where the highest levels of soluble ligand signaling occur. This idea of spatially regulated proteolysis will be revisited in the discussion of *Drosophila* EGF receptor signaling later in this chapter. Another potential consequence of the existence of two biologically active forms of TGF α is their differential ability to induce ligand-mediated endocytosis of the EGF receptor. In the case of EGF, occupation of EGFR by the soluble ligand and subsequent internalization is responsible for much of the receptor downregulation which occurs following stimulation (Sorkin 1998, Gill 1990). While such receptor internalization can also occur upon stimulation with soluble TGF α , it is unlikely to occur with transmembrane TGF α . It is conceivable that binding to EGFR on an adjacent cell could stimulate proteolysis of TM-TGF α to allow conventional internalization of the newly generated soluble form, but this has not been demonstrated experimentally.

The relative importance of the soluble ligand is becoming more apparent, thereby challenging the conventional “active-to-active” paradigm. First, the TACE knockout mouse displayed a phenotype similar to the EGFR knockout mouse (Peschon *et al.* 1998), suggesting that very little EGFR signaling was occurring in these mice. If the transmembrane forms of TGF α were equal in biological activity to their soluble counterparts, then one would have expected a much milder phenotype, since EGFR signaling would be preserved. One problem with this argument is that in the absence of TACE, the release of *several* soluble EGFR ligands from their transmembrane counterparts is likely to be reduced. This is the simplest explanation for the severity of the phenotype. Therefore, one cannot draw any straightforward conclusions about the

relative importance of the different forms of any one ligand such as TGF α . Nonetheless, the results suggest that *in vivo* the soluble forms of the whole group of ligands regulated by TACE may be more “active” than their membrane-anchored counterparts. This could either be due to their altered structure or their ability to diffuse through tissue and engage receptors in cells at a distance from the cells that were the original source of the ligand. Indeed, as will be discussed in detail later in this chapter, *spatially controlled* ligand processing has emerged as an important regulatory mechanism in the development of lower organisms.

A second challenge of the “active-to-active” paradigm comes from a study of autocrine signaling through EGFR (Dong *et al.* 1999). These authors point out several caveats to the studies that had previously demonstrated activity of transmembrane forms of growth factors such as TGF α . First, some of these studies relied on protease-resistant mutants of TGF α as the source of transmembrane ligand and evaluated the cleavage resistance by the lack of detectable soluble TGF α in the medium (Wong *et al.* 1989). Dong *et al.* suggest that the inability to detect the soluble TGF α could have been due to the high capture efficiency of EGFR on the ligand expressing cells (Wiley *et al.* 1998, Dempsey *et al.* 1994). They also point to evidence that soluble TGF α can be detected from cells expressing “noncleavable” forms of TGF α if the cells are first treated with an antibody that blocks EGFR. Second, these authors note that the studies on juxtacrine signaling by TGF α used cell types that might be “hypersensitive” to EGFR ligands due to the fact that they overexpress EGFR. Therefore these *in vitro* studies may overestimate the actual importance of the juxtacrine mode of signaling *in vivo*. The authors note that few studies

have actually compared the relative contributions of soluble versus membrane-anchored ligand to total ligand activities. In those studies that have made this comparison, the soluble ligands were found to have much greater activity than the transmembrane forms (Brachman *et al.* 1989, Higashiyama *et al.* 1995, Ono *et al.* 1994). In one *in vivo* study, transgenic mice overexpressing cleavable TGF α , but not noncleavable TGF α , showed an increased cancer incidence (Sandgren *et al.* 1990). Finally, through the use of specific metalloprotease inhibitors and a cell line dependent on autocrine EGFR signaling for growth and proliferation, Dong *et al.* demonstrated that, at least in the case of autocrine signaling through EGFR, conversion from the transmembrane to the soluble form of TGF α was required to observe any significant biological activity (Dong *et al.* 1999). This is consistent with the apparent requirement for EGFR ligand conversion in lower organisms to be discussed shortly.

In summary, while the biological activity of the transmembrane forms of growth factors may be important in certain contexts, the cleavage of these proteins and the functions mediated by their soluble forms are emerging in importance.

EGF Receptor Signaling in *Drosophila melanogaster*

That the TGF α /EGFR duo is important biologically is evident in the fact that this same ligand/receptor system has been conserved throughout evolution. Indeed, some of the components of the EGFR-RAS-MAP kinase signaling pathway were first identified through genetic studies in simpler organisms such as worms and flies (reviewed in Egan and Weinberg 1993, Perrimon 1993). Homologues of all of the major components of the mammalian EGFR-RAS-MAP kinase pathway exist in *Caenorhabditis elegans* and *Drosophila melanogaster*, as illustrated in Table 1. Note that there are significantly fewer EGFR ligands and only one EGFR in each of these organisms. This reduced level of redundancy has permitted more straightforward and controlled investigation into the functions of these components in these simpler organisms, which are also more genetically manipulatable.

DER

The EGFR has increased importance in the development of simpler organisms since it is the only receptor for the EGF-like ligands. The *Drosophila* EGF receptor (DER) was the first receptor tyrosine kinase identified in this organism and was found to homologous to its mammalian counterpart, particularly in the extracellular ligand binding and cytoplasmic kinase domains (Livneh *et al.* 1985 Wadsworth *et al.* 1985). The importance of DER in fly development is not easily addressed by analysis of its expression pattern. Like mammalian EGFR, DER is ubiquitously expressed in nearly all tissues of ectodermal origin, although the levels of expression vary somewhat from one tissue to

Table 1 Major Components of EGFR-MAP Kinase Signaling Pathway in Mammals, *Caenorhabditis* and *Drosophila*

	Mammals	<i>C. elegans</i>	<i>D. melanogaster</i>	Description
Ligands	EGF, TGF α , HB-EGF, BTC, NDF, neuregulins, heregulins, Amphiregulin	Lin-3	Spitz, Gurken, Vein Argos	Peptide growth factor with EGF-domain
Receptors	EGFR (ERBB1) ERBB2, ERBB3, ERBB4	LET-23	DER	Transmembrane receptor tyrosine kinase
Effectors	Grb2 mSOS Ras Raf MEK1/2 MAPK (ERK1/2)	SEM-5 ? LET-60 LIN-45 MEK-2 MPK-1 (Sur-1)	Drk SOS ras1 D-raf Dsor1 rolled	SH2 containing adapter protein Guanine exchange factor for Ras GTPase MAPKK kinase; S/T kinase MAPK kinase; T kinase, Y kinase MAP kinase; S/T kinase

References: Widmann '99, Moghal and Sternberg '99 and references therein

another (Katzen *et al.* 1991, Zak *et al.* 1990, Kammermeyer and Wadsworth 1987, Schejter *et al.* 1986).

By analogy to the mouse EGFR knockout experiments, the various roles of DER were more clearly defined by the knockout and weaker mutant allele phenotypes. These experiments revealed that two levels of DER activity are required for normal fly development (reviewed in Bier 1998). The requirement for at least a low/basal level of DER activity was illustrated by the DER null phenotypes of embryonic lethality and widespread epidermal cell death (Price *et al.* 1989, Schejter and Shilo 1989). The requirement for higher level DER activity was illustrated by weak alleles of DER. In flies that expressed weak alleles, those tissues requiring lower levels of activity were adequately supplied, while those tissues requiring higher levels of DER activity displayed defects. These alleles fell into two major categories named *torpedo* and *faint little ball*. They were isolated by genetic mutagenesis screens that were originally performed to identify genes important for female fertility and the development of the larval cuticle, respectively (Schupbach 1987, Nusslein-Volhard *et al.* 1984, Jurgens *et al.* 1984). Only later was it discovered that these alleles were in fact mutant alleles of DER (Price *et al.* 1989, Schejter and Shilo 1989).

Several subsequent studies of these mutant DER alleles demonstrated a requirement for high level DER activity in a variety of tissues during all stages of development (reviewed in Schweitzer and Shilo 1997). In the ovary, high DER activity is required in the follicle cells surrounding the oocyte and contributes to the specification of both the dorsal/ventral

and anterior/posterior body axes (Gonzalez-Reyes *et al.* 1995, Price *et al.* 1989, Schupbach 1987). In the embryo, high DER activity determines cell fate in the ventral ectoderm (Raz and Shilo 1992, Clifford and Schupbach 1992) and the ventral midline cells of the central nervous system (Kim and Crews 1993, Raz and Shilo 1993). In later development high DER activity is required in developing wing veins (Diaz-Benjumea and Hafen 1994, Clifford and Schupbach 1992), photoreceptor cells of the eye (Freeman 1996, Freeman 1994, Tio *et al.* 1994,) and cells of the developing trachea (Wappner *et al.* 1997).

From these examples, it is clear that DER activity is required not only for cell viability, but also for cell fate determination and cell differentiation during development. The question naturally arises as to how the single DER can mediate so many different developmental processes in so many different tissues. The answer lies in the fact that several mechanisms exist which precisely regulate the location and magnitude of DER activity. These include both the use of multiple ligands and the existence of specificity factors with putative roles in the control of ligand presentation, ligand receptor interaction or signaling events downstream of receptor activation.

DER Ligands

As is the case for the mammalian EGFR, multiple ligands for DER exist that can activate the RTK in a tissue specific manner. Three stimulatory ligands of DER were identified through the characterization of mutants which display only a subset of the DER mutant phenotypes. The ligands encoded by the genes *spitz* (Rutledge *et al.* 1992), *gurken*

(Neuman-Silberberg and Schupbach 1993) and *vein* (Schnepf *et al.* 1996) all contain an EGF domain similar to that found in TGF α and the other mammalian EGF family members. A deficiency of any one of these ligands is not as severe as a deficiency of the receptor DER. This is similar to the case of the TGF α mouse versus the EGFR knockout mouse discussed previously. Gurken is a transmembrane ligand whose expression appears to be limited to the developing oocyte (Neuman-Silberberg and Schupbach 1996, Neuman-Silberberg *et al.* 1993). Vein contains an immunoglobulin-like domain in addition to the EGF domain, has no transmembrane domain, and is presumed to be a soluble secreted factor (Schnepf *et al.* 1996, Simcox *et al.* 1996). Spitz is also a transmembrane ligand but, unlike Gurken, is ubiquitously expressed. These features, along with its sequence similarity, make it a likely homologue of mammalian TGF α (Rutledge *et al.* 1992).

Regulation of DER Signaling

Since both DER and its principal activating ligand spitz are expressed widely during development, there must be an additional level(s) of regulation that explains how receptor activation is restricted. A breakthrough in understanding the regulation of DER signaling was achieved by the establishment of a connection between the DER signaling pathway and a set of genes termed the “spitz group.” In addition to *spitz*, this group included *star*, *rhomboid*, *pointed*, *single-minded* and *sichel* (Mayer and Nusslein-Volhard 1988). Most of these genes were identified in systematic mutagenesis screens for embryonic lethal mutations affecting the pattern of the larval cuticle (Nusslein-Volhard *et al.* 1984, Jurgens

et al. 1984). They were grouped together based on the finding that mutation of any one of these genes caused a similar reduction of the lateral extent of the ventral epidermal pattern. In this region, both epidermal and neural cells were affected. The link between DER and the spitz group became apparent once the *faint little ball* mutant alleles of DER were identified and shown to result in nearly identical ventral midline defects (Raz and Shilo 1992, Clifford and Schupbach 1992). This connection between DER and the spitz group was solidified by the identification of the group's namesake spitz as a putative EGF-like ligand of DER (Rutledge *et al.* 1992). Subsequent cloning of additional spitz group genes allowed for the formal demonstration of genetic interaction between these genes and various components of the DER signaling pathway (Raz and Shilo 1993, Sturtevant *et al.* 1993). From these studies and others, two of the spitz group genes *star* and *rhomboid* have emerged as specificity factors which appear to regulate the *spitz*-DER signaling pathway.

Star

The *star* mutation was first identified on the basis of its dominant rough eye phenotype (Bridges and Morgan 1919) and was later found to play a role in the early development of a subset of photoreceptor cells in the eye (Heberlein and Rubin 1991). *Star* also appeared in the context of embryonic development as a member of the spitz group as described above (Mayer and Nusslein-Volhard 1988). These observations established an apparent connection between *star* and DER. Later studies demonstrated dosage sensitive interactions between *star* and *Ras1* in the eye (Heberlein *et al.* 1993) and between *star* and other components of the DER signaling pathway in the development of wing veins

(Sturtevant *et al.* 1993). These studies confirmed the connection between *star* and the DER signaling pathway and demonstrated that *star* potentiated DER signaling. Finally, the *star* gene was cloned (Kolodkin *et al.* 1994).

Analysis of the cDNA sequence of the cloned *star* gene revealed that it encodes a protein of 598 amino acids with a calculated molecular mass of 66 kd with no similarity to any known proteins. The open reading frame does not contain an amino terminal signal sequence, but it contains an internal stretch of 22 hydrophobic residues comprising a single putative transmembrane sequence. The highly hydrophilic nature of the amino terminus and the relatively neutral carboxy terminus were consistent with a type II transmembrane protein with the amino terminus in the cytoplasm and the carboxy terminus extracellularly oriented. In addition, two putative PEST sequences, thought to be associated with proteins having short half lives (Rechsteiner and Rogers 1996, Rogers *et al.* 1986), were present in the amino terminal domain.

Cloning of the *star* gene permitted the identification of new genetic interactions with the *sevenless* RTK signaling pathway and provided further confirmation of the previously described interactions with the DER signaling pathway (Kolodkin *et al.* 1994). The precise mechanism(s) by which the *star* protein potentiates DER signaling is not yet known. Its expression pattern, like that of DER and *spitz*, is fairly widespread in the embryo, consistent with a requirement for basal EGFR activity in most cells. Therefore it has been difficult to conceptualize how *star* might serve as a specificity factor for promotion or enhancement of DER signaling. Recent studies have begun to shed some

light on possible mechanisms of *star* function. These possible mechanisms will be discussed shortly in the context of the following discussion of the major *spitz*-DER signaling specificity gene *rhomboid*.

Since it is the major focus of the work presented in this thesis, a comprehensive review of what is currently known about *rhomboid* is presented here.

Rhomboid

Unlike *star*, very little was known about the *rhomboid* gene prior to its cloning. It was first identified in the original mutagenesis screen for embryonic lethal mutations affecting the pattern of the larval cuticle (Nusslein-Volhard *et al.* 1984, Jurgens *et al.* 1984). Later *rhomboid* was classified into the *spitz* group of genes based upon the narrowed ventral epidermis of the mutant fly (Mayer and Nusslein-Volhard 1988). In addition to a narrowed ventral zone, *rhomboid* mutant cuticles displayed alterations at sites of abdominal muscle attachment, a fused head skeleton, and defects in peripheral and central nervous system precursors (Mayer and Nusslein-Volhard 1988). Finally, in contrast to *spitz* and *star*, *rhomboid* was found to be dispensible for the normal germ line development and showed no maternal influence on embryonic development. In other words, *rhomboid* was an exclusively somatically expressed gene (Mayer and Nusslein-Volhard 1988).

The cloning of the *rhomboid* gene permitted a structural analysis of the protein encoded by its cDNA sequence (Bier *et al.* 1990). It encoded a protein of 355 amino acids with a predicted molecular weight of 39,356 kd and no significant similarity to any known

proteins. Like *star*, the open reading frame did not contain an amino terminal signal sequence but did contain internal hydrophobic stretches, consistent with it being an integral membrane protein with a cytoplasmically oriented amino terminus. Unlike the single transmembrane protein *star*, hydrophobicity analysis suggested that rhomboid was a multi-membrane spanning protein with the number of transmembrane domains ranging from 3 to 7, depending on the computer algorithm used to identify these domains. Again like *star*, a putative PEST sequence was present near the amino terminus of rhomboid.

Expression Pattern of Rhomboid

Using the cloned cDNA as a probe for *in situ* hybridization, a detailed analysis of the expression of *rhomboid* transcripts during development was performed (Bier *et al.* 1990). The expression pattern was found to be both complex and highly dynamic. The earliest expression was detected in two longitudinal stripes in the ventrolateral domains on either side of the ventral midline. Later in development, two perpendicular stripes of rhomboid expression were detected in the head. As development proceeded, the two longitudinal stripes became progressively more narrow and migrated closer to the midline, eventually forming a single strip along the ventral midline. Later, transient expression was detected at other locations, including tracheal precursor cells and a peripheral nervous system structure known as the chordontal sense organ. In later stages of development *rhomboid* expression faded along the ventral midline and began to appear in cells of the central nervous system. Eventually, expression was detected in repeated stripes perpendicular to the midline and corresponding to the abdominal segmentation of the fly.

A noteworthy feature of the expression pattern of *rhomboid* was that virtually all expression was in linear arrays of cells that localized to boundaries between different developmental regions. For example, early in development *rhomboid* expression at the midline marked the boundary between the left and right halves of the embryo and between the neuroectoderm and mesoderm. Later in development, *rhomboid* was expressed at the abdominal segment boundaries. In development, these boundary regions often correlate with, and are most likely formed by, strictly controlled high level signaling activity. Hence, the expression pattern of *rhomboid* suggests a role for high level DER signaling activity at these important developmental boundaries and is consistent with a proposed role of *rhomboid* as the major *spitz*-DER signaling specificity factor.

Overall, the expression pattern described above directly correlated with the mutant phenotypes observed in flies expressing weak *rhomboid* alleles (Bier *et al.* 1990). For example, the early expression in the head region correlated with the head defects discussed earlier that resulted in a pointed head skeleton. In another example, later expression in stripes corresponding to the abdominal segments of the fly correlated with observed disorganization of the abdominal muscles believed to attach at these locations. This tight correspondence between the rhomboid expression pattern and the cells affected by its loss suggested that rhomboid acted in a cell autonomous fashion (i.e. that rhomboid was required for the proper development of the cells that express rhomboid).

As discussed previously, the *rhomboid* mutant phenotypes were similar to the phenotypes of the other spitz group mutants, and these phenotypes were virtually identical to those produced by the various *faint little ball* weak alleles of DER. These observations, combined with the striking correlation of the rhomboid expression pattern with the mutant phenotypes, suggest that rhomboid required at precisely those locations which require the highest levels of DER signaling.

This connection between *rhomboid* and high level *spitz*-DER signaling activity was reinforced by three sets of studies that were performed subsequent to the cloning of the gene: studies of wing vein development, oogenesis, and ventral midline formation. These genetic interaction and gene dosage studies utilized either weak or strong *rhomboid* expression constructs or mutants in various combinations with weak or hyperactive alleles of various components of the DER signaling pathway. Collectively, they demonstrate a role for rhomboid in modulating both the location and magnitude of DER signaling.

Role of Rhomboid in Wing Vein Development

The function of *rhomboid* as a DER specificity factor was convincingly demonstrated in a study that investigated the role of *rhomboid* in wing vein formation (Sturtevant *et al.* 1993). A role for *rhomboid* in this developmental process might have been hypothesized from the previously identified requirement for DER signaling for proper wing vein formation (Clifford and Shupbach 1992). This was confirmed by the fortuitous identification of viable partial loss-of-function allele *rhomboid^{nc}*, apparently the result of

a deletion in the promoter of the *rhomboid* gene (Sturtevant *et al.* 1993, Diaz-Benjumea and Garcia-Bellido 1990). Flies homozygous for *rhomboid*^{nc} lack distal segments of wing veins, especially longitudinal veins L4 and L5 (wing longitudinal veins are designated L1 – L5 from anterior to posterior). In the present study, *in situ* hybridization revealed that *rhomboid* transcripts were present in wing vein primordia during development and were sharply restricted to the 5 longitudinal veins, on both the dorsal and ventral surfaces, in older wings (Sturtevant *et al.* 1993).

To test the hypothesis that localized *rhomboid* expression dictated the vein cell fate, Sturtevant *et al.* ectopically expressed *rhomboid* under the control of a heat shock promoter. A range of abnormal wing vein phenotypes was obtained which correlated with the induced level of *rhomboid* expression. In the weakly expressing lines, slight deltas were observed at the junctions of some of the longitudinal veins with the wing margin. The moderately expressing lines has more pronounced deltas in these locations and also displayed rudiments of ectopic wing veins, especially between L3 and L4. In the strongly expressing lines, wing veins were thickened or fused, extensive ectopic veins were present, and the wings often had large blisters due to the abnormal separation of the dorsal and ventral wing surfaces. Finally, dosage sensitive interactions were identified between *rhomboid*^{nc} and heat shock *rhomboid* by analysis of the wing veins of progeny resulting from crosses between these two lines of flies. For example, heterozygous weak heat shock *rhomboid* was able to strongly suppress the homozygous *rhomboid*^{nc} phenotype. This type of reciprocal interaction, along with the loss of vein material in the *rhomboid*^{nc} mutants and the excess vein material present in the overexpressing lines,

demonstrated that *rhomboid* was necessary for wing vein formation, and that *rhomboid* expression must be strictly localized along wing vein primordia to limit the number of cells which differentiate as vein tissue.

Given the strict localization requirement for *rhomboid* in the wing veins and the fact that *spitz* and DER are ubiquitously expressed in the wing, it appeared that *rhomboid* was acting as a spatial cue to specifically localize high *spitz*-DER signaling activity to promote the development of wing veins. To formally test this concept, genetic interaction studies were performed using various combinations of the *rhomboid*^{ne} allele, heat shock *rhomboid*, and either hyperactive or hypoactive alleles of DER, *spitz* group genes, and components of the DER signaling pathway (Sturtevant *et al.* 1993). Strong genetic interactions were observed between *rhomboid* and DER. Combination of gain of function alleles of both *rhomboid* (heat shock *rhomboid*) and DER (*Egfr*^{ellipse}) synergistically enhanced the formation of ectopic wing veins. Combinations of loss of function alleles of these genes (*rhomboid*^{ne} and *Egfr*^{torpedo}) synergistically enhanced the loss of vein phenotype. Lastly, combination of loss of function *rhomboid* (*rhomboid*^{nc}) with gain of function DER (*Egfr*^{ellipse}) resulted in nearly wild type wing vein development. These data suggested that *rhomboid* acted upstream or in parallel with DER to permit and/or amplify DER signaling activity. Using the same wing vein assay, additional strong genetic interactions were identified between alleles of *rhomboid* and *spitz*, *rhomboid* and *star*, *rhomboid* and *ras1*, and *rhomboid* and *gap1*. In all cases, the data were consistent with a model in which *rhomboid* potentiated *spitz*-DER signaling activity.

Role of Rhomboid in Oogenesis

A role for *rhomboid* in spatially restricting DER activity was demonstrated in another important study which established a requirement for spatially localized *rhomboid* in the generation of the dorsal-ventral axis during *Drosophila* oogenesis (Ruohola-Baker *et al.* 1993). Recall that high DER activity in the ovarian follicle cells surrounding the oocyte was previously shown to be required for proper specification of the dorsal-ventral axis of the eggshell and the embryo (Price *et al.* 1989, Schupbach 1987). Ruohola-Baker *et al.* demonstrated by *in situ* hybridization and immunostaining that *rhomboid* transcripts and protein, respectively, were present in both the somatic follicle cells and the germline (Ruohola-Baker *et al.* 1993). In addition, this study confirmed the result from previous studies that *rhomboid* is not required in the germline for proper oogenesis (Mayer and Nusslein-Volhard 1988). Therefore, the effects of *rhomboid* in oogenesis are most likely mediated by its expression in the DER expressing follicle cells. It is noteworthy that *rhomboid* expression was tightly localized to the follicle cells on the dorsal-anterior end of the egg chamber (Ruohola-Baker *et al.* 1993). To determine whether this localization was important for the determination of the dorsal-ventral axis, *rhomboid* was ectopically overexpressed using a heat shock promoter. This resulted in dorsalization (an expansion of the dorsal material at the expense of the ventral material) of both the eggshell and the embryo. In contrast, when an anti-sense version of *rhomboid* was ectopically overexpressed using the heat shock promoter, both the eggshell and the embryo were ventralized (ventral material expanded at the expense of dorsal material). This suggested that *rhomboid* was required for specifying the dorsal-ventral axis of both the follicle cell layer and the oocyte (Ruohola-Baker *et al.* 1993).

Given the strict localization requirement for *rhomboid* in the dorsal-anterior follicle cells and the fact that DER is ubiquitously expressed in all of the follicle cells, it again appeared that *rhomboid* was acting as a spatial cue to specifically localize high DER signaling activity to dorsal locations. To formally test this concept, a genetic interaction study was performed by ectopically expressing heat shock *rhomboid* in the *torpedo* (an oogenesis specific DER loss-of-function allele) mutant background. The resulting eggshells and embryos were ventralized, demonstrating that DER was epistatic to *rhomboid*. Furthermore, when heat shock *rhomboid* was ectopically expressed in a *gurken* (the oocyte specific transmembrane ligand homologous to TGF α) mutant background, the eggshells and embryos were again ventralized, demonstrating that *gurken* was also epistatic to *rhomboid*. Therefore, *rhomboid* action required DER in the follicle cells and *gurken* in the oocyte. Given that *rhomboid* encodes a transmembrane protein, these results suggested that *rhomboid* was involved in signaling between the oocyte and the dorsal follicle cells (Ruohola-Baker *et al.* 1993).

In the preceding two examples of wing vein development and oogenesis, it appeared that *rhomboid* expression was required by the cells expressing it, which were also the cells receiving the DER signal. In other words, *rhomboid* appeared to be acting in a cell autonomous fashion. However, the results from two subsequent studies on ventral midline development suggested that the primary mode of action for *rhomboid* might be to participate in the generation of the DER signal by acting in a cell non-autonomous fashion. These studies also demonstrated the importance of ligand processing for

signaling activity, a topic discussed earlier in this chapter in the context of an alternate paradigm for TGF α ligand activity.

Role of Rhomboid in Spitz Processing and Ventral Midline Development

The first study suggested a new position for *rhomboid* (and *star*) in the genetic hierarchy of DER signaling (Schweitzer *et al.* 1995). While the preceding studies suggested *rhomboid* might be acting immediately upstream or at the level of the receptor, this study putatively placed *rhomboid* (and *star*) upstream of the processing event that results in the generation of the secreted spitz ligand of DER. This was determined through epistasis experiments whereby ventral ectoderm defects in flies carrying a homozygous mutant allele of *rhomboid* (or *star*) were rescued by ventral ectoderm expression of a constitutively secreted form of spitz consisting of only the extracellular domain of the ligand.

Interestingly, this same study showed both *in vitro* and *in vivo* that secreted spitz was the active form of the ligand, while the transmembrane precursor had no activity. This was achieved *in vitro* by generating stable *Drosophila* Schneider cell lines expressing either *spitz* or DER. Two *spitz* cell lines were generated, one expressing the full-length transmembrane spitz protein (*m-spitz*), and one expressing a constitutively secreted spitz protein lacking the transmembrane and cytoplasmic domains (*s-spitz*). The conditioned medium from the *s-spitz* cells, but not *m-spitz* cells, was capable of activating DER tyrosine phosphorylation when applied to Schneider cells stably expressing DER (Schweitzer *et al.* 1995). More importantly, cell membranes prepared from the *m-spitz*

cells were incapable of activating DER in these same cells. Note that these results were dramatically different from the results obtained in mammalian cell culture systems with the TGF α ligand (Brachman *et al.* 1989, Wong *et al.* 1989). *In vivo*, a similar effect was observed. When *m-spitz* was ectopically overexpressed in the ventral ectoderm of wild-type flies, no change in the morphology of the cuticle was observed. However, when *s-spitz* was overexpressed, a dramatic ventralization of the cuticle and embryo was observed (Schweitzer *et al.* 1995).

A second study both extended and refined these results (Golembo *et al.* 1996). First, it demonstrated that ectopically overexpressed *rhomboid* could ventralize a wild-type embryo in a manner similar to that observed previously with secreted *spitz*. Importantly, this study further demonstrated that a functional DER pathway was required for this ventralizing activity of *rhomboid*, as this effect was not observed in *Egfr^{faint little ball}* mutant embryos. Interestingly, similar to *m-spitz*, no aberrant phenotype was observed as a result of ectopic overexpression of *star* in wild-type embryos. This demonstrated that *rhomboid* was the only limiting component in the ventral ectoderm with regard to the machinery required to generate a *spitz*-DER signaling activity.

Next, this study showed that *rhomboid* or *star* expressed in the ventral midline cells could function non-autonomously to help pattern the immediately adjacent ventral ectoderm. This was demonstrated by the ability of *rhomboid* (*star*) expressed exclusively in the midline to rescue all of the ventral ectoderm defects of *rhomboid* (*star*) mutant embryos.

The results from these two studies supported the notion that the *rhomboid* acts as a specificity factor for DER by controlling the localization of *spitz*-DER signaling.

However, these studies also extended this concept by suggesting a cell non-autonomous mechanism by which the effects of *rhomboid* might be mediated. The model put forth was that *rhomboid* modulates a processing event, occurring at the midline, which converts the transmembrane *spitz* precursor into a secreted ligand. The secreted *spitz* then diffuses into the surrounding ventral ectoderm and activates the DER signaling necessary for correct cell fate determination in this region of the developing embryo.

Results from a recent study support this model of a non-autonomous action of the midline on the patterning of neighboring ventral epidermal cells (Gabay *et al.* 1997). This paper examined the *in situ* activation pattern of DER signaling in the developing fly embryo using the monoclonal antibody dp-ERK, specific for the activated form of the *Drosophila* MAPK. A striking feature of the dp-ERK staining pattern was that it mirrored every component of the complex pattern of *rhomboid* expression in the early embryo, including both the ventral ectoderm and wing vein primordia. In later embryos, when *rhomboid* expression was confined to the midline, 3 to 4 rows of ventral ectoderm cells on either side of the midline were stained by dp-ERK. This corresponded precisely to the previously determined range of DER signaling activated by *spitz* emanating from the midline (Kim and Crews 1993, Raz and Shilo 1993). Importantly, these staining patterns were absent in embryos mutant for *rhomboid* or *spitz* or DER, thus demonstrating both a cell autonomous and non-autonomous requirement for *rhomboid* in *spitz*-DER induced activation of MAP kinase (Gabay *et al.* 1997).

This concept of spatially regulated ligand proteolysis as a means of controlling receptor mediated signaling events was discussed earlier in this chapter in the context of TACE processing of TM-TGF α . It has emerged as an important general mechanism for the regulation of a wide variety of biologically relevant ligand-receptor interactions (for reviews see Merlos-Suarez and Arribas 1999, Kiessling and Gordon 1998, Werb and Yan 1998).

Additional aspects of Rhomboid Function

As this thesis was being prepared, additional reports were published which both enhance and complicate the model of *rhomboid* action in *Drosophila* development. Until recently, most models placed the rhomboid, star and spitz proteins on the plasma membrane where rhomboid and star are hypothesized to modulate spitz processing (e.g. Fig. 1 of Perrimon and Perkins 1997). A recent paper by Pickup and Banerjee has demonstrated by immunoelectronmicroscopy that the star protein localizes to the nuclear and contiguous endoplasmic reticulum membranes but not to the plasma membrane (Pickup and Banerjee 1999). This suggests that *star*, and possibly *rhomboid* as well, might influence earlier spitz processing events which might occur in these subcellular locations. Indeed, the paper went on to demonstrate that while three major forms of endogenous spitz protein could be detected in wild-type eye discs, only the smaller two forms were detected in flies overexpressing *star* in the eye disc (Pickup and Banerjee 1999). By analogy to the processing of TM-TGF α described earlier in this chapter, this result suggests that star might enhance the post-translational removal of the glycosylated pro-domain from the spitz protein. In another experiment, overexpression of both *star* and *m-spitz* in the wing

produced a blistered wing phenotype similar to that seen in strong *rhomboid* overexpressing flies (Pickup and Banerjee 1999, Sturtevant *et al.* 1993). Together these results suggest that *star* enhancement of intracellular spitz processing may translate into increased production of the soluble ligand.

Another recent report has shown that *rhomboid* and *star* act synergistically to enhance DER signaling in wing vein development (Guichard *et al.* 1999). Only a minimal amount of ectopic vein material was present in wings of wild-type flies overexpressing *star* or in the wings of a line of flies expressing weak heat shock *rhomboid*. However, when *star* was overexpressed in the weak heat shock *rhomboid* background, large amounts of ectopic vein material were present. This paper also confirmed the previous finding that mutant alleles of *star* could strongly suppress *rhomboid* induced ectopic wing vein phenotypes. This result was extended further by demonstrating that overexpressed *rhomboid* had no ectopic vein phenotype in *star* null mitotic clones, nor could overexpressed *rhomboid* rescue the loss-of-vein phenotype in *star* null mitotic clones (Guichard *et al.* 1999). The authors interpreted these results to mean that *rhomboid* requires *star* to function.

Lastly, another recent paper (Wasserman and Freeman 1998) has attempted to clarify the discrepancy between *rhomboid* acting to generate the DER signal in a cell non-autonomous manner (i.e. in the ventral midline as described above) versus *rhomboid* functioning in the receipt of the DER signal in a cell autonomous manner. (i.e. in the dorsal follicle cell of the ovary as described earlier). Previous work had shown that

rhomboid and DER function were both required in the follicle cells but not the oocyte (Mayer and Nusslein-Volhard 1988, Ruohola-Baker *et al.* 1993, Price *et al.* 1989, Schupbach 1987) and the *gurken* ligand was only present and required in the oocyte (Neuman-Silberberg and Schupbach 1993). Therefore, it appeared that, at least in the ovary, *rhomboid* was not involved in ligand processing to generate a DER signal. Rather, it seemed that *rhomboid* was acting in a cell autonomous manner in the follicle cell in the receipt of the DER signal from *gurken* (Ruohola-Baker *et al.* 1993). Gurken was the only ligand previously reported to activate DER during oogenesis. By analyzing the eggs laid by adult females from a weak mutant *spitz* line of flies, Wasserman and Freeman were able to demonstrate the additional requirement for *spitz* ligand in normal egg development (Wasserman and Freeman 1998). Furthermore, contrary to a previous report (Mayer and Nusslein-Volhard 1988), Wasserman and Freeman were able to demonstrate that *spitz* was not required in the oocyte. Therefore they concluded that the requirement for *spitz* was in the follicle cell, the same cell where *rhomboid* and DER are required. Through genetic manipulation, the authors were able to remove *spitz* from the follicle cells. The resulting phenotype resembled that caused by a reduction of DER signaling (Schupbach 1987). However, the absence of *gurken* completely eliminated DER signaling and also rhomboid protein expression. This suggested a model in which first *gurken* signals from the oocyte to DER on the follicle cell to activate *rhomboid* expression. In turn, *rhomboid* expression in the follicle cell allows *spitz* to become a ligand on the follicle cell to further amplify DER signaling (Wasserman and Freeman 1998). Hence, the role of *rhomboid* in this model is to shift the mode of signaling from paracrine (*gurken*-DER) to autocrine (*spitz*-DER). These experiments and this model

suggested that, just as does in other tissues, *rhomboid* acts in the ovary to potentiate *spitz*-DER signaling. However, since *rhomboid*, *spitz* and DER are all present together in the follicle cell, this experimental system cannot address the issue of whether *rhomboid* acts to process the ligand or to enhance its reception by DER.

Models of Rhomboid Function

This final issue of how rhomboid potentiates *spitz*-DER signaling is crucial for the understanding of its function as a major DER specificity factor. At least three classes of models are conceivable: 1) The rhomboid protein might function in concert with star, another rhomboid molecule, or other adhesion molecules, to increase cell-cell adhesion between communicating cells. This would in turn increase the probability of *spitz*-DER interaction. While certainly plausible, this model is insufficient to explain those instances where rhomboid potentiates signaling in distant cells or when rhomboid, *spitz* and DER are all present on the same cell. 2) The rhomboid protein might increase the affinity of the *spitz*-DER interaction, increase the intrinsic tyrosine kinase activity of the DER or promote/increase the interaction of DER with downstream RAS-MAP kinase signaling components. This model would nicely explain those instances when rhomboid functions in a cell autonomous fashion in cells expressing both rhomboid and DER. However, it would not easily account for the ability of rhomboid to potentiate signaling in distant DER expressing cells. 3) The rhomboid protein may function in the proteolytic conversion of *spitz* from an inactive transmembrane ligand to an active soluble ligand. This model has been used to explain the ability of rhomboid to act in a cell non-autonomous fashion to potentiate DER signaling in non-adjacent cells. The creation of a

source of secreted ligand by rhomboid has also been invoked to explain how graded signaling levels might be achieved in settings where both the spitz and DER are ubiquitously expressed. However, this mode of action would not be optimal in those circumstances where DER signaling must be more narrowly confined.

These models are certainly not meant to be mutually exclusive, nor does it seem that any one model can adequately explain all of the intricate ways in which rhomboid seems to function as a specificity factor for DER signaling. All of these mechanisms are by definition biochemical in nature and therefore cannot be easily addressed by purely genetic experiments.

Project Goals and Thesis Organization

To address these various possible mechanisms and gain additional insight into the functions of rhomboid, a model system in which biochemical experiments could be performed was needed. In addition, it was of interest to determine whether a rhomboid-like gene existed in higher organisms and played similar roles in modulating EGFR signaling. The work presented in this thesis was predicated on the assumption that at least one human homologue of *Drosophila rhomboid* existed. Two major hypotheses, based on the above models of *rhomboid* function, guided these studies: the human rhomboid protein acts directly on EGFR or downstream signaling components to potentiate EGFR-MAP Kinase signaling, and human *rhomboid* expression potentiates EGFR signaling by modulating the processing of the TM-TGF α ligand. The experiments

presented in the following chapters were performed to test these hypotheses. Chapter 2 describes the cloning of a human homologue of *Drosophila rhomboid*. This gene was then used in the experiments described in Chapter 3 to physically characterize the human rhomboid protein. Chapter 4 describes studies that utilized mammalian cell culture systems and *in vivo* methods to elucidate the biochemical basis of *rhomboid* function.

Chapter 2

Cloning of a Human Homologue of *Drosophila rhomboid*

INTRODUCTION

All of the available information about rhomboid has been obtained through genetic studies in *Drosophila* (see Chapter 1). No biochemical data has been obtained as to the nature of the protein-protein interactions underlying *rhomboid* function. To obtain this kind of information, the cloning of a human homologue of *rhomboid* was performed so that mammalian cell culture systems could be used to explore *rhomboid* function biochemically. This chapter details the cloning of a full-length cDNA coding for a human homologue of *Drosophila rhomboid*.

MATERIALS AND METHODS

Cloning of pSK-hRho and pHRM

Dr. Hong-Zong Zhang, a postdoctoral fellow in our lab, performed database searches using the dRho sequence and identified an expressed sequence tag (GenBank Accession #D82416) from a human pancreatic islet cDNA library:

```
                                upstream -->
GTCCTGCGGGACTGGAGAAGCTGGCAGGCTGGCACCGCATAGCCATCATCTACCTGCTGA
GTGGTGTCAACCGCAACCTGGCCAGTGCCATCTTCTGCCATACCGAGCAGAGGTGGGTC
CTGCTGGCTCCCAGTTCGGCATCCTGGNCTGNCTCTTCGTGGAGCTCTTCCAGAGCTGGN
AGATCCTGGCGCGGCCCTGGCGTGCCTTCTCAAGCTGNTGGNTGTGGTGCTCTTCCTCT
TCACCTNTGGGNTGCTGCCGTGGATTGACAACTGTGCCACATCTCGGGGTTTCATCAGTG
GTCTCTTCCTCTCCTTCGTCTTCTTGCCCTACATCAGGTTTG
                                <-- downstream
```

When used as primers for PCR on primary aliquot #6 of a >4 kb human placental cDNA library in λ gt10, the underlined “upstream” and “downstream” sequences yielded the expected 305 base pair product.

This aliquot was diluted $1:5 \times 10^3$ and plated on 14 plates yielding ~ 4000 plaques/plate. The pooled plaques from each plate were screened by the same PCR, and the pool from plate #11 was positive (i.e. yielded the expected 305 base pair product). This pool was diluted $1:1 \times 10^4$ and plated on 19 plates yielding ~ 1000 plaques/plate. The pool from plate #18 was positive by PCR. This pool was diluted $1:6 \times 10^4$ and plated on 20 plates yielding ~ 300 plaques/plate. The pools from plates #1, #7, #9, #12, #13 and #17 were positive by PCR. Pool #12 was chosen, diluted $1:3 \times 10^5$ and plated on 14 plates yielding ~ 75 plaques/plate. The pool from plate #3 was positive by PCR.

At this point, the pool (#6-#11-#18-#12-#3) was tested with an antisense version of the “upstream” primer and the “ λ gt10 forward” primer 5’-ctttgagcaagttcagcctggtaag-3’ and yielded a ~ 1 kb PCR product. It was also tested with a sense version of the “downstream” primer and the “ λ gt10 reverse” primer 5’-gaggtggcttatgagtatttctccaggta-3’ and yielded a ~ 0.5 kb product. The combination of antisense “upstream” and “ λ gt10 reverse” primers yielded no product nor did the combination of sense “downstream” and “ λ gt10 forward.” This analysis indicated that the insert was in the forward orientation with respect to the λ gt10 vector backbone and that the predicted total cDNA insert size was ~ 1.8 kb (1 kb + 0.5 kb + 0.3 kb of EST sequence).

The pool was diluted $1:2 \times 10^4$ and plated on a single plate yielding 110 plaques. 18 single plaques were picked and screened by PCR with the “upstream” and “downstream” primers. #16 was positive and λ DNA was prepared from this phage clone. The cDNA insert was released by Eco RI digestion and gel purified. The fragment was then ligated

into the Eco RI site of pBluescript-SK (Stratagene) to generate pSK-hRho. DNA sequencing was performed on this plasmid.

A C-terminal Myc tag was then added to the hRho coding region by subcloning into pRK5M (generously provided by Xin-Hua Feng). The primers “up-hRho”: 5’-ttcagaattctgggcatgggtgggacggct-3’ and “down-hRho”: 5’-ctcagtgtcgacgtggagctgagcgtccagttc-3’ were used to PCR hRho out of pSK-hRho without its stop codon. The Eco RI site in “up-hRho” and the Sal I site in “down-hRho” are underlined. The PCR product and pRK5M were both digested with these two enzymes, gel purified and ligated to form pHRM.

Generation of pHRF

The Eco RI-Sal I fragment from pHRM was gel purified using GeneClean (Bio 101) and ligated into the pRK5F vector (a gift from Xin-Hua Feng) which was sequentially digested with Sal I and Eco RI, dephosphorylated with CIP (Boehringer) and gel purified. Ligation reactions were performed at room temperature for 3 hrs using high concentration T4 DNA ligase (Gibco/BRL).

Generation of pHRF-short

The “short hRho” primer 5’-gcggaattctagaacaat**gcgccaggacccgcaggtgc**-3’ and the “hRho 3” primer 5’-ttcggaggagggtcatcacac-3’ were designed to amplify a 264 base pair DNA fragment stretching from the final in frame ATG to just beyond the unique Bam HI site of the original hRho cDNA sequence. The Eco RI site engineered onto the 5’ end is underlined in the “short hRho” sequence and the initiation codon is shown in bold. PCR

was performed on an MJ Research PTC-200 DNA Engine using Pfu polymerase (Stratagene) and 10 ng of the pSK-hRho as the target. The program used was one cycle at 95 C for 5 minutes followed by 30 cycles of 95 C for 5 minutes 60 C for 30 seconds 72 C for 2 minutes, followed by one cycle at 72 C for 10 minutes and a 4 C hold. 4 duplicate 50 ul reactions were run and pooled. The 264 base pair fragment was gel purified, digested with Eco RI and Bam HI, and cleaned up using a Qiaquick column (Qiagen). This fragment was ligated into pHRF which had been digested with Eco RI and Bam HI and gel purified. Ligation reactions were performed at 16 C overnight using high concentration T4 DNA ligase (Gibco/BRL).

Generation of pHRF-long

The “large hRho” primer: 5’-gcggaattctagaacaat**gccggctccctccagg**-3’ was designed based on the genomic sequence (GenBank accession #Z69719) surrounding a newly identified putative start site (in bold) and included an Eco RI site to assist in cloning (underlined).

This primer, when used in conjunction with the “rho 259R” primer:

5’-catgtcctcgatctggcgcttgac-3’, was designed to amplify a 275 base pair product stretching from the newly identified putative start site to a site 72 base pairs downstream of the first ATG in the original cDNA obtained from the library.

The target human genomic DNA was generated from a near confluent 100 mm plate of HeLa cells as follows: The cells were washed once with PBS and then removed from the plate with 0.05% trypsin and pelleted. The pellet was washed once with ice cold PBS-CMF, resuspended in 4 ml of ice cold PBS and aliquoted into 4 equal portions in eppendorf tubes. The cells were repelleted in the eppendorf tubes and each pellet was

resuspended in 17 ul of digestion buffer (50 mM Tris pH 8, 20 mM NaCl, 1 mM EDTA, 1% SDS). 3 ul of proteinase K stock (14 mg/ml, Gibco/BRL) was added to each tube, and the tubes were incubated at 55 C for several hours until the pellets were completely digested. 500 ul of H₂O was added to each tube and the tubes were boiled for 5-10 minutes to inactivate the proteinase K. The genomic DNA was then extracted with phenol/chloroform and EtOH precipitated. Following a 70% EtOH wash, each DNA aliquot was resuspended in 25 ul of T.E. and stored at 4 C.

PCR amplification using “large rho” and “rho 259R” was performed as indicated for the generation of pHRF-short using 2 ul (~60 ng) of the HeLa genomic DNA prep per reaction. 4 duplicate 50 ul reactions were run and pooled. The 275 base pair product was gel purified and used in a subsequent round of PCR.

A second round of PCR was used to add the newly obtained sequence to the original cDNA sequence. The last 110 base pairs of the 275 base pair product amplified from HeLa genomic DNA overlapped the original cDNA sequence in pSK-hRho and this allowed for easy joining of these two target DNAs using the “large hRho” primer:

5’-gcggaattctagaacaatgccggctccctccagg-3’ and “rho sal 3” primer:

5’-ctcagtgctcgacgtggagctgagcgtccagttc-3’. PCR was performed as indicated for the generation of pHRF except that the 72 C extension time was increased from 2 minutes to 4 minutes to allow sufficient time for the amplification of the larger product by the Pfu polymerase. 5 identical 50 ul reactions were run and pooled. The pool was cleaned up using a Qiaquick column (Qiagen), digested sequentially with Sal I and Eco RI and gel

purified. The purified fragment was ligated into pRK5F which was sequentially digested with Sal I and Eco RI, dephosphorylated with CIP (Boehringer) and gel purified. Ligation reactions were performed at 16 C overnight using high concentration T4 DNA ligase (Gibco/BRL).

***In vitro* transcription/translation**

Coupled *in vitro* transcription/translation reactions were carried out using a TnT SP6 kit (Promega). 1 ug of plasmid DNA was used per 50 ul reaction prepared according to the manufacturer's instructions. Reactions were performed at 30 C for 2 hours. 5 – 10 ul of each reaction was run on SDS-PAGE. The gel was fixed 1 hour in 20% MeOH + 10% HAc, soaked in Amplify (Amersham) for 30 minutes, dried and exposed to autoradiography film (BioMax MR).

Cell culture and transfection

COS-1 and HEK-293 cells were maintained in DME-H16 3g/L glucose (UCSF Cell Culture Facility) supplemented with 10% fetal bovine serum (Hyclone), 100 U/ml penicillin and 100 ug/ml streptomycin at 37 C, 5% CO₂. Cells were transiently transfected in 100 mm dishes using Lipofectamine (Gibco/BRL) according to the manufacturer's instructions.

Immunofluorescent staining

Transiently transfected COS-1 cells were seeded onto multi-chamber slides and allowed to reattach overnight. The cells were rinsed with PBS, fixed for 5 minutes with cold (-20 C) methanol, rinsed again with PBS and then blocked overnight at 4 C in PBS + 3% Bovine Serum Albumin (BSA, Sigma). The cells were then incubated in a 1:500 dilution of anti-Flag M2 (Kodak IBI) in PBS + 2% horse serum (Vector Labs) for 1 hour at 37 C. The cells were washed 3 x 5 minutes with PBS + 3% BSA and then incubated in a 1:200 dilution of Texas red conjugated goat anti-mouse IgG (Jackson ImmunoResearch) in PBS + 2% horse serum for 45 minutes at room temperature. Again the cells were washed 3 x 5 minutes in PBS + 3% BSA followed by a final wash in PBS before mounting. The stained cells were visualized on a Zeiss Axioplan Universal microscope equipped with a short arc mercury lamp and standard filters for immunofluorescence.

Preparation of cell lysates and immunoprecipitation

At ~48 hours following transfection, cells were washed once with PBS and then lysed in 1 ml/100 mm plate of Myc lysis buffer (20 mM Tris pH 8, 137 mM NaCl, 1% NP-40, 2 ug/ml pepstatin A, 4 ug/ml aprotinin, 10 ug/ml leupeptin, 1 mM PMSF) or Flag lysis buffer (25 mM Tris pH 7.5, 300 mM NaCl, 1% Triton X-100, 2 ug/ml pepstatin A, 4 ug/ml aprotinin, 10 ug/ml leupeptin, 1 mM PMSF) at 4 C for 20 minutes on a rotating platform. Each plate was then scraped and the cell lysate and debris was passed twice through a 25 gauge needle and deposited into an eppendorf tube on ice. The lysates were clarified by centrifugation at 14,000 RPM 4 C for 25 minutes and the supernatants transferred to fresh tubes on ice. Per 500 ul of clarified lysate 2 ul of anti-Myc antibody

(Clone 9E10, generously provided by J.M. Bishop, UCSF) or 2 ul anti-Flag antibody (Clone M2, Kodak IBI) were added and the tubes were rotated at 4 C for 1 hour. 30 ul of PAM (protein A sepharose (Sigma) to which rabbit anti-mouse IgG (Jackson ImmunoResearch) had been previously coupled) was added to each tube and they were rotated at 4 C for an additional 1 hour.

SDS-PAGE and Western Blotting

Immunoprecipitates were washed 3 times in either Myc or Flag lysis buffer, resuspended in 30 ul of the same plus 10 ul of 4X SDS loading dye containing β -ME, and proteins were resolved on either 8% or 10% SDS-PAGE minigels using a BioRad minigel apparatus. Proteins were transferred to PVDF membranes (Immobilon P, Millipore) using a BioRad minitransfer apparatus. The membranes were typically blocked overnight at 4 C in TBST (tris buffered saline + 0.05% Tween-20) + 5% nonfat dry milk.

Following a brief rinse in TBST, the blots were incubated for 2 hours at room temperature in either Myc or Flag primary antibody at a 1:1000 dilution in TBST. The blots were washed with several changes of TBST for ~30 minutes and then incubated for 1 hour at room temperature in horseradish peroxidase conjugated goat anti-mouse secondary antibody (BioRad) at a 1:5000 dilution in TBST + 5% nonfat dry milk.

Following several washes with TBST, the blots were developed with ECL (Amersham) and exposed to film (Kodak BioMax MR).

Protein sequence analysis and structural predictions

Molecular weight prediction and high cysteine content were determined using the SAPS (Statistical Analysis of Protein Sequences, Brendel *et al.* 1992) software which was

accessed through the ISREC homepage on the internet (<http://www.isrec.isb-sib.ch/software/software.html>)

Transmembrane domain prediction was performed using the program TM-Pred (Hofmann and Stoffel 1993) which was accessed through the ISREC homepage.

Alternative predictions were also obtained using the program SOSUI available on the internet (http://www.tuat.ac.jp/~mitaku/adv_sosui/).

Protein sequence comparison for identity/similarity and multiple sequence alignments were performed using the GCG programs GAP and PILEUP, respectively (University of Wisconsin Genetics Computing Group). Both programs were available through the Socrates server at UCSF and were run using a gap penalty = 2 and the default values for all other parameters. The PILEUP output was displayed by copying its output (in .msf format) into the BOXSHADE program available on the internet through the ISREC homepage.

PEST domain prediction was performed using the PESTfind program (Rogers *et al.* 1986) available at the Genetic Data Environment WWW Server at IMB-Jena (<http://genome.imb-jena.de/cgi-bin/GDEWWW/menu.cgi>). The minimum number of amino acids positive between flanks was set to 5.

Additional features of the protein were determined by using the ScanProsite program to scan the protein against the Prosite database. This program was available through the ExPASy molecular biology server home page (<http://www.expasy.ch/>).

RESULTS

Cloning of a human homologue of *Drosophila rhomboid*

To clone a homologue of *Drosophila rhomboid* from a human cDNA library, Dr. Hong-Zong Zhang made several attempts to design degenerate PCR primers using short stretches of amino acids that appeared to be conserved in *Drosophila rhomboid* (hereafter referred to as “dRho”) and apparent *C. elegans* homologues of dRho. None of these attempts were successful. Eventually Dr. Zhang designed PCR primers based on an expressed sequence tag from a human pancreatic islet cDNA library (GenBank accession #D82416) found in an EST database search for sequences homologous to dRho. This primer pair successfully amplified the expected sized product from a human placental cDNA library. The library was then diluted and pools of plaques were screened by PCR using this primer pair. Positive pools were further diluted and screened until eventually a single positive plaque was identified.

DNA sequencing and subsequent alignment of the deduced amino acid sequence with that of dRho confirmed that the isolated sequence was in fact a homologue of dRho. The alignment may not have been optimal since the translation initiation site remained ambiguous. There were three in frame putative start sites, and no in frame stop codon was present in the small amount of sequence preceding the first ATG of the isolated cDNA. The insert was subcloned from the vector used for sequencing into pRK5M, a mammalian expression vector with a C-terminal Myc epitope tag, to generate the plasmid pHRM (for a diagram of the hRho constructs discussed in this chapter, see Figure 2.1).

Expression of pHRM in mammalian cells

The pHRM plasmid containing the hRho cDNA was transiently transfected into COS-1 cells. As a positive control, the plasmid pTGF α -myc was transfected in parallel. Cell lysates were subjected to myc IP-western analysis. While the TGF α -myc protein was easily detected, no specific hRho-myc protein was detected (Figure 2.2).

Generation of pHRF and expression *in vitro*

Since it was possible that the myc epitope was buried in the protein or otherwise inaccessible to the antibody, a different epitope tag was tried. The hRho cDNA was subcloned out of pHRM and into pRK5F, a mammalian expression vector with a C-terminal FLAG epitope tag, to generate the plasmid pHRF (Figure 2.1).

Before using pHRF in mammalian transfection experiments, the plasmid was first tested in a coupled *in vitro* transcription/translation reaction. As a positive control the pTACE-FLAG plasmid was used in a separate reaction. 90% of each reaction was then subjected to FLAG immunoprecipitation. The precipitated protein was then subjected to SDS-PAGE along with the remaining 10% of each reaction. As shown in Figure 2.3, the pHRF reaction produced a strong doublet that migrated at an apparent MW of ~50 kD, and this doublet could be immunoprecipitated with FLAG antibody.

Expression of pHRF in mammalian cells

It appeared that the pHRF plasmid generated a protein of the appropriate size *in vitro*, and the ability to immunoprecipitate the protein with an anti-Flag antibody verified the presence of a functional in frame C-terminal epitope tag. To see if the protein could be synthesized *in vivo*, the pHRF plasmid was then transiently transfected into HEK-293 cells. As a positive control, the TACE-Flag plasmid was transfected. Lysates were then subjected to Flag IP-western analysis. While the TACE-Flag protein was easily detected, no specific hRho-Flag protein was detected (Figure 2.4).

To determine if Flag tagged hRho protein could be detected in transiently transfected cells *prior to cell lysis*, COS-1 cells were transfected with pHRF. As a positive control p59-Flag was transfected. The cells were fixed and immunostained using anti-Flag antibody along with a Texas Red conjugated secondary antibody. Immunofluorescence microscopy (not shown) demonstrated that while p59-Flag could be easily detected, hRho-Flag was not detected.

Generation of pHRF-short

One reason for the inability to detect hRho-Flag might have been that one of the downstream in frame methionines represented the actual start site and that the upstream methionines were acting to suppress translation initiation from a downstream site. To determine if this was the case, PCR was used to generate a shorter version of hRho that initiated at the third in frame methionine. The PCR product was cloned into pRK5F to generate pHRF-short (Figure 2.1).

Expression of pHRF-short in mammalian cells

The pHRF-short plasmid was transiently transfected into HEK-293 cells. As a positive control, the TACE-Flag plasmid was transfected. Lysates were then subjected to Flag IP-western analysis. While the TACE-Flag protein was easily detected, no specific hRho short-Flag protein was detected (Figure 2.5).

To determine if Flag tagged short hRho protein could be detected in transiently transfected cells *prior to cell lysis*, COS-1 cells were transfected with pHRF-short. As a positive control, p59-Flag was transfected. The cells were fixed and immunostained using Flag antibody along with a Texas Red conjugated secondary antibody.

Immunofluorescence microscopy (not shown) demonstrated that while p59-FLAG could be easily detected, hRho short-Flag was not detected.

Generation of pHRF-long

A remaining possibility was that the hRho cDNA clone obtained from the library was incomplete at its 5' end and that the initiation codon was present in upstream sequence not represented in the cDNA library. Fortuitously, a continuous stretch of genomic sequence was found in the GenBank database (accession #Z69719) in which the coding region represented in the hRho cDNA obtained from the library was located. Close inspection of the genomic sequence upstream from the most 5' ATG of the original cDNA clone revealed yet another in frame (assuming no intervening exons) ATG with an in frame stop codon immediately preceding it and a recognizable TATA box further upstream. This was therefore the most likely translational start site. Using the genomic

sequence, PCR primers were designed to amplify the sequence between the newly discovered start site and the 5' most start site in the cDNA clone. The sequence was amplified from a preparation of HeLa cell genomic DNA and then an additional round of PCR was used to add this sequence to the existing cDNA. This addition resulted in an additional 186 bp that coded for an additional 62 amino acids at the N-terminus of the protein. The PCR product was cloned into pRK5F to generate pHRF-long (Figure 2.1). Figure 2.6 shows the sizes of the three different clones: pHRF-short, pHRF, and pHRF-long.

Expression of the three pHRF clones *in vitro*

The plasmids pHRF-short pHRF and pHRF-long were each tested in a coupled *in vitro* transcription/translation reaction. As a positive control the pTACE-Flag plasmid was used in a separate reaction. 10% of each reaction was then subjected to SDS-PAGE. As shown in Figure 2.7, the pHRF-short reaction produced a strong doublet which migrated at apparent MW of ~47 kD and the pHRF reaction produced a strong triplet at ~55 kD. The pHRF-long reaction resulted in a weaker, but still prominent, single band which migrated at ~55 kD.

Expression of pHRF-long in mammalian cells

The pHRF-long plasmid was transiently transfected into HEK-293 cells. As a positive control, the TACE-Flag plasmid was transfected. Lysates were then subjected to Flag IP-western analysis. The hRho long-Flag protein was detected as a band running just above the heavy chain IgG band at an apparent MW of ~60 kD. In addition, a band running at

~47 kD was detected as well as a high MW band near the top of the gel (Figure 2.8). None of these bands was present in the lysate from cells transfected with the pRK5F vector nor in the lysate from cells transfected with TACE-Flag.

Sequence analysis and predicted features of hRho

The cDNA and deduced amino acid sequence of hRho is shown in Figure 2.9. The hRho protein contains 543 amino acid residues has a calculated MW ~62 Kd. Like dRho and Star there is no signal sequence present at the N-terminus, despite the fact that they are all predicted to be transmembrane proteins. The program TM-Pred suggests that hRho has a total of seven putative transmembrane spans (Figure 2.10), similar to dRho. However, the spacing between the first and second transmembrane domains of hRho is significantly larger than in dRho. The spacing between the remaining six is similar.

A comparison of the protein sequences of dRho and hRho was performed using the GAP program (University of Wisconsin Genetics Computing Group) with a minimal gap penalty and with the alignment of amino acid 167 of hRho with the first residue of dRho. Using these parameters, hRho was found to be 36% identical and 45% similar to dRho. An alignment of the hRho amino acid sequence with that of dRho, cRho1 and cRho2 (two apparent *C. elegans* homologues) and rrp (another human homologue, see Discussion) is shown in Figure 2.11. The similarity among the proteins is particularly apparent within the predicted transmembrane regions. HRho, rrp and cRho1 all have longer N-termini than dRho.

Another similarity between hRho and dRho is the presence of a strong PEST sequence from residue 241 to 252 in the hRho sequence (PESTFind score = 12.1). Additional features of the hRho protein include two potential N-glycosylation sites at residues 69 and 27, a potential tyrosine phosphorylation site between residues 133-141, several potential protein kinase C and casein kinase II phosphorylation sites and several possible N-myristoylation sites. The protein is also above the 95th percentile in cysteine content (4.6%). There are no other identifiable protein domains that give clues as to the function of hRho.

The hRho gene most likely resides in the subtelomeric region on the short arm of human chromosome 16. A laboratory sequencing near the alpha globin locus control region on this chromosome, isolated a partial cDNA which is identical to that which codes for amino acids 278– 357 of the full length hRho (Kielman *et al.* 1993). Since residue 278 is methionine, this group believed they had the 5' end of a gene and deposited into the GenBank database (accession #M99624) as “human EGF receptor- related gene, 5' end.” The basis for this designation is unclear although comparison of this partial sequence with the human EGFR sequence revealed a possible alignment with a stretch of EGFR containing its transmembrane domain and some adjacent cytoplasmic sequence (not shown).

DISCUSSION

The goal of the work described in this chapter was to clone and express a full-length cDNA that coded for a human homologue of dRho. The strategy that proved successful was PCR from a human placental cDNA library. This resulted in the generation of the plasmid pSK-hRho whose insert (later determined to be a partial cDNA for hRho) was sequenced. The alignment of the deduced amino acid sequence for the partial hRho cDNA with the amino acid sequence of dRho showed the two sequences to be 36% identical and 45% similar. While these percentages were not remarkably high, there was similarity throughout the entire length of the protein. The alignment may not have been optimal since, at that point in the cloning process, the translation initiation site remained ambiguous. There were three in frame putative start sites, and no in frame stop codon was present in the small amount of sequence preceding the first ATG of the isolated cDNA. In addition, the hRho protein shared some important structural features (discussed below) with dRho. The evidence therefore supported the conclusion that the gene which was isolated was indeed a homologue of dRho. The insert from pSK-hRho was subcloned to generate pHRM which was subsequently subcloned to generate pHRF.

Despite the fact that pHRF could be transcribed/translated into protein *in vitro*, immunofluorescence demonstrated that cells fail to synthesize the protein *in vivo*. This explains why the IP-western analysis was unsuccessful: no protein was made and therefore none was detected. That the plasmid could be transcribed/translated *in vitro* was not surprising since in this artificial system, unlike in a cell, controls on translation initiation are quite relaxed. Translation can initiate from the first methionine in the

sequence regardless of whether it is the actual start codon of the protein. Recall that the original hRho cDNA clone contained three potential in frame start codons and it remained ambiguous as to whether the 5'most ATG represented the actual start site of the protein. The appearance of multiple bands suggested that more than one of these sites might be used *in vitro*, while inside the cell, stricter control of the translational machinery might prevent any of these putative sites from being utilized.

One formal possibility was that one of the downstream in frame methionines represented the actual start site and that the upstream methionines were acting to suppress translation initiation from a downstream site. This possibility was addressed by generating pHRF-short, a plasmid coding for a protein that initiated at the most downstream in frame methionine. The appearance of multiple forms *in vitro*, the inability to detect the protein by IP-western analysis of lysates from transfected cells, and the inability to detect the protein by immunofluorescence in cells prior to lysis all demonstrated that pHRF-short did not represent the full length hRho cDNA.

Quite often cDNA libraries are generated by oligo-dT primed reverse transcription from mRNA from the tissue or organ of interest. Thus synthesis of a given cDNA starts at its 3' end. As a result of limitations in the efficiency of the *in vitro* reverse transcription reaction, such libraries often contain partial cDNAs which are incomplete at their 5' ends. Given these facts and the cumulative experimental evidence, it seemed most likely that clone obtained was a partial cDNA clone and that the actual start site lay in sequence

further upstream which was not represented in the cDNA library from which the clone was obtained.

This hypothesis was testable due to the fortuitous discovery of genomic sequence in the GenBank database containing the coding regions represented in the hRho cDNA obtained from the library. The genomic sequence revealed an additional in frame initiation codon with an in frame stop codon immediately preceding it and a recognizable TATA box further upstream. This was therefore the most likely translational start site despite the fact that the surrounding sequence did not conform to a canonical consensus sequence (Kozak 1987).

PCR amplification of this additional 5' sequence from HeLa cell genomic DNA resulted in the addition of 186 base pairs to the cDNA sequence which translated into an additional 62 amino acids at the N-terminus of the putative hRho protein. This new start site was proven correct experimentally, since only pHRF-long produced a single band in an *in vitro* transcription/translation reaction and also resulted in a protein detectable in lysates from transiently transfected cells. Thus, pHRF-long contained the full-length hRho cDNA sequence.

An analysis of the protein sequence was performed using various software programs available on the internet. Interestingly hRho, like dRho and star, has no recognizable signal sequence despite the fact that they are all predicted to be transmembrane proteins. Therefore, the first hydrophobic alpha helix of the protein likely serves as a stop transfer

sequence during translocation of the protein across the membrane of the endoplasmic reticulum, and the N-terminus is predicted to be cytoplasmically oriented (Spiess and Lodish 1986). However, as will be discussed in greater detail in Chapter 3, the topology of the hRho protein in the membrane is not at all certain.

Transmembrane prediction programs predicted anywhere from 4 to 7 transmembrane domains for dRho. Similarly, the TM-Pred program predicted 7 transmembrane domains for hRho while the SOSUI program predicted 6. These differences are likely due to differences in the algorithms used and the default parameters that dictate how likely a hydrophobic stretch is to be an actual transmembrane domain.

The most profound feature of hRho is the presence of a large loop between the first and second putative transmembrane domains. This distinguishes it from dRho and the other homologues. While the significance of this is not clear, it is tempting to speculate that if hRho exists on the plasma membrane, the loop could serve as a receptor domain for an as yet undiscovered ligand. Alternatively this loop might mediate interactions between hRho and other proteins which are either membrane associated or in the cytoplasm. Another possibility is that the loop mediates homomeric interaction of more than one hRho molecule or heteromeric interactions with related family members either in the same cell or at cell-cell junctions (again assuming that some hRho exists on the plasma membrane).

Another significant similarity between hRho and dRho is the prediction of a putative PEST domain. PEST domains are proline, glutamic acid, serine and threonine rich

sequences that are thought to target proteins for rapid destruction by the cellular proteolytic machinery (Rechsteiner and Rogers 1996, Rogers *et al.* 1986). The PESTfind program is a software program developed to predict the presence of PEST domains in protein sequences. The algorithm produces a score from -50 to +50. By definition, a score above 0 denotes a possible PEST region and a value above +5 is quite likely to be an actual PEST domain. The PEST domain of the hRho protein scored a +12.1.

Studies of dRho have indicated that the protein turns over rapidly (as does the mRNA) (Sturtevant *et al.* 1996). There is also some evidence that the dRho protein is recycled from the plasma membrane, since it appears to be stabilized on the membrane in Shibire mutant flies which have a defect in dynamin mediated vesicle endocytosis (Sturtevant *et al.* 1996). Hence by analogy, the PEST domain may represent a means by which the levels of hRho are regulated, and by which any signal or process requiring hRho activity is terminated.

As indicated previously, the hRho amino acid sequence is 36% identical and 45% similar to dRho. While the level of identity is not particularly impressive, the identity and similarity exist throughout the entire length of the protein and are strongest in the predicted transmembrane domains of the proteins. Also, the similarity of structural features such as a lack of signal sequence, 7 predicted TM domains, and a PEST domain suggest that hRho is indeed a homologue of dRho. Of course this does not rule out the possibility that other, more similar homologues exist. In fact, while the work described in this thesis was in progress, a group reported the cloning of another human homologue

of dRho which they named rhomboid related protein, or rrp (Pascall and Brown 1998). The fact that another human homologue exists is not surprising given that two homologues were identified in *C. elegans* and also that redundancy tends to increase with the complexity of the organism. Rrp is a protein of 438 amino acids. Like hRho and dRho, it contains no signal sequence and is predicted to contain 7 transmembrane domains with an intracellular N-terminus. Pascall and Brown reported 30% identity and 56% similarity to dRho, although with the minimal gap penalty used here to characterize hRho, these numbers would be significantly higher. This would make rrp more similar to dRho than hRho is. This is evident in Figure 2.11, which shows the alignment of all known rho sequences. The PILEUP alignment algorithm automatically puts the most similar sequences toward the top of the alignment, and rrp appears immediately below dRho. The only other data available about rrp is that in a survey of expression levels in human tissues (multiple tissue Northern blot), the highest levels were seen in brain and kidney and weaker signals were detected in heart, skeletal muscle and pancreas (see Fig. 3 Pascall and Brown 1998). Interestingly, the group reported what they believed to be cross-hybridization of their probe to larger species than would be predicted by their sequence. The authors suggested that this might be due to the expression of a related gene(s) in the tissues tested. It is tempting to speculate that their probe was cross hybridizing to hRho, especially since the gene for hRho is larger than rrp.

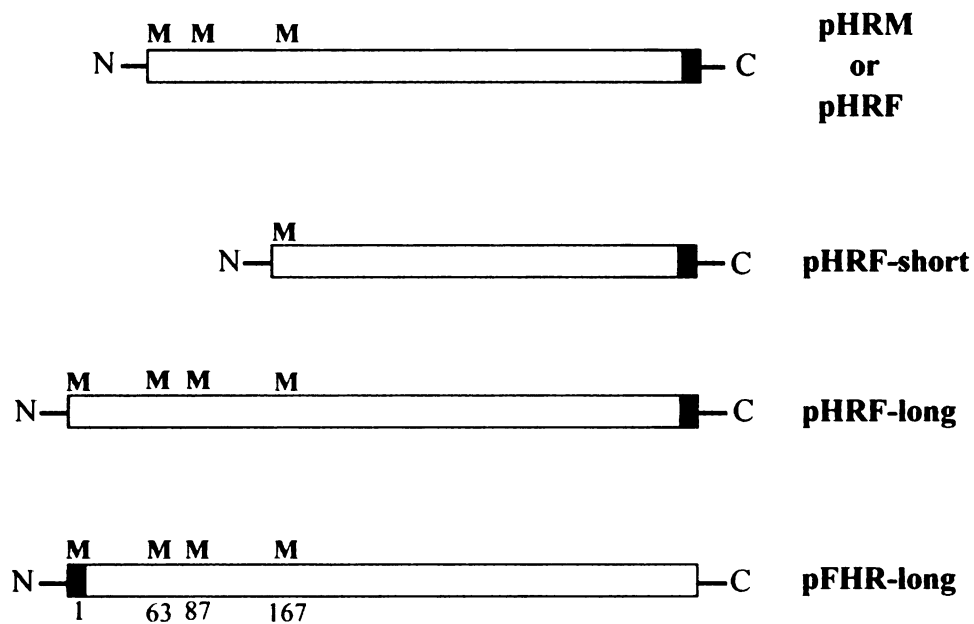


Figure 2.1 Schematic diagrams of the various hRho constructs mentioned in the text. The multiple in frame methionines are indicated by **M** both in this figure and in the amino acid sequence of full length hRho in Figure 2.9. The shaded box represents the location of the epitope tag. The nomenclature used is as follows: HR = hRho, M = myc epitope tag, F = flag epitope tag, short = construct initiating from the most C-terminal in frame methionine, long = construct initiating from the most N-terminal in frame methionine.

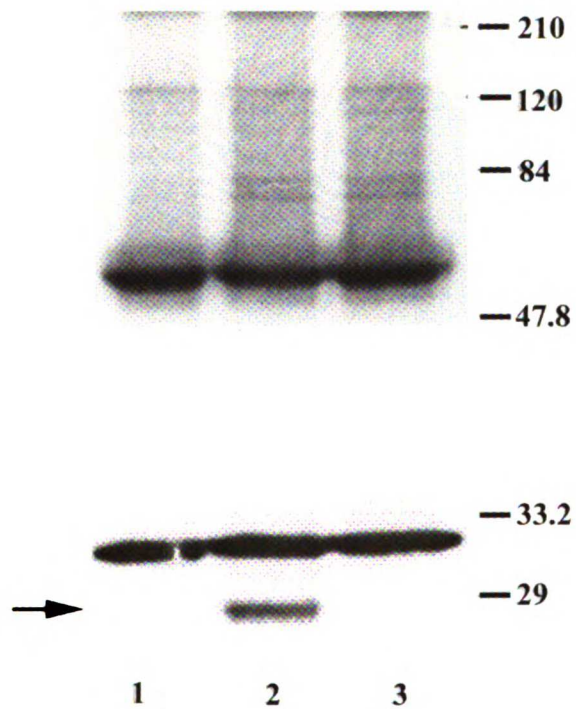


Figure 2.2 Myc IP-western analysis of lysates from COS-1 cells transiently transfected with vector (lane 1), TGFalpha-myc (lane 2) or pHRM (lane 3). The TGFalpha band is indicated by the arrow. hrho is not expressed.

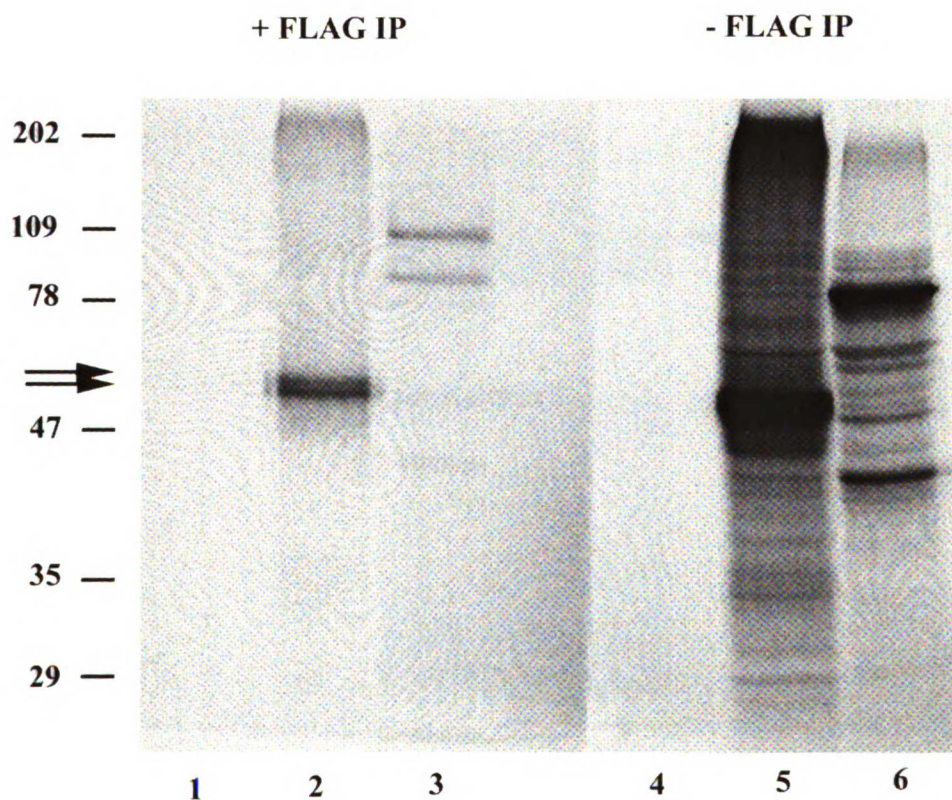


Figure 2.3 In vitro transcription/translation of no DNA (lanes 1,4), pHRF (lanes 2,5) and pTACE-F (lanes 3,6). Lanes 1-3 are FLAG IPs from 90% of the reaction. Lanes 4-6 are the remaining 10% of the reaction not subjected to FLAG IP. The hrho doublet is indicated by the double arrows.

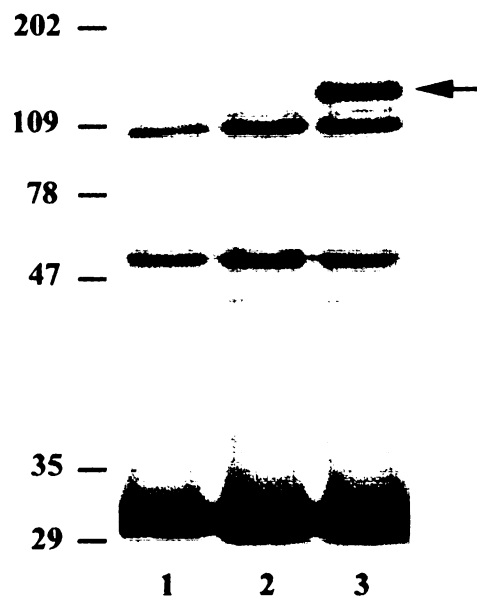


Figure 2.4 Flag IP-western analysis of lysates from HEK-293 cells transiently transfected with vector (lane 1), pHRF (lane 2) or pTACE-F (lane 3). The TACE band is indicated by the arrow. hrho is not expressed.

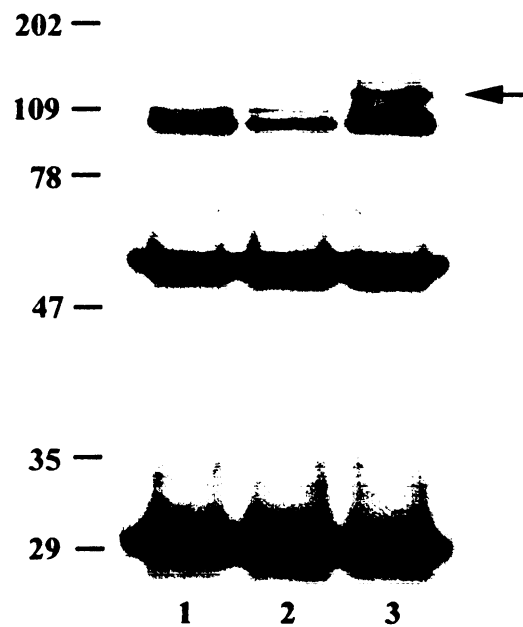


Figure 2.5 Flag IP-western analysis of lysates from HEK-293 cells transiently transfected with vector (lane 1), pHRF-short (lane 2) or pTACE-F (lane 3). The TACE band is indicated by the arrow. hrho short is not expressed.

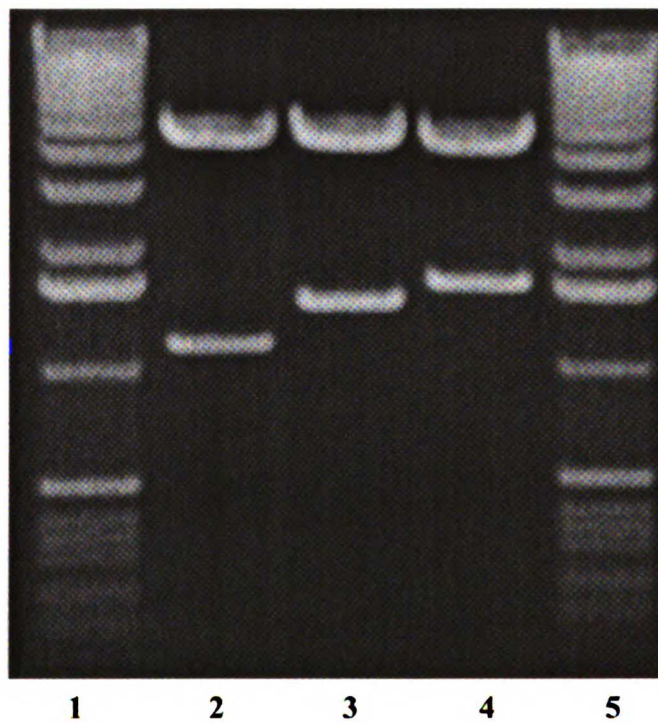


Figure 2.6 Agarose gel showing the sizes of the various hrho constructs. Lanes 1,5: 1 kb ladder, Lane 2: pHRF-short, Lane3: pHRF, Lane 4: pHRF-long. In each lane, the upper band is the pRK5F vector and the lower band is the insert released by an Eco RI and Sal I double digest.

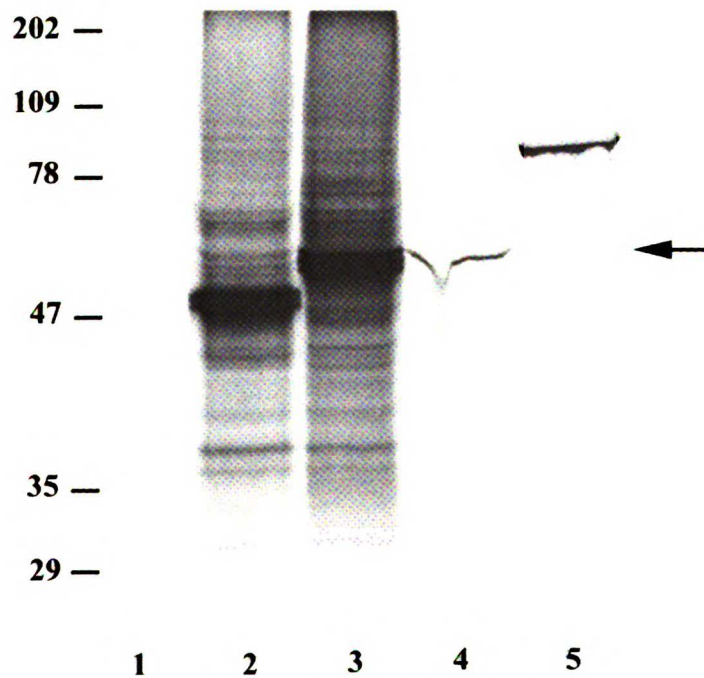


Figure 2.7 In vitro transcription/translation reactions showing the products formed from the various hrho plasmids: no DNA (lane 1), pHRF-short (lane 2) pHRF (lane 3), pHRF-long (lane 4) and pTACE-F (lane 5). pHRF-short and pHRF resulted in multiple forms. The single form produced by pHRF-long is indicated by the arrow.

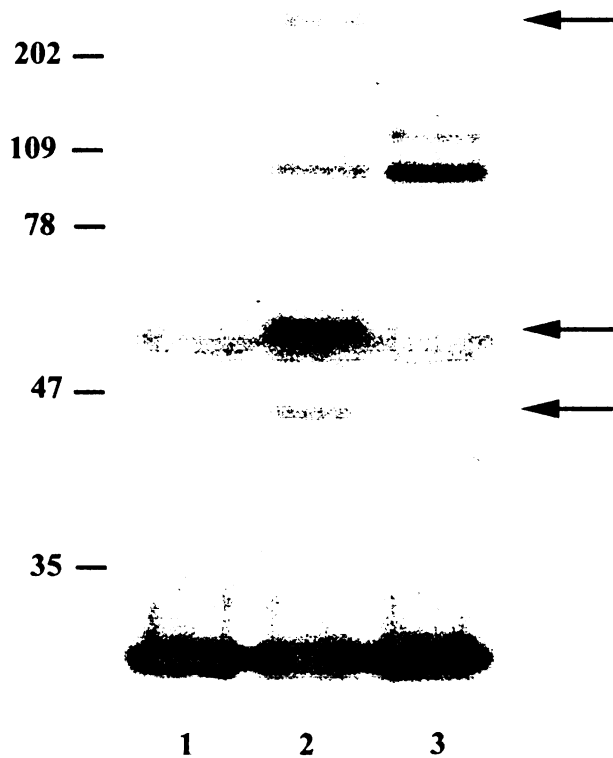


Figure 2.8 Flag IP-western analysis of lysates from HEK-293 cells transiently transfected with vector (lane 1), pHRF-long (lane 2) or pTACE-F (lane 3). The various species of hrho long are indicated by arrows. The high MW species most likely represents incompletely reduced aggregates of hrho long. The ~47 kd band might represent a degradation product of hrho long which retains the C-terminal epitope tag. The ~55 kd size of the species just above the heavy chain IgG most closely matches the MW predicted from the deduced amino acid sequence of hrho long.

aggTGAatgccggctccctccaggcccttgagcgaggctggcgggaagcagaaggagggc
M P A P S R P L E R G W R K Q K E G 18
 gccgcagccccgcagcccaaggtgcggtccgcacaggaggtggtgagcaccgccccggc
 A A A P Q P K V R L R Q E V V S T A G P 38
 cgacggggccagcgtatcgcggtgccggtgcgcaagctcttcgccgggagaagcggccg
 R R G Q R I A V P V R K L F A R E K R P 58
 tatgggctgggcatgggtgggacggctaccaaccgcacctaccgcaagcgcacgcagc
 Y G L G **M** V G R L T N R T Y R K R I D S 78
 ttcgtcaagcggcagatcgaggacatggacgaccacagcccttcttcacctactggctt
 F V K R Q I E D **M** D D H R P F F T Y W L 98
 accttcgtgcactcgctcgtcaccatcctagccgtgtgcatctatggcatcgccccgtg
T F V H S L G V T I L A V C I Y G I A P V 118
 ggctctcgcagcatgacgggtggactcgggtgctgcggaaccgccccgggtctacgagaac
G F S Q H E T V D S V L R N R G V Y E N 138
 gtcaagtacgtgcagcaggagaacttctggatcggggccagctcggaggccctcatccac
 V K Y V Q Q E N F W I G P S S E A L I H 158
 ctggggcccaagtttccgccctgcatgcgccaggaccgcaggtgcacagcttcattcgc
 L G A K F S P C **M** R Q D P Q V H S F I R 178
 tcggcgcgcgagcgcgagaagcactccgcctgctgcgtgcgcaacgacaggtcgggtgc
 S A R E R E K H S A C C V R N D R S G C 198
 gtgcagacctcggaggaggagtgtcgtccacgctggcagtggtggaagtggcccatc
 V Q T S E E E C S S T L A V W V K W P I 218
 catcccagcggccccagagcttgcgggccacaagagacagtttggtctgtctgccaccag
 H P S A P E L A G H K R Q F G S V C H Q 238
 gatcccagggtgtgatgagccctcctcgaagacctcatgagtggccagaaagacatc
 D **P R V C D E P S S E D P H E W P E D I** 258
 accaagtggccgatctgcacaaaaacagcgtgggaaccaccaaaccatccccacatg
 T K W P I C T K N S A G N H T N H P H M 278
 gactgtgtcatcacaggacggccctgtgcatggcaccaagggcaggtgtgagatcacc
 D C V I T G R P C C I G T K G R C E I T 298
 tcccgggagtactgtgactcattgaggggtacttccatgaggaggccacgctctgctct
 S R E Y C D F M R G Y F H E E A T L C S 318
 caggtgcactgcatggatgatgtgtgtgggtcctgcttttctcaacccccaggtgct
 Q V H C M D D V C G L L P F L N P E V P 338
 gaccagttctaccgctgtggctatccctcttctcgcacgccccgggatcttgacgctg
 D Q F Y R L W L S L F L H A G I L H C L 358
 gtgtccatctgcttccagatgactgtcctgcgggacctggagaagctggcaggtggcac
V S I C F Q M T V L R D L E K L A G W H 378
 cgcatagccatcatctacctgctgagtggtgtcaccggcaacctggccagtgccatcttc
 R **I A I I Y L L S G V T G N L A S A I F** 398
 ctgccataccgagcagaggtgggtcctgctggctcccagttcggcatcctggcctcctc
 L P Y R A E V G P A G S Q F G I L A C L 418
 ttcgtggagctcttccagagctggcagatcctggcgccctggcgtgccttcttcaag
F V E L F Q S W Q I L A R P W R A F F K 438
 ctgctggctgtggtgctcttctcttcaccttgggctgctgcccgtggattgacaactt
L L A V V L F L F T F G L L P W I D N F 458
 gcccacatcagggttcatcagtggcctcttctctccttcgcttcttgcctacatc
 A H I S G F I S G L F L S F A F L P Y I 478
 agcttggcaagttcgacctgtaccggaacgctgccagatcatcatcttccaggtggtc
S F G K F D L Y R K R C Q I I I F Q V V 498
 ttctgggctcctggctggcctgggtgctcctcttacgtctatcctgtccgctgtgag
F L G L L A G L V V L F Y V Y P V R C E 518
 tgggtgagttctcactgcactccctcactgacaagttctgtgagaagtacgaactg
 W C E F L T C I P F T D K F C E K Y E L 538
 gacgctcagctccactga
 D A Q L H *

Figure 2.9 cDNA and deduced amino acid sequence of full length hrho. The 4 in frame methionines are in bold. The 7 predicted TM domains are underlined. The PEST domain is in bold italics. Also note the in frame stop codon preceding the initiator methionine.

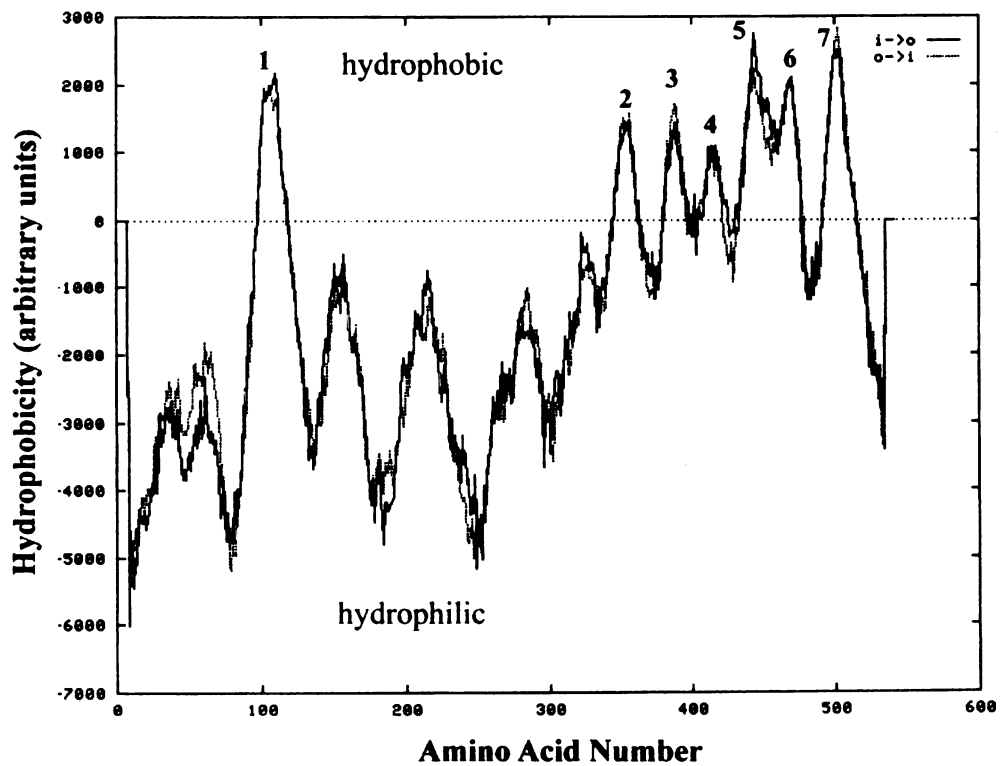


Figure 2.10 Hydrophobicity plot of the full-length hrho protein. The plot was generated by the transmembrane prediction program TM-Pred. The numbered peaks correspond to the seven predicted transmembrane domains.

Chapter 3

Descriptive Characterization of Human Rhomboid

INTRODUCTION

The previous chapter presented the details of the cloning of a full length cDNA coding for a human homologue (hereafter designated “hRho”) of *Drosophila rhomboid*. Next, a descriptive characterization of the hRho protein was undertaken. First, attempts were made to establish the subcellular localization of the protein using both immunofluorescence and cell surface biotinylation. Then, the tissue expression pattern of the gene was analyzed by RT-PCR. Finally, two techniques were used to begin to understand the types of protein-protein interactions in which hRho is involved. The more general of these was a screen for interacting proteins using metabolic labeling followed by immunoprecipitation. In addition, based on genetic interaction data from *Drosophila* (Chapter 1), physical interaction studies were designed using specific proteins with which hRho might be predicted to interact - the EGF receptor and TGF α . The aim of the work described in this chapter was to generate a thorough description of the hRho protein in the hope of revealing possible clues about its function in mammalian cell biology.

MATERIALS AND METHODS

Generation of plasmid constructs

The plasmid pFHR-long was generated from pHRF-long by PCR using the primers “NFlag rho5”: 5’-gcggaattcccggctccctccaggcccttg-3’ to bypass the ATG and “Nrho Sal3”: 5’-gcggtcgactcagtgagctgagcgtccagttc-3’ to incorporate a stop codon shown (in bold). The Eco RI and Sal I sites are underlined. PCR was performed using Pfu polymerase (Stratagene) as described in Chapter 2 for the generation of pHRF. The PCR product was digested sequentially with Sal I and Eco RI and gel purified. The purified

fragment was ligated into the Eco RI and Sal I sites of pXF1F (generously provided by Xin-Hua Feng), which is the same vector as pRK5F except that the Flag tag includes an ATG and is located between the Cla I and Eco RI sites to provide an N-terminal epitope tag.

The plasmids pRK5-EGFR and pRK5-EGFRc688 were generated from the plasmids pXER and pXERc688 (gifts from Gordon Gill, UCSD). The wild-type or mutant insert was released from these plasmids by digestion with Xba I and Hind III and the gel purified fragment was ligated into the Xba I and Hind III sites of pRK5.

The plasmid pT β RIIM was described previously (Chen and Derynck '94). It contains a wild-type TGF β type II receptor with a C-terminal Myc epitope tag ligated into the Eco RI and Xba I sites of the vector pRK5.

The expression plasmids pRK7-TGF α for wild-type TGF α and pRK7-TGF α Δ C for cytoplasmically truncated TGF α were described previously (Shum *et al.* '94). The plasmid pRK5-TGF α Δ E was generated using PCR to insert a Myc epitope tag flanked by diglycines (GGEQKLISEEDLGG) between amino acids 93 and 94 and to remove the 50 amino acid core TGF α from the extracellular domain. The TGF α Δ E sequence was ligated into the Eco RI and Hind III sites of pRK5.

Immunofluorescent staining and microscopy

Transiently transfected cells were replated on tissue culture chamber slides 24 hours after transfection and allowed to reattach overnight. The cells were then washed with PBS and fixed either with cold (-20 C) methanol for 5 minutes or with 4% paraformaldehyde (Sigma) in PBS at room temperature for 15 minutes. An additional 5 minute incubation in 0.2% Triton X-100 (Sigma) was used to permeabilize the cells following fixation with paraformaldehyde. Nonspecific binding sites were blocked with 3% bovine serum albumin (BSA, Sigma) in PBS for 2 hours at room temperature or overnight at 4 C. The cells were then incubated in a 1:500 dilution of anti-Flag M2 antibody (Kodak IBI) in PBS + 2% horse serum (Vector Labs) for 1 hour at 37 C. Following 3 x 5 minute washes with PBS + 3% BSA, the cells were incubated in a 1:200 dilution of Texas red conjugated goat anti-mouse IgG (Jackson ImmunoResearch) in PBS + 2% horse serum for 45 minutes at room temperature. The cells were again washed 3 x 5 minutes in PBS + 3% BSA followed by a final wash in PBS before mounting in Vectashield mounting medium (Vector Labs). The stained cells were visualized on a Zeiss Axioplan Universal microscope equipped with a short arc mercury lamp and standard filters for immunofluorescence.

Co-immunofluorescent staining was performed essentially as described above, except that HeLa cells stably transfected with hRho (see Chapter 4) were used to allow detection of hRho in every cell, and donkey serum was used as a blocking agent. Endogenous mp30 was detected with a 1:500 dilution of a rabbit polyclonal antibody generated against a glutathione S transferase (GST) fusion to a C-terminal peptide from dog mp30

(a generous gift from Peter Walters, UCSF). The hRho signal was detected with a 1:400 dilution of Cy-3 conjugated donkey anti-mouse IgG (Jackson ImmunoResearch) and the mp30 signal was detected with a 1:200 dilution of fluorescein conjugated goat anti-rabbit IgG (Jackson ImmunoResearch). Staining for the two proteins was performed sequentially. Microscopy was performed on a Zeiss LSM 410 confocal microscope equipped with a krypton-argon laser and optimized photomultiplier tubes.

Cell surface biotinylation

Transiently transfected COS-1 cells were washed twice in ice cold PBS* (PBS-CMF + 0.5 mM MgCl₂, pH 7.8). 3 ml of ice cold, freshly dissolved, membrane impermeable sulfo-NHS-LC biotin (1 mg/ml in PBS*; Pierce #21335) was added per 100 mm dish of cells and the plates were incubated for 45 minutes at 4 C. The biotinylation reaction was quenched by washing the cells twice in 50 mM glycine in PBS* and then allowing the cells to incubate in this buffer at 4 C for an additional ~15 minutes.

Following biotinylation and quenching, the cells were lysed, immunoprecipitated with anti-Flag antibody, run on SDS-PAGE and electroblotted as described in Chapter 2. The membrane was then blocked overnight at 4 C in TBST (tris buffered saline + 0.05% Tween-20) + 5% nonfat dry milk. The membrane was then blocked an additional 45 minutes at room temperature in SuperBlock (0.2 M glucose, 10% glycerol, 3% BSA, 0.5% Tween-20 and 1% nonfat dry milk in PBS). Following 3 x 10 minute washes in PBS + 0.5% Tween-20, the membrane was incubated in a 1:2000 dilution of streptavidin-HRP (1 mg/ml; Pierce #21126H) in PBS + 0.1% Tween-20 for 45 minutes at room

temperature. Following an additional 3 x 10 minute washes in PBS + 0.5% Tween-20, the blots were developed with ECL (Amersham) and exposed to autoradiography film (Kodak BioMax MR).

RT-PCR

Tissues were freshly dissected from adult C57BL/6 mice (a generous gift from Anne Neil of the Hormone Research Institute at UCSF) and flash frozen in liquid nitrogen. Each frozen tissue was then transferred to a separate culture tube (Falcon 2059) on ice containing ~4 ml of Trizol Reagent (Gibco/BRL) and immediately homogenized using a homogenizer (Omni International 2000) at full speed for 1-2 minutes until the tissue was completely thawed and homogenized. The Trizol homogenate was aliquoted into equal portions in microcentrifuge tubes (typically 4-6) on ice. Total RNA was then prepared from the homogenate as per the manufacturer's instructions. The RNA was stored at -80 C at the isopropanol precipitation step until further use.

For use in RT-PCR, the RNA was thawed on ice and precipitated by centrifugation at 12,000 RPM for 30 minutes at 4C. The pellet was washed once in 70% EtOH prepared with DEPC (Sigma) treated H₂O, resuspended in DEPC H₂O, and quantified using a Shimadzu UV160U Spectrophotometer ($1 A_{260} = 40 \text{ ug/ml}$). 3 ug of RNA in a volume of 10 ul was DNase treated by adding 40 ul DNase Mix (10 ul 5X Transcription Buffer (Promega), 5 ul 10 mM DTT, 21 ul DEPC H₂O, 2 ul RNAsin (Promega), 2 ul RQ1 DNase (Promega)). Following DNase treatment, the RNA was extracted with phenol/chloroform and EtOH precipitated. Each RNA sample was resuspended in 6 ul of

random hexamers (50 uM Gibco/BRL) and 4 ul of DEPC H₂O, heated at 68 C for 10 minutes and then cooled on ice. The samples were then divided equally into two tubes. 14 ul of RT Mix (4 ul of 5X RT buffer (Promega), 2 ul of 10mM DTT (Gibco/BRL), 1 ul of 10 mM dNTPs (Boehringer Mannheim), 0.5 ul RNAsin and 6.5 ul of DEPC H₂O) was added to each tube. 1 ul of M-MLV reverse transcriptase (Gibco/BRL) was added to one of the tubes and both tubes were incubated at 42 C for 2 hours. The samples were boiled for 3 minutes to inactivate the reaction and diluted with an additional 80 ul of H₂O.

The first strand cDNA prepared as described above was used as a target for PCR using several different primer sets. A portion of the mRho sequence was amplified using the primers “mhRho5”: 5'-aggaggagtgctcgtccacg-3' and “mhRho3” 5'-agccacaggcggtagaac-3'. These primers were designed based on the mouse sequence designated “mouse EGF receptor related gene, 5' end” (accession #M99623) which was obtained by a group sequencing upstream of the alpha globin locus on mouse chromosome 11 (Kielman *et al.* '93) and which is >90% identical in sequence to that which codes for amino acids 278-357 of hRho. The predicted size of the mRho RT-PCR product was 432 base pairs.

A portion of the mEGFR sequence (accession #U03425) was amplified using the primers “mEGFR5”: 5'-gttgctgaccgcgctctgcg-3' and “mEGFR3”: 5'-tgagggcaatgaggacatagcc-3'.

The predicted size of the mEGFR RT-PCR product was 244 base pairs. A portion of the mTGF α (accession #M92420) sequence was amplified using the primers “mTGF α 5”: 5'-**ggacagctcgctctgctagcg-3'** and “mTGF α 3”: 5'-cttctcatgtctgcagacgagg-3'. The predicted *size* of the mTGF α RT-PCR product was 410 base pairs.

As an internal control for cDNA synthesis, a portion of the structural gene β -actin was amplified from the same cDNA samples using the primers “m β -actin5”: 5’-cgtgggccgccttaggcacca-3’ and “m β -actin3”: 5’-ttggccttagggtcagggggg-3’. The predicted size of the β -actin RT-PCR product was 243 base pairs.

PCR reactions were performed using 5 ul of 10X PCR Buffer with 1.5 mM MgCl₂ (Boehringer Mannheim), 25 pmol of each primer, 5 ul of 10X dNTPs (2 mM each, Boehringer Mannheim), 3 ul of first strand cDNA and 5U of Taq polymerase (Boehringer Mannheim) in a final volume of 50 ul. The PCR program used for all of the primer sets was 1 cycle at 95 C for 5 minutes followed by 30 cycles of 95 C for 5 minutes, 60 C for 30 seconds, 72 C for 2 minutes, followed by one cycle at 72 C for 10 minutes and a 4 C hold. PCR products were run on 1.8% ethidium bromide stained agarose TBE gels and photographed on Polaroid 667 film.

Metabolic labeling

Transiently transfected cells in 100 mm dishes were grown to ~80% confluency and then starved in serum free, cysteine-methionine free DME-H16 3g/L glucose (UCSF Cell Culture Facility) at 37 C for one hour. The cells were then labeled overnight at 37 C in cysteine-methionine free medium + 10% dialyzed FBS (Gibco/BRL) + 400 uCi of Easy Tag EXPRESS (NEG-772, NEN) in a final volume of 5 ml. After labeling, the medium was removed and the cells were washed twice with PBS prior to lysis and immunoprecipitation as described above. The washed immunoprecipitates were run on an 8% or 10% SDS-PAGE minigel. The gel was fixed 1 hour in 20% MeOH + 10% HAc,

soaked in Amplify (Amersham) for 30 minutes dried and exposed to autoradiography film (BioMax MR).

Co-immunoprecipitation Studies

HEK-293 cells in 100 mm dishes were transiently transfected with plasmids in a 1:1 ratio using Lipofectamine (Gibco/BRL) according to the manufacturer's instructions.

Preparation of cell lysates, immunoprecipitation and western blotting were performed essentially as described in Chapter 2. For EGFR, the EGFR Ab-5 antibody (Calbiochem) was used at 1 ug/ml for immunoprecipitation and a 1:1000 dilution of anti-EGFR (#324862, Calbiochem) was used for western blotting. For detection of EGFRc688, a 1:2000 dilution of anti-EGFR(KSM), a rabbit polyclonal antibody which recognizes the extracellular domain of EGFR (a generous gift from Gordon Gill, UCSD), was used for western blotting. For TGF α , the α 1 Ab (Bringman *et al.* '87) was used at ~4 ug/ml for immunoprecipitation and a 1:100 dilution of anti-TGF α Ab-1 (#GF06, Calbiochem) was used for western blotting. For the tripartite complex study, Flag peptide (Sigma) was used according to the manufacturer's instructions to elute the Flag immunoprecipitates from the protein A sepharose beads. Two 50 ul elutions were pooled and then diluted to 500 ul with Py lysis buffer prior to the second round of immunoprecipitation.

RESULTS

Subcellular localization of hRho protein

To determine the subcellular localization of the hRho protein, COS-1 cells were transiently transfected with pHRF-long. The cells were fixed and immunostained using anti-Flag antibody along with a Texas red conjugated secondary antibody. When the cells were fixed with methanol (which also permeabilizes the cells), intense non-nuclear staining was observed which was feathery or reticular in appearance and which extended throughout the cytoplasm (Figure 3.1). Paraformaldehyde fixation resulted in the same localization and quality of staining but the signal was only detectable when the cells were permeabilized following fixation (not shown).

To further address the issues of the membrane topology and localization of hRho, a construct was generated with the Flag epitope tag at the N-terminus. The rationale was that if the protein localized to the plasma membrane and if a C-terminal tag could only be detected upon permeabilization of the cell, then the N terminus would be extracellular (if the protein had the predicted 7 transmembrane domains). Therefore, the protein tagged at the N-terminus would be detectable without the need to permeabilize the cell. PCR was used to amplify hRho-long from pHRF. The PCR product was cloned into pXF1F, a mammalian expression vector with an N-terminal Flag epitope tag (identical to pRK5F except for the location of the tag) to generate pFHR-long (see Chapter 2, Figure 2.1).

In order to verify expression from this plasmid, it was transiently transfected into HEK-293 cells and Flag IP-western analysis was performed on cell lysates. A ~60 Kd protein

was detected and the expression level appeared higher than that obtained with the C-terminally tagged hRho construct pHRF-long (Figure 3.2 lanes 2 and 3). The smaller ~47 kd band seen with pHRF-long was not detected with pFHR-long, suggesting that it was either a C-terminal degradation product or a product resulting from the use of an alternative translation initiation site, both of which would retain a C-terminal epitope tag but not an N-terminal tag.

Immunofluorescence performed on COS-1 cells transiently transfected with pFHR-long gave the same results as for pHRF-long. Again, intense non-nuclear staining was visible only when the cells were permeabilized either by methanol fixation or by incubation in a detergent solution following paraformaldehyde fixation (not shown). Because the N and C terminally tagged proteins gave the same results, the membrane topology of the protein remained ambiguous.

Given the location and quality of the staining, it appeared that the protein localized to an intracellular membrane. The feathery appearance and the fact that the staining extended throughout most of the cytoplasm were consistent with localization to the endoplasmic reticulum (ER). In order to address this possibility, an experiment was performed to determine if hRho co-localized with the ER membrane protein mp30. Co-immunofluorescent staining was performed on HeLa cells stably transfected with hRho (see Chapter 4) to detect the overexpressed hRho protein and the endogenous mp30 protein. The hRho staining appeared throughout most of the cytoplasm with a slightly increased concentration in the perinuclear region. The mp30 staining was more

concentrated in the perinuclear region with a weaker signal throughout the rest of the cell. While there were some areas of hRho staining that did not overlap with mp30 staining, a convincing overlap of the two signals was observed (Figure 3.3 yellow/orange areas).

Cell surface labeling of hRho protein

An additional experiment was performed to establish whether any of the total cellular hRho protein localized to the plasma membrane. Live transiently transfected COS-1 cells were cell surface biotinylated, quenched with glycine, lysed and immunoprecipitated with anti-Flag antibody. Western blots were then probed with streptavidin HRP to detect biotinylated proteins. A ~60 kd protein was detected in cells transfected with hRho but not in cells transfected with vector alone (Figure 3.4 lanes 1 and 2). As a control for incomplete quenching and/or leakage of the biotin across the plasma membrane where it could label intracellular proteins, a parallel analysis was performed on cells transfected with the plasmid p59F. p59 is an intracellular protein believed to localize to the golgi (Kuo '99). No p59 was detected (Figure 3.4 lane 3) despite very high expression as determined by a separate FLAG IP/western performed on the same lysate (not shown). Therefore it seemed that at least some portion of the total cellular hRho localized to the plasma membrane.

Analysis of the tissue expression of rho

Determining the tissue expression pattern of a protein is often useful in helping to establish its potential function. Therefore an effort was made to characterize hRho localization on this more macroscopic scale. The laboratory that identified the “human

EGF receptor related gene 5' end" cDNA upstream of the alpha globin locus on human chromosome 16 also identified a nearly identical sequence on a syntenic region upstream of the alpha globin locus of mouse chromosome 11 (Kielman *et al.* 1993). It was designated "mouse EGF receptor-related gene, 5' end" (accession #M99623). The human and mouse cDNAs and the corresponding amino acid sequences are >90% identical. Therefore, this sequence likely represents part of a putative mouse homologue (mRho) of *Drosophila rhomboid*. This remarkable identity between the human and mouse cDNA sequences was exploited in order to analyze mRho expression in mouse tissues as an alternative to analyzing hRho expression in human tissues that are more difficult to obtain.

PCR primers were generated using regions of the cDNAs that were identical in human and mouse. Total RNA was prepared from several normal tissues dissected from adult mice and RT-PCR analysis was performed using these primers. A corresponding analysis of EGF receptor and TGF α expression was performed on these same cDNAs using primers designed from the murine sequences for these genes. The mouse gene mRho was expressed in all of the tissues tested, which included brain, heart, lung, stomach, liver, spleen, kidney, uterus and skeletal muscle (Figure 3.5). The signal was equally robust in all tissues tested. The EGF receptor expression pattern coincided with mRho, and again all tissues tested gave an equally strong signal (Figure 3.6 top). While TGF α was also expressed in all tissues tested, a few tissues gave very weak signals. These included heart, spleen and skeletal muscle (Figure 3.6 bottom).

Metabolic labeling and immunoprecipitation

To look for proteins with which the hRho protein might interact, HEK-293 cells were transiently transfected with pHRF-long and metabolically labeled. Cell lysates were then immunoprecipitated with anti-Flag antibody. The predicted ~60 kd hRho band was identified in cells transfected with pHRF-long but not in cells transfected with vector alone (Figure 3.7 lanes 1 and 2). Interestingly, a weaker ~36 kd band reproducibly co-precipitated with hRho. This band could have been either an associated protein or a C-terminal degradation product of hRho that retained the epitope tag.

A repeat of this metabolic labeling experiment in HEK-293 cells with the N-terminally tagged clone pFHR-long again resulted in the detection of the ~60 kd hRho protein and the same ~36 kd band seen which co-precipitated with the C-terminally tagged clone (not shown). As an additional confirmation of the association with the ~36 kd protein, the metabolic labeling experiment was repeated in another human cell line, HeLa. Again the ~36 kd protein was detected co-precipitating with both N and C-terminally tagged hRho, confirming that the ~36 kd protein was not unique to HEK-293 cells (Figure 3.7 lanes 4-6).

Given the discovery of a protein which appeared to associate with hRho, an N-terminally histidine tagged, C-terminally FLAG tagged hRho construct was generated as a reagent that could potentially be used to purify and identify the ~36 kd protein using a metal column. This construct was transiently transfected into HEK-293 cells and shown to generate a protein slightly greater in size than the ~60 kd hRho protein, consistent with the addition of the 6-his tag (not shown).

Co-immunoprecipitation of EGFR with hRho

As discussed in Chapter 1, rhomboid appears to positively regulate DER signaling in flies. One possibility is that this is achieved by a direct physical interaction with the receptor. To test for a physical interaction between hRho and EGF receptor, HEK-293 cells were transiently transfected with vector, pFHR-long, pRK5-EGFR or both pFHR-long and pRK5-EGFR. Cell lysates were then immunoprecipitated with anti-Flag antibody and western blotted with an anti-EGF receptor antibody. The ~170 kd EGFR protein was only detected in the lane corresponding to cells which had been transfected with both hRho and EGFR (Figure 3.8 lanes 1-5).

This experiment was repeated with the added variable that parallel transfections were treated with 5 ng/ml EGF for 5 minutes immediately prior to lysis and analysis. This was done because hRho might preferentially bind to activated EGF receptor as has been shown with other proteins known to bind the EGF receptor. The co-precipitation of EGF receptor with hRho was reproduced but was not enhanced (or diminished) by the addition of soluble ligand (not shown).

As a control, HEK-293 cells were co-transfected with pFHR-long and pT β RIIM, an expression plasmid for Myc tagged TGF- β type II receptor, another transmembrane receptor kinase. Cell lysates were prepared and immunoprecipitated with anti-Flag antibody under the same conditions used to co-precipitate EGF receptor with hRho. The western blot was then probed with anti-Myc antibody. No TGF- β type II receptor was detected co-precipitating with hRho (Figure 3.8 lanes 6-8).

The interaction between hRho and EGFR was further characterized using EGFR c688, a truncation mutant of EGFR missing the most of the cytoplasmic domain of the receptor, including the kinase domain. Co-transfection of pFHR-long and pRK5-EGFRc688 and IP-western analysis performed as above failed to detect an interaction of hRho with this mutant form of the receptor (Figure 3.9). Therefore, the interaction of hRho with EGFR appeared to be mediated by the cytoplasmic domain of EGFR.

Co-immunoprecipitation of TM-TGF α with hRho

In flies, dRho has also been postulated to play a role in regulating Spitz proteolysis. It therefore seemed reasonable to test for a direct physical interaction between hRho and transmembrane TGF α (TM-TGF α). HEK-293 cells were transiently transfected with vector plus pRK7-TGF α or pFHR-long plus pRK7-TGF α . Cell lysates were then immunoprecipitated with anti-Flag antibody and western blotted with an anti-TGF α antibody. The smaller two of the three forms of TM-TGF α which run in the range of 20 - 30 Kd were detected in cells transfected with both hRho and TGF α (Figure 3.10 lane 2). These represent the core glycosylated proTM-TGF α species and the mature TM-TGF α that has undergone processing to remove its glycosylated prodomain. The slowest migrating, complex glycosylated proTGF α species did not co-precipitate despite its presence in the cell lysate (Figure 3.10 lane 8).

The interaction between hRho and TM-TGF α was further mapped using TGF α Δ C, a truncation mutant of TM-TGF α missing most of its cytoplasmic domain, and TGF α Δ E, a mutant in which the extracellular core 50 amino acid EGF-like domain has been replaced

with a Myc epitope tag. Co-transfection of pFHR-long with pRK7- TGF α Δ C or with pRK7-TGF α Δ E and IP-western analysis performed as above detected an interaction with TGF α Δ C (again with the same two of the three forms) but not with TGF α Δ E (Figure 3.10 lanes 4 and 6). Therefore, the interaction of hRho with TM-TGF α appeared to be mediated by the extracellular domain of TGF α .

Co-immunoprecipitation of EGFR and TM-TGF α with hRho

Since EGFR and TM-TGF α each individually co-immunoprecipitated with hRho, it seemed likely that the three proteins could form a tripartite complex since TGF α and EGFR were already known to interact as ligand and receptor, respectively. To formally test this possibility, HEK-293 cells were transiently co-transfected with pFHR-long + pRK7-TGF α + pRK5-EGFR. Cell lysates were then immunoprecipitated with anti-Flag antibody. The immunoprecipitates were washed and the hRho protein, along with any associated proteins, were eluted using Flag peptide. A second round of immunoprecipitation was then performed on the eluates using anti-TGF α or anti-EGFR antibody, and parallel western blots were performed using anti-EGFR and anti-TGF α antibody. On the EGFR western blot, the 170 kd EGFR was detected co-immunoprecipitating with TM-TGF α which had been previously co-immunoprecipitated by hRho (Figure 3.11A lane 2). However, the EGFR was difficult to detect in a control immunoprecipitation using anti-EGFR (Figure 3.11A lane 1). On the TGF α western blot, only the mature TM-TGF α lacking the glycosylated pro-domain could be detected co-immunoprecipitating with EGFR which had been previously co-immunoprecipitated by hRho (Figure 3.11B lane 1). Both the core glycosylated proTM-TGF α and the mature

DISCUSSION

The work in this chapter was undertaken with the intent of providing as complete a description of the hRho protein as possible in order to provide a foundation for the functional characterization of the protein.

Often one of the most important clues about the function of a protein is where it localizes in the cell. The literature on dRho suggests (but does not prove) that it localizes to the plasma membrane along with star and spitz to regulate spitz proteolysis (reviewed in Perrimon and Perkins 1997). Hence one might predict a similar localization for hRho. The immunofluorescence experiments described in this chapter were aimed at determining the subcellular localization of hRho. A secondary aim was to attempt to determine the topology of hRho in the membrane. The pFHR construct was generated in part for this purpose because it has the Flag epitope on the N-terminus while pHRF has it on the C-terminus. If hRho does indeed localize to the plasma membrane, and if it has an odd number of transmembrane domains, one would expect that only one of the two versions of the protein would be detectable when the cells are fixed but not permeabilized. The detectable version would have that terminus extracellularly oriented and the opposite terminus intracellularly oriented.

The staining results for hRho turned out to be more complex than anticipated. First, there did not appear to be intense staining around the rim of the cell as one might expect for a plasma membrane protein. Rather, the staining was non-nuclear, feathery or reticular in appearance, and appeared to extend throughout most of the cytoplasm. This pattern was

highly suggestive of some internal membrane localization (see below). Second, the hRho could only be clearly detected if the cells were permeabilized either by using methanol as a fixative or by using detergent to permeabilize paraformaldehyde fixed cells. This was true of both the N and C-terminally tagged hRho.

One possible interpretation of the fact that detection of both the N and C-terminally tagged hRho required permeabilization of the cell is that the protein does localize to the plasma membrane but the Flag epitope is not easily accessible to the antibody following fixation. Permeabilization could serve “loosen” the fixed material and allow access to the epitope. An alternative interpretation is that the protein localizes to the plasma membrane but has an even number of transmembrane domains and both the N and C terminus are on the intracellular side of the membrane. The most likely explanation, especially given the location and quality of the staining, is that the protein localizes to an intracellular membrane. The feathery appearance and the fact that the staining extends throughout most of the cytoplasm are consistent with localization to the endoplasmic reticulum (ER), although distribution of some of the protein to the plasma membrane cannot be completely ruled out.

As a means of addressing the possibility that at least some of the hRho protein localizes to the plasma membrane, cell surface proteins were biotinylated prior to cell lysis, immunoprecipitation and detection. Indeed, using this approach some hRho could be detected on the plasma membrane, but this method has some inherent limitations that complicate the interpretation of the results. One technical problem is that the

biotinylation reagent can “leak” cross the plasma membrane and label intracellular proteins. In addition, if insufficiently quenched, the reagent can label intracellular proteins following cell lysis. To control for these possibilities, a protein known to be intracellular was used in parallel and found not to be labeled.

From the data discussed thus far, one might conclude that the majority of the protein localizes to some intracellular membrane such as the ER but that a small portion of it localizes to the plasma membrane. However, these experiments might not accurately represent the true localization of the protein because in the artificial system used the protein is massively overexpressed relative to the likely endogenous levels of the protein. For example, all secreted transmembrane proteins pass through the ER whether or not it is their final destination. If a protein is overexpressed, it is possible that the secretory system of the cell might become overloaded. There might be more of the protein present in the ER and golgi than would normally be the case. Alternatively, a protein might escape the normal control mechanisms that prevent an intracellular membrane protein from being delivered to the plasma membrane.

Recent evidence has shown that star, a genetically related single transmembrane protein, localizes not to the plasma membrane but rather to the outer nuclear membrane and the ER membrane which is contiguous (Pickup *et al.* 1999). Given the strong genetic interaction between dRho and star (Guichard *et al.* 1999), it is very likely they co-localize, and some preliminary evidence even suggests that they physically interact (personal communication with Ethan Bier, unpublished results). Therefore it seems quite

likely that dRho, and by analogy hRho, might exist on the ER membrane instead of, or in addition to, the plasma membrane. In this context, it is interesting to note that a study of the role of dRho in retinal photoreceptor development showed expression of dRho in what appeared to be intracellular vesicles of the R2, R5 and R8 photoreceptor cells (Freeman *et al.* 1992). Furthermore, the immunostaining was improved by inclusion of the nonionic detergent NP-40 (which permeabilizes cells) in the fixative used to prepare the specimens (Freeman *et al.* 1992).

Note that an ER localization is not inconsistent with a hypothesized role for dRho in regulating spitz proteolysis. Spitz is likely to undergo the same types of intracellular processing that have been described for TGF α , such as cleavage to remove the glycosylated pro-domain. It is possible that dRho is involved in regulating this proteolysis event rather than the one which results in the release of the soluble ligand. Also, it is not at all clear that the release of spitz (and TGF α) from the membrane to generate a soluble ligand occurs at the plasma membrane. This processing event could occur at an intracellular membrane location since these membranes are topologically equivalent to the plasma membrane. A soluble ligand released into an intracellular lumen, such as the ER lumen or the lumen of a secretory vesicle, would also be delivered extracellular space.

To further explore the possibility that hRho localizes to the ER, an immunostaining experiment was performed to determine if hRho co-localized with the ER membrane protein mp30. This protein was once thought to be involved in the binding of the signal

recognition particle to (SRP) to its receptor on the ER membrane (Tajima *et al.* 1986). A convincing overlap of the two signals was observed, but there were also areas of hRho staining that did not overlap with mp30 staining and which might be interpreted as cell surface/plasma membrane staining. While the results do not prove definitively that hRho localizes to the ER, they are certainly consistent with this hypothesis. However, given the results of both this experiment and the biotinylation experiment, the localization of at least some of the protein to the plasma membrane cannot be completely ruled out.

To obtain a more macroscopic picture of where hRho is expressed, experiments turned to the evaluation of the tissue expression pattern of hRho. This was accomplished by utilizing a partial cDNA sequence for an apparent mouse homologue of rhomboid that was present in the GenBank database. The remarkable similarity between this mouse partial cDNA and a portion of the hRho cDNA sequence was exploited in order to analyze mRho expression in mouse tissues as an alternative to analyzing hRho expression in human tissues. RT-PCR analysis performed on RNA isolated from various mouse tissues demonstrated equally robust expression of mRho in all tissues tested. Similarly, equally robust expression of mEGFR was detected in all of the tissues. mTGF α was strongly expressed in all tissues except heart, spleen and skeletal muscle where the signal was present but weaker. Given the inherently non-quantitative nature of RT-PCR, no definitive statement can be made about the relative levels of the three proteins in the tissues tested. Nonetheless, the co-expression of mRho with mEGFR and mTGF α in most of the tissues tested is consistent with a possible role for mRho, and by inference hRho, in TGF α mediated EGFR signaling.

Additional clues about the function of a novel protein such as hRho might also be obtained from a careful examination of the proteins with which it interacts. Using a co-immunoprecipitation approach, protein-protein interactions in which hRho is likely to participate were analyzed. A non-biased search for hRho interacting proteins was performed by metabolically labeling cells and then looking for endogenous cellular proteins which appeared to specifically co-immunoprecipitate with hRho. In addition, candidates were chosen based on the available genetic data from studies of dRho in flies. An obvious way in which hRho might positively regulate EGFR signaling is by physically interacting with the receptor itself or with the transmembrane ligand TGF α (or both). Therefore co-immunoprecipitation experiments were performed on cells transiently co-transfected with plasmids for hRho and one or more of these candidate proteins.

The first approach resulted in the detection of a ~36 kd protein. The possibility that this protein was merely a degradation product of hRho itself that retained the epitope tag was ruled out based on the fact that it was detected co-precipitating with both the N and C terminally tagged versions of the protein. If it were a degradation product of hRho one would not expect to detect a band of the exact same size with both the N and C terminally tagged clones (except in the unlikely event that some sort of cleavage happens at precisely the middle of the protein). The fact that the ~36 kd protein was reproducibly detected in two different human cell lines lends additional support to the notion that it is not a technical artifact, but rather a real endogenous human protein abundant enough to be detected by this method. The identity of the protein was not determined; however, one

interesting candidate is the protein EGF Response Factor-1 (ERF-1). A rat version of this protein was originally isolated in a differential display screen for EGF responsive genes (Gomperts *et al.* 1990). The human gene was cloned by homology and found to encode a 338 amino acid protein of 36 kd (Bustin *et al.* 1994). Interestingly, two of the researchers involved in the isolation of both the rat and human ERF-1 proteins later isolated rrp, the other human homologue of dRho (Pascall and Brown 1998). As described earlier in this chapter, a 6-His tagged hRho cDNA construct was generated. This reagent could potentially be used to purify enough of the ~36 kd protein to pursue this question further.

The candidate approach also yielded interesting results. An interaction between hRho and EGFR was detected by immunoprecipitating the hRho protein with anti-Flag antibody and then western blotting with an anti-EGFR antibody. Co-immunoprecipitation in the opposite direction was not detected (i.e. IP with anti-EGFR and western with anti-FLAG), however this is not uncommon in this type of experiment. One explanation is that the interaction with antibody alters the conformation or otherwise interferes with the ability of the precipitated protein to interact with other proteins. The EGFR species which co-precipitated with hRho appeared to migrate slightly faster on SDS-PAGE than that which was precipitated directly with an anti-EGFR antibody (Figure 3.9 top, compare lanes 2 and 4). EGFR is known to undergo post-translational modifications including glycosylation (Soderquist and Carpenter 1984). It is also functionally regulated by phosphorylation on several tyrosine and threonine residues and can exist in a hypophosphorylated or hyperphosphorylated state (Countaway *et al.* 1989, Yarden and Schlessinger 1987, Whitely and Glaser 1986, Downward *et al.* 1985, Bertics

et al. 1985). As such, it often migrates as either a wide band or multiple bands on SDS-PAGE. Thus it appears that hRho selectively interacts with either unglycosylated EGFR or hypophosphorylated forms of the receptor. The significance of this observation is unclear, but it might suggest that hRho interacts with an immature form of the receptor in an intracellular compartment rather than with the fully mature form of EGFR at the cell surface.

The TGF β type II receptor, another transmembrane receptor kinase, did not co-precipitate with hRho demonstrating at least some degree of specificity of hRho for the EGF receptor. The fact that the cytoplasmically truncated EGFRc688 did not co-precipitate with hRho also supports the specificity of the interaction by demonstrating that a particular domain of the receptor is required for the interaction to occur. The interaction between hRho and EGFR is consistent with the ability of dRho to positively regulate DER signaling. A direct interaction might facilitate the assembly/dimerization of the receptor, enhance its affinity for ligand or potentiate its signal transduction capacity by modulating interactions with downstream mediators.

An interaction between hRho and TM-TGF α was also detected by immunoprecipitating the hRho protein with anti-Flag antibody and then western blotting with an anti-TGF α antibody. Again co-immunoprecipitation in the opposite direction (i.e. IP with anti-TGF α and western with anti-Flag) was not detected. Interestingly, the largest form of TM-TGF α representing the complex glycosylated proTGF α did not co-precipitate with hRho despite its presence along with the other two major forms in the cell lysate. The

simplest explanation is that the bulky sugars attached to the pro domain sterically interfere with the ability of hRho to access the protein. This explanation is supported by the fact that TGF α Δ E, a TGF α mutant with the core 50 amino acid TGF α domain replaced by a Myc epitope tag, failed to co-precipitate with hRho. Hence, the interaction with hRho appears to be mediated by an extracellular domain of TM-TGF α , and such an interaction could conceivably be blocked by a large carbohydrate moiety on the nearby prodomain. The interaction between hRho and TGF α is consistent with a potential role for hRho in the regulation of TGF α processing. This regulation might occur at any one of a number of steps, including transportation of the transmembrane ligand to the cell surface, removal of the glycosylated prodomain from the protein, proteolytic cleavage of TM-TGF α to release the soluble ligand or stabilization of the interaction between the ligand and its receptor.

From the above discussion another intriguing possibility may be inferred, namely that hRho interacts with both EGFR and TGF α in a tripartite protein complex. For example, a cytoplasmic domain of hRho might interact with the cytoplasmic domain of EGFR, while at the same time, a luminal/extracellular domain of hRho interacts with the 50 amino acid core extracellular domain of TGF α . This possibility was formally tested by co-expressing all three proteins in HEK-293 cells. The hRho protein and any associated proteins were immunoprecipitated with anti-Flag, eluted with Flag peptide, and then subjected to a second round of immunoprecipitation. To prove that the three proteins form a complex, it was necessary to demonstrate in the second round of immunoprecipitation that the second protein (TM-TGF α or EGFR) could

immunoprecipitate the third (EGFR or TM-TGF α). This was indeed found to be the case in both directions: EGFR could be detected in the anti-TGF α immunoprecipitate, and at least one form of TM-TGF α could be detected in the anti-EGFR immunoprecipitate.

The second round anti-EGFR immunoprecipitation appeared to be significantly less efficient than the anti-TGF α immunoprecipitation, since no EGFR could be detected in the former while it was easily detected in the latter (Figure 3.11A compare lanes 1 and 2). The anti-EGFR antibody used for immunoprecipitation in these studies recognizes an epitope in the extracellular domain. The inefficiency might be due, at least in part, to the occupation of the ligand binding site of the receptor by TGF α . This occupancy changes the conformation of the receptor and this might alter the epitope or render it less available to the antibody. The efficiency of the anti-EGFR immunoprecipitation in the second round was not zero, however, since some TM-TGF α could be detected by western blot (Figure 3.11B lane 1). The fact that TGF α could be detected in the anti-EGFR immunoprecipitate while no EGFR was detected might reflect a greater sensitivity of the anti-TGF α western blotting antibody relative to the anti-EGFR western blotting antibody under the conditions used in this experiment.

Only the mature TM-TGF α lacking the prodomain was detected interacting with EGFR in the second round of immunoprecipitation, despite the fact that the core glycosylated proTM-TGF also co-precipitated with hRho in the first round (Figure 3.11B compare lanes 1 and 2). This might have been due to the inevitable loss of sensitivity that occurs when successive rounds of immunoprecipitation are performed and a relatively greater

abundance of the mature TM-TGF α . A more interesting possibility is that the mature form is the predominant transmembrane form capable of interacting with the EGF receptor. No comprehensive study has been performed to date on the role of the pro-domain in signaling by TM-TGF α . It seems plausible that signaling by the transmembrane ligand might be negatively regulated by its pro-domain. Removal of the pro-domain might serve to “activate” the ligand by enabling it to better engage its receptor. HB-EGF, another EGF-like transmembrane ligand, is believed to operate through such a mechanism (Nakagawa *et al.* 1996).

The hRho protein could potentiate signaling by bringing together ligand and receptor, thereby enhancing their affinity for one another or prolonging/stabilizing their interaction. This might occur in a paracrine fashion on the plasma membrane or an intracellular membrane of a single cell or, if hRho is present on the plasma membrane, in a juxtacrine fashion with TM-TGF α \pm hRho on one cell and EGFR \pm hRho on a neighboring cell. This idea, that hRho might potentiate signaling through EGFR in a manner analogous to the enhancement of DER signaling by dhro, served as the basis for the functional studies described in the next chapter.

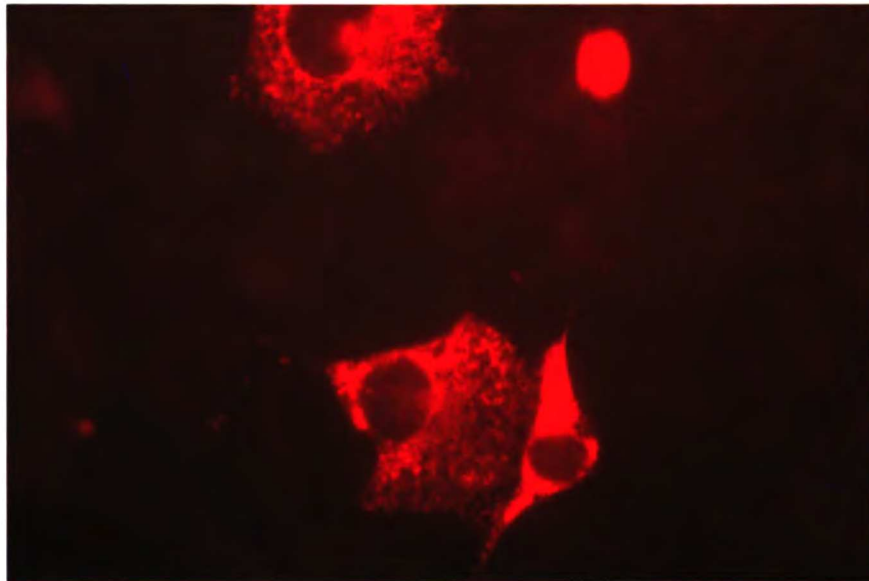


Figure 3.1 Immunofluorescent staining of hrho long in COS-1 cells transiently transfected with pHRF-long. Flag was used as the primary antibody and Texas red conjugated anti-mouse IgG was used as a secondary antibody. Transfection efficiency is always less than 100 %, so not all cells in the field shown are stained. Note the reticular quality of the cytoplasmic staining which is suggestive of an internal membrane localization for hrho.

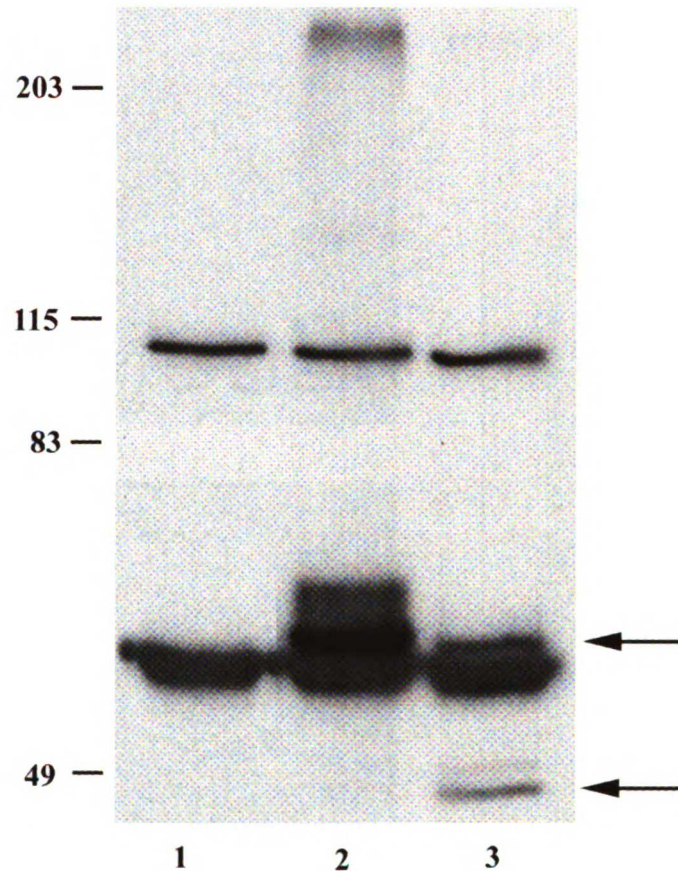


Figure 3.2 Flag IP-western analysis of lysates from HEK-293 cells transiently transfected with vector (lane 1), pFHR-long (lane 2) or pHRF-long (lane 3). The various species of hrho long are indicated by arrows. The expression level of pFHR-long is higher than that of pHRF-long, and the smear suggests post-translational modification. The ~47 kd band is either a C-terminal degradation product or a product resulting from the use of an alternative translation initiation site. It therefore retains the epitope tag and is detected when generated from pHRF-long (lane 3) but not from pFHR-long (lane 2).

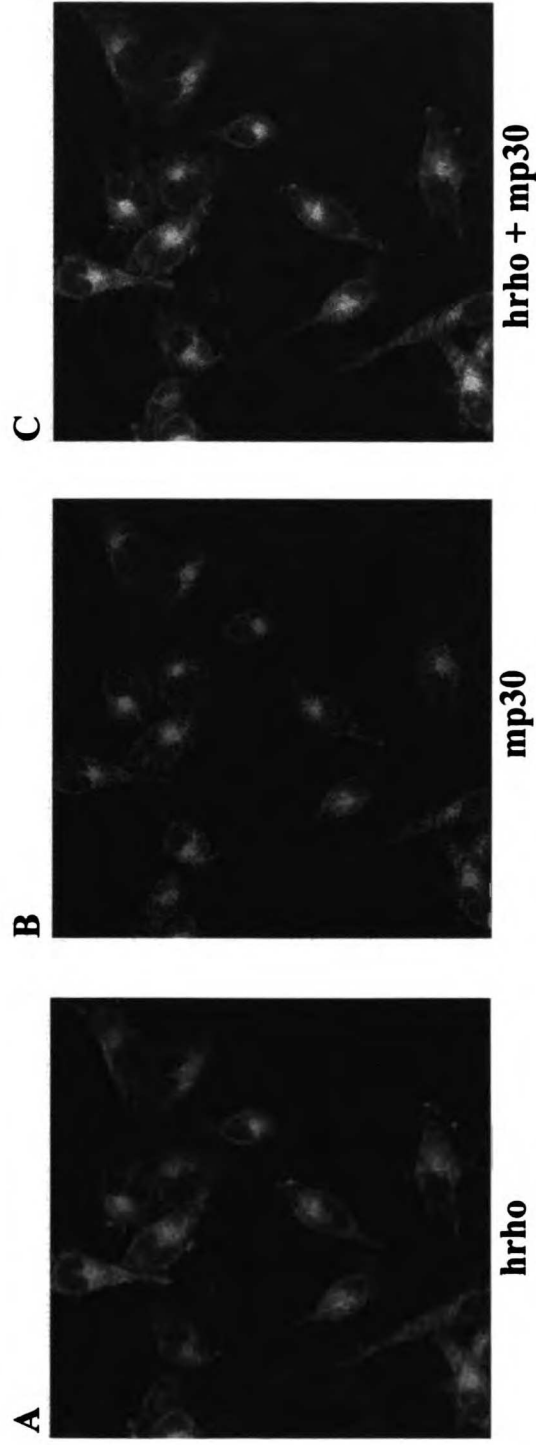


Figure 3.3 Co-localization of hrho and the ER membrane protein mp30. HeLa-tTA cells stably expressing hrho (see Chapter 4) were immunostained sequentially with anti-Flag/Texas Red and anti-mp30/Fluorescein. Confocal microscopy was performed to visualize hrho (A), mp30 (B) or both hrho and mp30 (C). Areas of overlap of the two signals appear yellow/orange in (C).

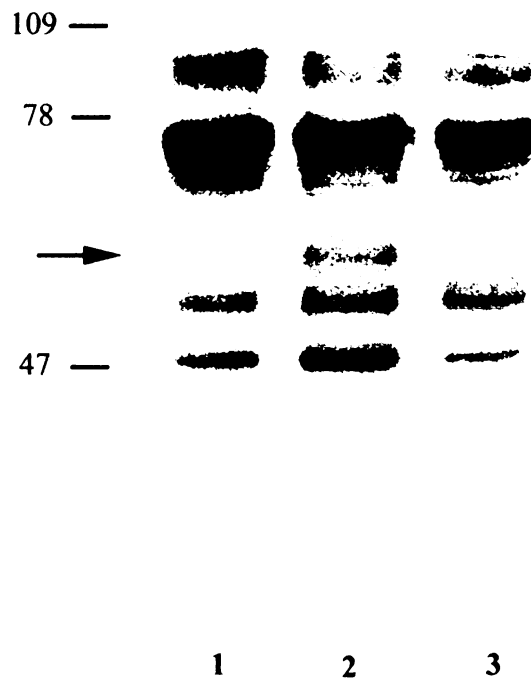


Figure 3.4 Cell surface biotinylation followed by Flag IP-streptavidin western analysis of COS-1 cells transiently transfected with vector (lane 1), pHRF-long (lane 2) or p59-F (lane 3). No p59-F was detected, as would be expected for an intracellular protein. hrho was detected (arrow) indicating that at least some portion of the total hrho present in the cell localizes to the plasma membrane.

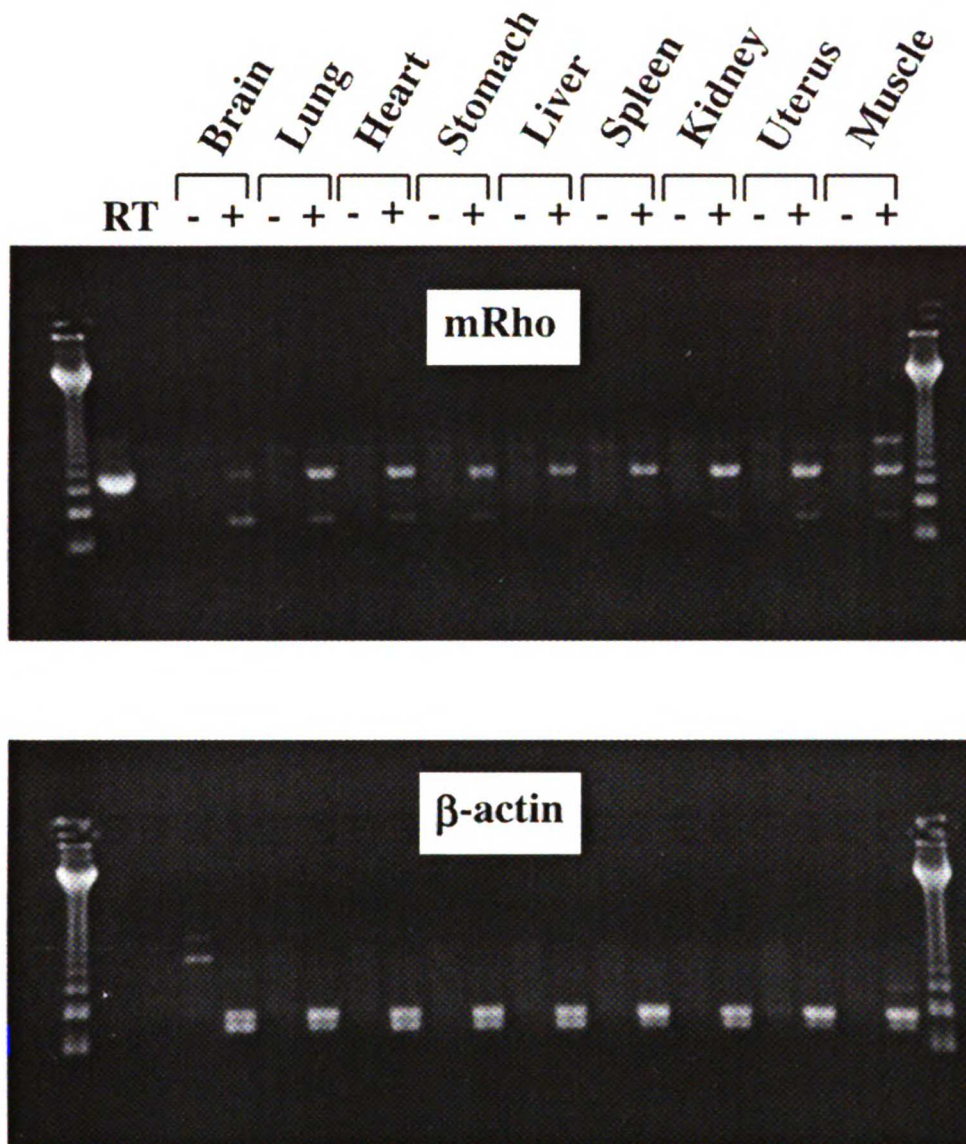


Figure 3.5 RT-PCR analysis of rho expression in various mouse tissues. Each RNA sample was reacted without (-) or with (+) reverse transcriptase (RT) prior to PCR with either a primer set for mrho or a primer set for the structural gene β -actin.

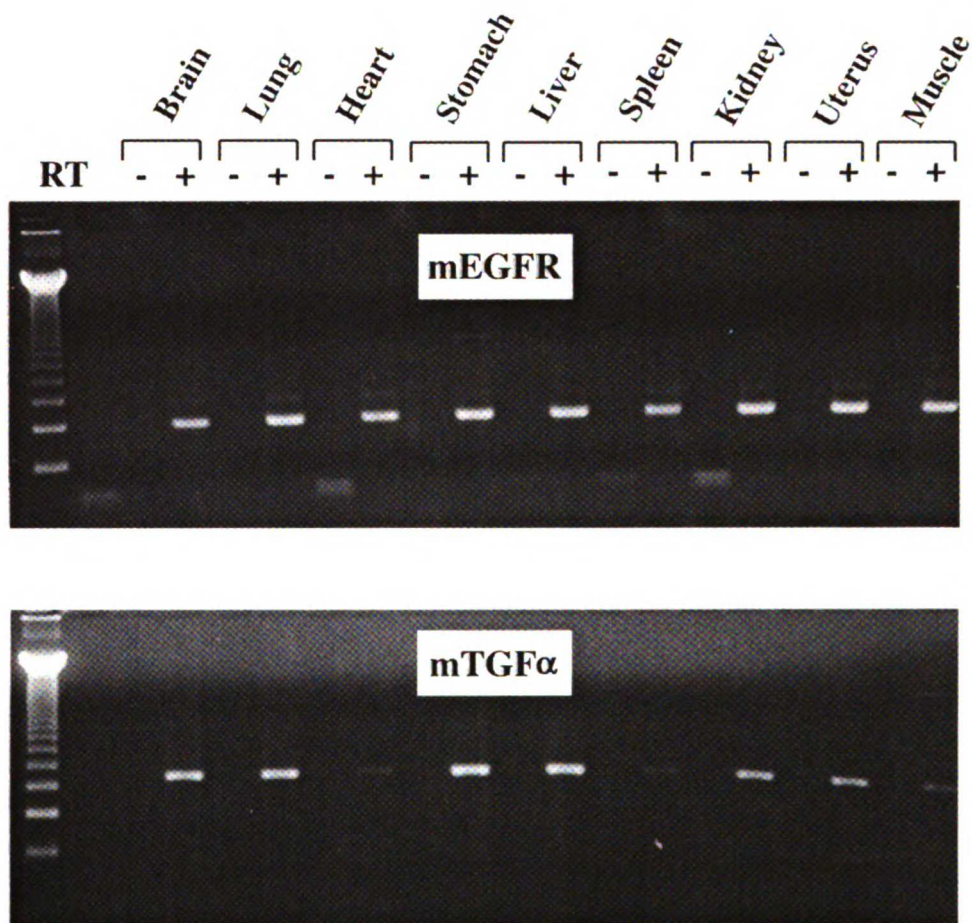


Figure 3.6 RT-PCR analysis of EGFR and TGF α expression in various mouse tissues. The same cDNAs generated to produce Figure 3.7 were used for PCR with either a primer set for mEGFR or a primer set for mTGF α .

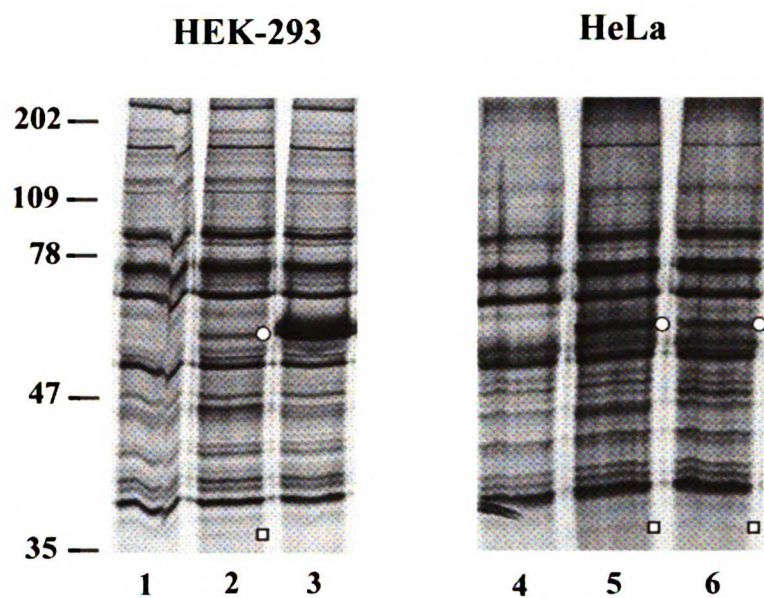


Figure 3.7 Flag immunoprecipitation of cell lysates prepared from metabolically labeled HEK-293 cells (lanes 1-3) or HeLa cells (lanes 4-6) which were transiently transfected with vector (lanes 1,4), pHRF-long (lanes 2,6), p59F (lane 3) or pFHR-long (lane 5). The hrho band is indicated by a small white circle. The identity of the ~36 kd protein that co-precipitates with hrho (small white square) is unknown.

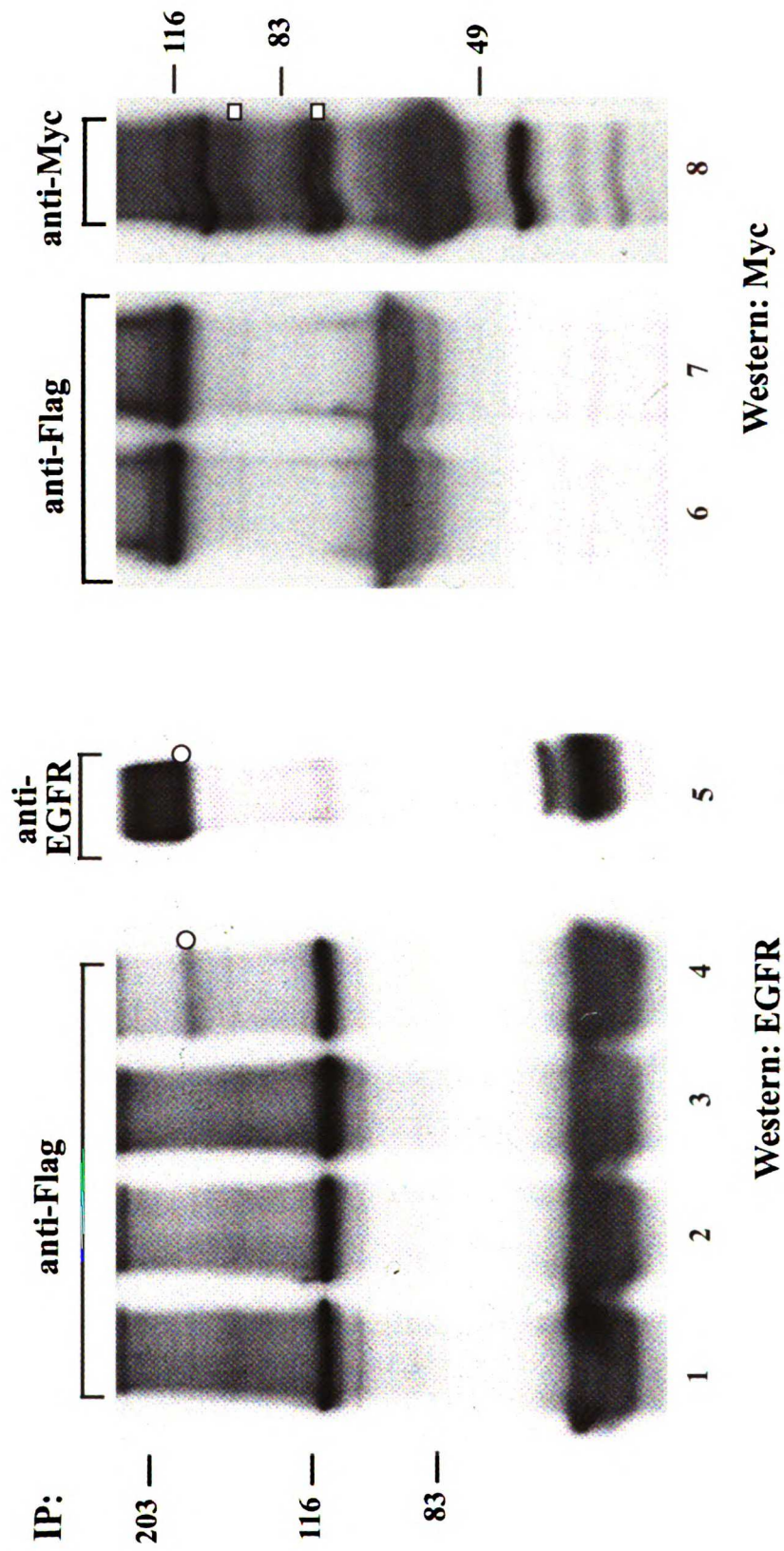


Figure 3.8 Co-immunoprecipitation of hrho and EGF receptor. Lysates from HEK-293 cells transiently transfected with vector (lane 1), pFHR-long (lane 2), pRK5-EGFR (lane 3), pFHR-long + pRK5-EGFR (lanes 4,5), pTBR1IM (lane 6), pFHR-long + pTBR1IM (lanes 7,8) were immunoprecipitated with anti-Flag (lanes 1-4, lanes 6-7) or anti-Myc (lane 8) and western blotted with an anti-EGFR antibody (lanes 1-5) or an anti-Myc antibody (lanes 6-8). The ~170 kd EGFR is indicated by small white circles. The unglycosylated and glycosylated TBR1I are indicated by small white squares.

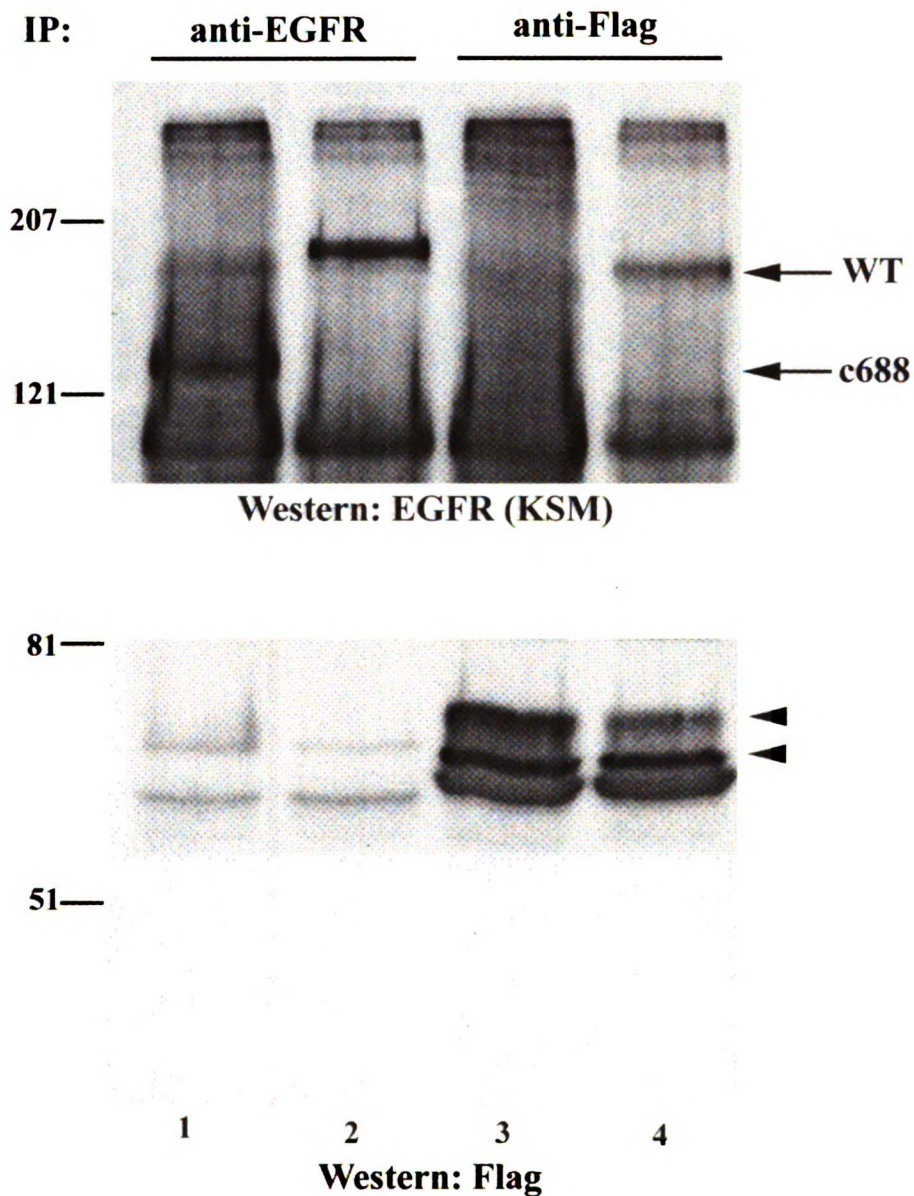


Figure 3.9 Co-immunoprecipitation of wild-type but not cytoplasmically truncated EGFR with hrho. Lysates from HEK-293 cells transiently transfected with pFHR-long + pRK5-EGFRc688 (lanes 1,3) or pFHR-long + pRK5-EGFR (lanes 2,4) were immunoprecipitated with anti-EGFR (lanes 1,2) or anti-Flag (lanes 3,4) and western blotted with anti-EGFR(KSM) (top) or anti-Flag (bottom). The positions of the two forms of EGFR are shown. The double arrowheads indicate forms of hrho detected migrating just above the heavy chain IgG.

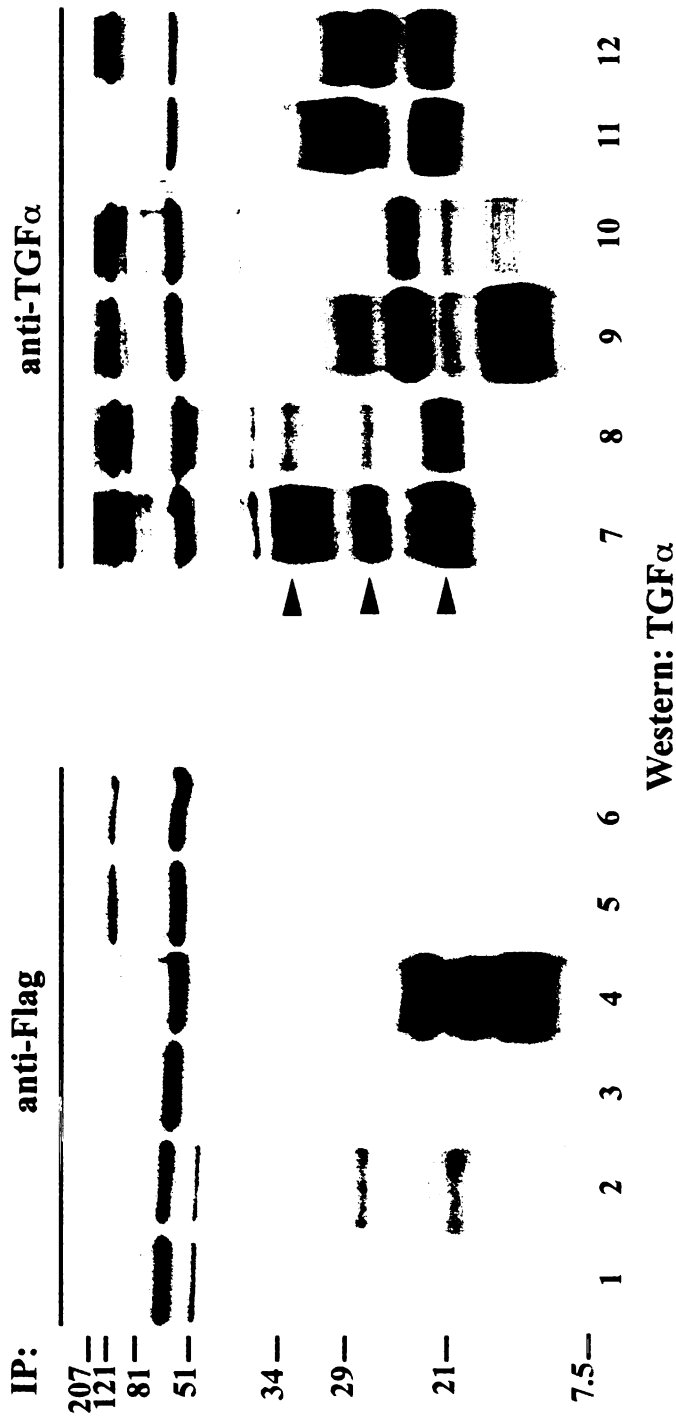


Figure 3.10 Co-immunoprecipitation of wild-type and cytoplasmically truncated but not extracellularly deleted TM-TGF α with hrho. Lysates from HEK-293 cells transiently transfected with vector + pRK7-TGF α (lanes 1,7), pFHR-long + pRK7-TGF α (lanes 2,8), vector + pRK7-TGF α Δ C (lanes 3,9), pFHR-long + pRK7-TGF α Δ C (lanes 4,10), vector + pRK7-TGF α Δ E (lanes 5,11) or pFHR-long + pRK7-TGF α Δ E (lanes 6,12) were immunoprecipitated with anti-Flag (lanes 1-6) or anti-TGF α (lanes 7-12) and western blotted with an anti-TGF α antibody. Arrowheads indicate the three major forms of wild-type TM-TGF α .

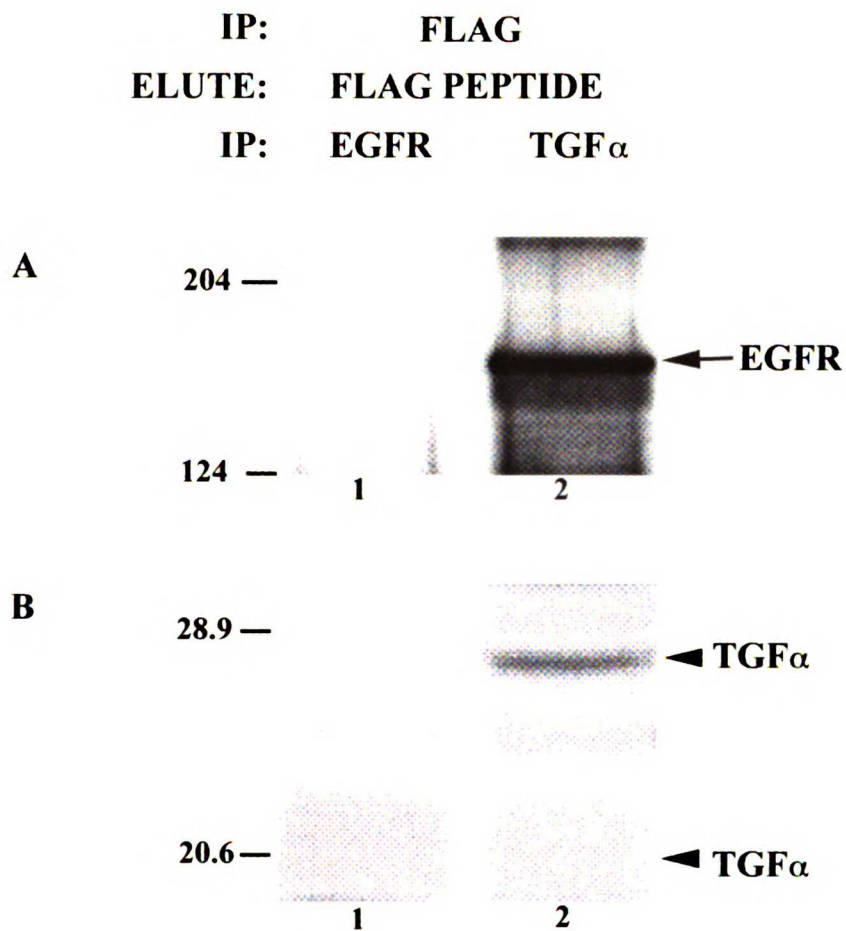


Figure 3.11 Co-immunoprecipitation of EGFR and TGF α with hrho in a tripartite complex. HEK-293 cells were transiently transfected with pFHR-long + pRK5-EGFR + pRK7-TGF α . Cell lysates were immunoprecipitated with anti-FLAG, and the precipitated proteins were eluted with FLAG peptide. The eluted proteins were then immunoprecipitated with anti-EGFR (lanes 1) or anti-TGF α (lanes 2) and western blotted with anti-EGFR (**A**) or anti-TGF α (**B**).

Chapter 4

Functional Characterization of Human Rhomboid

INTRODUCTION

The preceding chapter presented a thorough descriptive characterization of the hRho protein. The hRho protein was found to be structurally similar to dRho, particularly with regard to the lack of a signal sequence, the presence of multiple transmembrane domains, and the presence of a putative PEST domain. The hRho protein was found to localize predominantly in the ER and to a lesser extent at the plasma membrane of the cell. It was shown to physically interact with EGFR, and this interaction specifically required the cytoplasmic domain of EGFR. The hRho protein was also shown to physically interact with TM-TGF α , and this interaction specifically required the core 50 amino acid extracellular domain of TM-TGF α . Finally, some preliminary evidence was presented which suggested that hRho, EGFR, and TGF α might exist in a tripartite protein complex.

All of these data regarding hRho were consistent with the two major hypotheses about the function of dRho in *Drosophila* presented in Chapter 1. The localization data were consistent with a role in processing of the transmembrane TGF α ligand, either intracellularly or at the cell surface. The TM-TGF α physical interaction data were also consistent with a role in processing of the ligand. The EGFR physical interaction data were consistent with additional hypothesized functions of hRho, such as the stabilization of the ligand-receptor interaction or the potentiation of activation of EGFR or downstream signaling molecules.

The studies presented in this chapter sought to evaluate if hRho shared some of these functional properties commonly attributed to dRho. Using the information from

Drosophila genetic studies of dRho, along with the descriptive data accumulated on hRho (Chapter 3), experiments were designed in mammalian cell culture systems to elucidate the cell biological function of this novel protein.

To investigate if hRho expression had an effect on EGFR-MAPK signaling, the pathway was examined at multiple levels. Initial studies used transient transfection methods.

First, transient co-transfection luciferase assays were used to examine the transcription of *c-fos*, a well-characterized early response gene downstream of EGFR-MAPK. Next, the effects of hRho on activation of the EGF receptor were studied. These initial studies proved to be only marginally informative due to technical problems with the transient transfection experiments that will be described in detail.

For additional functional studies, HeLa cells stably expressing hRho were generated.

Using these stable cells, the effects of hRho expression on the soluble or transmembrane ligand induced activation of endogenous EGFR and downstream MAP kinases were examined. In addition, the effect of hRho expression on the rate of DNA synthesis by the stable cells was determined.

To evaluate a putative role for hRho in the processing of the transmembrane TGF α ligand, transient transfection methods were again employed. Pulse-chase experiments were conducted to analyze the effect of hRho on the post-translational processing events involved in TM-TGF α secretion.

Finally, the biological consequences of hRho overexpression were examined *in vivo* by generating hRho transgenic flies. The sensitive wing-vein assay was used to assess the phenotype of hRho itself and to screen for genetic interactions between hRho and the various components of the drosophila EGFR-MAPK signaling pathway.

The overall aim of the work presented in this chapter was to functionally characterize hRho. The experiments were specifically designed to test the hypotheses that hRho overexpression, by analogy to dRho, would result in the potentiation of EGFR-MAPK signaling and/or would affect TM-TGF α processing.

MATERIALS AND METHODS

Plasmid constructs

The c-fos luciferase reporter plasmid p2FTL (a gift from Dr. Gordon Gill, UCSD) was previously described (Chen *et al.* 1987). The plasmid pRK7- β gal (a gift from Xin-Hua Feng) was generated by subcloning the Hind III-Eco RI fragment containing the β -galactosidase coding region from the pSV- β gal plasmid (Promega) into the same sites of the pRK7 vector. The plasmid pRK7-Hygro (a gift from Wen Shi) was generated by subcloning the Xho I-Xba I fragment containing the hydromycin resistance coding region from the pBS-Hygro plasmid (InVitrogen), filling the ends and ligating into pRK7 which had been digested with Hpa I and treated with CIP (Boehringer).

The plasmid pBi5-FHR-long was generated by PCR of the Flag tagged hRho from pFHR-long using the primers “NFLAGRho5”: 5’-
ataagaaagcggccgcatggactacaaggacgacgatgac-3’ and “NrhoSal3”: 5’-
gcggtcgactcagtgaggctgagcgtccagttc-3’ which incorporate a Not I and Sal I restriction site, respectively (underlined). PCR was performed using Pfu polymerase (Stratagene) as described for constructs generated in Chapter 2. The pooled PCR product was cleaned up using a Qiaquick column (Qiagen), sequentially digested with Not I and Sal I, and gel purified. The purified fragment was ligated into the the bidirectional tet response plasmid pBi5 (a gift from Hermann Bujard, ZMBH Heidelberg, Germany; Baron *et al.* 1995) which was sequentially digested with Not I and Sal I, dephosphorylated with CIP (Boehringer) and gel purified. Ligation reactions were performed at room temperature for 3 hours using high concentration T4 DNA ligase (Gibco/BRL).

The plasmid pUAST-FHR-long was generated by sequential digestion of pBi5-FHR-long with Not I and Xba I. The gel purified insert was ligated into the *Drosophila* upstream activator sequence plasmid pUAST (a gift from Ethan Bier, UCSD) which had been sequentially digested with Not I and Xba, dephosphorylated with CIP (Boehringer) and gel purified. Ligation reactions were performed as described above.

The plasmid pUAST-HR-long was generated by digesting the plasmid pHRF-long with Eco RI and Bam HI and the plasmid pFHR-long with Bam HI and Kpn I. The two inserts were ligated into pUAST which had been sequentially digested with Eco RI and Kpn I,

dephosphorylated with CIP (Boehringer) and gel purified. Three way ligation reactions were performed as previously described.

The plasmid pUAST-HRF-long was generated by digesting the plasmid pHRF-long sequentially with Eco RI and Kpn I with a cleanup step in between. The insert was gel purified and ligated into pUAST which had been sequentially digested with Eco RI and Kpn I, dephosphorylated with CIP (Boehringer) and gel purified. Ligation reactions were performed as described above.

c-fos induction experiments

CHO cells grown to ~50% confluence in 6-well plates were transiently transfected with 0.5 ug pRK5-EGFR, 0.5 ug p2FTL, 0.25 ug pRK7- β gal and 0.1 ug of either vector or pFHR-long per well using Lipofectamine (Gibco/BRL) according to the manufacturer's instructions. After transfection, the cells were grown in serum free medium overnight. Followed by stimulation with 5 ng/ml EGF (#324856, Calbiochem) for 24 hours. Cells were lysed in 300 ul/well of 1X Reporter Lysis Buffer (Promega) for 20 minutes at room temperature with rocking, and the lysates were clarified by centrifugation at 14,000 RPM for 3 minutes at 4 C. For luciferase assays, 100 ul of each clarified lysate was mixed with 100 ul of Luciferase Substrate A solution (PharMingen) and assayed on a luminometer (Monolight 2010, Analytical Luminescence) programmed to automatically inject 100 ul of Luciferase Substrate B (PharMingen) and then count light units for 10 seconds. For β -gal assays, typically 10 ul of the same clarified lysate was mixed with 100 ul of 1X Galacton-Plus Reaction Buffer (Tropix) and incubated at 37 C for 30 minutes. The

samples were assayed on the same luminometer programmed to automatically inject 100 μ l of Accelerator II Solution (Tropix) and then count light units for 10 seconds. All experiments were performed in triplicate. Each luciferase value was normalized to its corresponding β -gal value and the mean of the three normalized values was computed along with the standard error of the mean.

β -gal staining experiment

CHO cells grown to ~50% confluence in 6-well plates were transiently transfected with 0.25 μ g pRK7- β gal and 0, 0.05, 0.1, 0.2, 0.4 or 0.8 μ g of pFHR-long per well using Lipofectamine (Gibco/BRL) according to the manufacturer's instructions. As needed, vector DNA was added to achieve the same total amount of DNA for transfection. 48 hours after transfection, the cells were rinsed once in PBS and then fixed in PBS-CMF + 2% paraformaldehyde (Sigma) + 0.2% glutaraldehyde (Sigma) for 5 minutes at room temperature. Following 3 washes with PBS-CMF, the cells were incubated in β -gal Staining Solution (PBS-CMF + 5 mM K-Ferrocyanide (Sigma) + 5 mM K-Ferricyanide (Sigma) + 2 mM $MgCl_2$ (Sigma) + 0.1% X-gal (Gibco/BRL)) at 37 C for 6 hours. The staining solution was then removed, and the cells were rinsed once with water, overlaid with 70% glycerol (Sigma) and stored at 4 C until photography.

EGFR Phosphorylation Assay – Transient Transfections

HEK-293 cells grown to ~60% confluence in 100 mm dishes were transiently transfected with 0.5 μ g of vector or pFHR-long, 2.5 μ g of vector or pRK7-TGF α and 2.5 μ g of pRK5-EGFR using Lipofectamine (Gibco/BRL) according to the manufacturer's

instructions. For the dose response experiment, 2.1 ug of pRK5-EGFR, 2.1 ug of pRK7-TGF α and 0, 25, 50, 100, 200 or 400 ng of pFHR-long were transfected. As needed, vector DNA was added to keep the total amount of transfected DNA constant. The transfected cells were grown in normal growth medium for 48 hours. Preparation of cell lysates and western blots were performed essentially as described in Chapter 2 except that Py Lysis Buffer (25 mM Tris pH 7.5, 150 mM NaCl, 1% NP-40, 2 ug/ml pepstatin A, 4 ug/ml aprotinin, 10 ug/ml leupeptin, 1 mM PMSF, 2 mM EDTA, 50 mM NaF and 0.2 mM Na₃VO₄) was used. Protein concentrations were determined using Protein Assay Reagent (Biorad) and measuring the absorbance at 595 nm on a Shimadzu UV160U Spectrophotometer. Equal amounts of total protein (30 ug) were analyzed on parallel western blots for phosphorylated EGFR, total EGFR, TGF α or hRho using a 1:1000 dilution of anti-phosphotyrosine (Py99, Santa Cruz), a 1:1000 dilution of anti-EGFR (#324862, Calbiochem), a 1:100 dilution of anti-TGF α Ab-1 (#GF06, Calbiochem) or a 1:1000 dilution of anti-Flag M2 (Kodak IBI), respectively. For phosphotyrosine western blotting, the blocking and secondary antibody incubation steps were performed using 5 % bovine serum albumin (BSA, Sigma) instead of non-fat dry milk.

Generation of tetracycline regulated hRho stable cell lines

HeLa-tTA-1 cells (a gift from Dave Morgan, UCSF) were maintained in DME-H16 3g/L glucose (UCSF Cell Culture Facility) supplemented with 10% fetal bovine serum (Hyclone), 100 U/ml penicillin and 100 ug/ml streptomycin (UCSF Cell Culture Facility), and 200 ug/ml G418 (Geneticin, Gibco/BRL) at 37 C, 5% CO₂. The cells were

grown in 100 mm dishes to ~60-80% confluence. 9 ml of fresh medium was added to the cells 2 hours before transfection. The cells were transfected in a 5:1 molar ratio of pBi5-FHR-long or pBi5 to pRK7-Hygro using calcium phosphate precipitation essentially as described (Ausubel *et al.* 1998). Briefly, a total of 10 ug of plasmid DNA was diluted in H₂O to a final volume of 450 ul, to which 50 ul of 2.5 M CaCl₂ was added. This DNA solution was added dropwise to 500 ul of 2X HBS (0.28 M NaCl, 0.05 M HEPES, 1.5 mM Na₂HPO₄ pH 7.05) which was agitated by bubbling air through the solution. The solution was vortexed for 5 seconds and precipitates were allowed to form for 20 minutes at room temperature. The complexes were then added dropwise to the cells. After 16 hours of incubation at 37 C, the transfected cells were rinsed with PBS and fresh medium was added. At ~72 hours, the cells were trypsinized and diluted 1:25 – 1:35 onto several 100 mm dishes and allowed to reattach overnight. At ~96 hours the medium was changed to selection medium (maintenance medium supplemented with 250 ug/ml Hygromycin B (Gibco/BRL) and 1 ug/ml tetracycline-HCl (Sigma)). After 7 to 10 days of selection, single cell colonies were picked with a 20 ul pipette tip and dispersed in trypsin in 48-well plates. 48 pBi5-FHR-long clones and 15 pBi5 clones were expanded in selection medium.

For screening, each clone was seeded into two 35 mm dishes, one containing 1 ug/ml tetracycline and the other containing no tetracycline, and grown for 48 hours. After 48 hours with or without tetracycline, the cells were lysed in 300 ul 1X Reporter Lysis Buffer (Promega) and luciferase assays were performed as described above for the c-fos induction studies. The 7 tet-repressible, luciferase positive clones were grown in the

absence of tetracycline for 48 hours. As a secondary screen, cell lysates were prepared and anti-Flag western blots were performed to detect hRho expression as previously described. To test their tet-repressibility, each of the 3 hRho positive clones was seeded into two 60 mm dishes, one containing 1 ug/ml tetracycline and the other containing no tetracycline, and grown for 48 hours. Cell lysates were prepared and anti-Flag western blots were performed as previously described. Clone #19 was used in subsequent functional studies.

Endogenous EGFR Expression and Phosphorylation in hRho stable cells

To analyze endogenous EGFR expression, stable clone #19 was grown in 100 mm dishes in normal growth medium (DME H-16 3 g/L glucose (UCSF Cell Culture Facility) supplemented with 10% fetal bovine serum (Hyclone), 100 U/ml penicillin and 100 ug/ml streptomycin (UCSF Cell Culture Facility)) with or without 1 ug/ml tetracycline HCl (Sigma) for 48 hours. Cell lysates were prepared in Py Lysis buffer and protein was quantified as described previously. The proteins were resolved on 8% SDS-PAGE and transferred to PVDF membranes as described in Chapter 2. The membrane was then cut with a scissors horizontally below the 121 kd marker. EGFR and Flag western blotting of the top and bottom pieces of the membrane, respectively, were performed as described in Chapters 2 and 3 except that the ECL+ Plus reagent (Amersham) was used according to the manufacturer's instructions to achieve enhanced detection sensitivity.

For analysis of EGFR phosphorylation in response to soluble TGF α ligand, stable clone #19 was grown for 24 hours in in 100 mm dishes in normal growth medium with or

without 1 ug/ml tetracycline HCl (Sigma) for 24 hours. The cells were then grown an additional 24 hours in serum free medium with or without tetracycline and then stimulated for 0, 1 or 5 minutes with 2 ng/ml TGF α (#616430, Calbiochem). The cells were rinsed in PBS, cell lysates were prepared in Py Lysis buffer and protein was quantified as described previously. EGFR immunoprecipitation was performed from equal amounts of total protein (250 ug) as described in Chapter 3. Antiphosphotyrosine western blotting was performed as described above for the transient transfection experiments.

For analysis of EGFR phosphorylation in response to TM-TGF α , stable clone #19 was plated in 60 mm dishes in normal growth medium with 1 ug/ml tetracycline and allowed to adhere overnight. The cells were transiently transfected with 1 ug of either vector or pRK7-TGF α using the Effectene transfection reagent (Qiagen) according to the manufacturer's instructions. Transfections were performed in normal growth medium in the presence of 1 ug/ml tetracycline and were allowed to proceed for 24 hours. The cells were then grown 24 hours in normal growth medium with or without tetracycline followed by 24 hours in serum free medium with or without tetracycline. Cell lysates were prepared in Py Lysis buffer and protein was quantified as described previously. Equal amounts of protein (250 ug) were immunoprecipitated with anti-EGFR and western blotted with anti-phosphotyrosine as described above. In addition, equal amounts of protein (30 ug) were analyzed in parallel TGF α and Flag western blots as described previously.

Endogenous MAP kinase activation in hRho stable cells

For analysis of endogenous p42 and p44 MAP kinase phosphorylation in response to soluble ligand, stable clone #19 was grown in 100 mm dishes in normal growth medium with or without 1 ug/ml tetracycline HCl (Sigma) for 24 hours. The cells were then grown an additional 24 hours in serum free medium with or without tetracycline and then stimulated for 0 or 30 minutes with 20 ng/ml EGF (#324856, Calbiochem). The cells were rinsed in PBS, cell lysates were prepared in Py Lysis buffer and protein was quantified as described previously. Equal amounts of protein (30 ug) were resolved on 8% SDS-PAGE and the transferred to PVDF membranes as described in Chapter 2. The membrane was then cut with a scissors horizontally below the 51 kd marker. A 1:1000 dilution of anti-Flag (Kodak IBI) and a 1:1000 dilution of phosphospecific anti-MAPK (NEB) were used for western blotting of the top and bottom pieces of the membrane, respectively. Western blotting was performed essentially as described previously except that for the phosphospecific anti-MAPK, the primary antibody was diluted in blocking solution containing 5 % non-fat dry milk and the incubation was performed overnight at 4 C.

For analysis of endogenous p42 and p44 MAP kinase phosphorylation in response to TM-TGF α , stable clone #19 was transiently transfected with either vector or pRK7-TGF α using Effectene (Qiagen) as described above. The cells were then grown 24 hours in normal growth medium with or without tetracycline followed by 24 hours in serum free medium with or without tetracycline. Cell lysates were prepared in Py Lysis buffer and

protein was quantified as described previously. Equal amounts of protein (30 ug) were analyzed in parallel TGF α and phosphospecific MAPK western blots as described above.

³H-Thymidine incorporation assays

Stable clone #19 cells were plated at $\sim 2 \times 10^4$ cells per well of a 24-well dish in normal growth medium supplemented with 1 ug/ml tetracycline and allowed to adhere overnight. The cells were grown for 24 hours in normal growth medium in the presence or absence of 1 ug/ml tetracycline. They were then grown for an additional 24 hours in either serum free medium or normal growth medium with or without tetracycline. ³H-thymidine (4 ul/ml; 1 mCi/ml, Dupont-NEN) was then added to the media in each well and allowed to incorporate into newly synthesized DNA for 4 hours at 37 C. The medium was removed, and the cells were washed twice with ice cold PBS to remove unincorporated label. This was followed by fixation/precipitation with 500 ul/well of ice cold 10% trichloroacetic acid (Fisher) for 20 minutes at room temperature. The resulting precipitates were washed twice with 500 ul/well H₂O and solubilized in 250 ul/well of 1 M NaOH by mixing for 20 minutes at room temperature. 250 ul/well of 1 M HCl was added to neutralize the mixture. The samples were transferred to scintillation vials, 4 ml of scintillation fluid (Scintiverse, Fisher) were added and the samples were measured on a Wallac 1409 liquid scintillation counter. Triplicate samples were analyzed for each condition, and the data were presented as the mean \pm standard error of the mean.

Pulse-Chase Experiments

For studies of intracellular TGF α processing, COS cells grown to ~60% confluence in 60 mm dishes were transiently transfected with 2 μ g plasmid DNA using Lipofectamine (Gibco/BRL) according to the manufacturer's instructions. Control cells were transfected with 1.9 μ g vector + 100 ng pRK7-TGF α . Experimental cells were transfected with 1.6 μ g vector + 200 ng pFHR-long + 200 ng pRK7-TGF α . Transiently transfected COS cells were grown in normal growth medium for ~30 hours and then in serum free medium for an additional 18 hours. Following serum starvation, the cells were incubated in cysteine-methionine free DME-H16 3g/L glucose (UCSF Cell Culture Facility) at 37 C for one hour. The cells were then pulse labeled for 20 minutes at 37 C in cysteine-methionine free medium + 250 μ Ci of Easy Tag EXPRESS (NEG-772, NEN) in a final volume of 1 ml. The plates of cells were then transferred to ice, the medium was removed and the cells were washed twice with ice cold PBS to remove unincorporated label. After washing, 1 ml of chase medium (DME-H16 3g/L glucose (UCSF Cell Culture Facility) + 100 μ g/ml cysteine (Sigma) and 100 μ g/ml methionine (Sigma) + 0.1% BSA (Sigma)) was added to the cells and they were returned to the 37 C incubator for 0, 15, 30, 60 or 100 minutes. At each timepoint, the appropriate plates were transferred to ice, the medium was removed and the cells were washed with PBS. Preparation of cell lysates in 1 ml of Py lysis buffer and immunoprecipitation with α 1 Ab (Bringman *et al.* 1987) was performed as previously described. The washed immunoprecipitates were run on 13% SDS-PAGE and the gel was fixed, amplified, dried and autoradiographed as described in Chapter 3.

For studies of TGF α ectodomain shedding, CHO cells grown to ~60% confluence in 60 mm dishes were transiently transfected with 2 μ g plasmid DNA using Lipofectamine according to the manufacturer (Gibco/BRL). Control cells were transfected with 1.85 μ g vector + 150 ng pRK7-TGF α . Experimental cells were transfected with 1.2 μ g vector + 400 ng pFHR-long + 400 ng pRK7-TGF α . Transiently transfected CHO cells were grown in normal growth medium for ~30 hours and then in serum free medium for an additional 18 hours. Following serum starvation, the cells were incubated in cysteine-methionine free DME-H16 3g/L glucose (UCSF Cell Culture Facility) at 37 C for one hour. The cells were then pulse labeled for 2 hours at 37 C in cysteine-methionine free medium + 250 μ Ci of Easy Tag EXPRESS (NEG-772, NEN) in a final volume of 1 ml. The plates of cells were then transferred to ice, the medium was removed and the cells were washed twice with ice cold PBS to remove unincorporated label. After washing, 1 ml of either serum free Chase Medium (DMEM/Ham's F12 (Gibco/BRL) + 0.1% BSA (Sigma)) or Chase Medium supplemented with 20% fetal bovine serum was added to the cells and they were returned to the 37 C incubator for 0 or 30 minutes. The plates of cells were then returned to ice and 900 μ l of the medium was removed from each and transferred to microcentrifuge tubes. The tubes were centrifuged for 1 minute to clarify the samples and then 800 μ l of each clarified sample was transferred to a fresh tube. 200 μ l of IP Mix (170 μ l Py lysis buffer + 30 μ l PAM + 0.5 μ l α 1 Ab) was added to each sample and the tubes were rocked end-over-end at room temperature for 1 hour and then washed in Py lysis buffer as previously described. The washed immunoprecipitates were run on 13% SDS-PAGE and the gel was fixed, amplified, dried and autoradiographed as described in Chapter 3.

Generation of hRho transgenic flies

Transgenic flies were generated by Dr. Annabel Guichard in the lab of Ethan Bier at the University of California, San Diego. White⁻ fly embryos were collected at age 0-1 hour, dechlorinated by bleach treatment (50% bleach, 2 hours and 30 minutes), aligned on double-sided tape and covered with mineral oil. The pUAST-HR-long plasmid and the Delta 2-3 helper construct encoding the P-element transposase (respective concentrations: 800 and 200 ng/ul) were co-injected at the posterior pole of the embryo (the site of germ cell development). The survivors that reached adulthood were crossed to white⁻ flies, and the transformants were scored in the progeny of this second cross. Transformants were identified by their orange colored eyes. Transformant lines were established individually, and the chromosomal location of each insert was established using standard genetic methods.

RESULTS

TRANSIENT TRANSFECTION EXPERIMENTS

Effect of hRho expression on c-fos induction

Transcription of the c-fos gene, a known downstream target of the EGFR-MAPK pathway (Marais *et al.* 1993, Hill *et al.* 1993, Muller *et al.* 1984), was used to determine the effect of hRho expression on this pathway. These experiments utilized the reporter construct p2FTL consisting of two tandem c-fos promoter elements in front of a thymidine kinase minimal promoter fused to the firefly luciferase gene (Chen *et al.* 1987). CHO cells were transiently transfected with pRK5-EGFR, p2FTL, a pRK7- β gal (as internal control) and either empty vector or pFHR-long. In a preliminary series of experiments, lysates were prepared from transfected cells that were either left untreated or treated with soluble EGF. The luciferase and β -galactosidase activities of each lysate were measured. When the data were analyzed in the standard fashion in which the luciferase activity is normalized to the β -galactosidase activity, there was an apparent increase in the EGF stimulated c-fos induction in the hRho transfectants compared to the vector transfected controls (Figure 4.1A). However, when the luciferase and β -galactosidase activities were analyzed separately, there was actually a decrease in the luciferase activity and an even more pronounced decrease in the β -galactosidase activity in the hRho transfectants relative to controls (Figure 4.1 B and C). Subsequent experiments utilizing transfected TM-TGF α , instead of exogenously added soluble EGF, yielded similar results (data not shown).

Downregulation of expression from genes co-transfected with hRho

The decrease in c-fos luciferase activity in the hRho transfectants could have been due to decreased expression of EGFR, resulting in a decreased responsiveness of the cells to the soluble EGF ligand. To address this possibility, CHO cells were transiently transfected with vector, vector + pRK5-EGFR, pRK7- β gal + pRK5-EGFR, or pFHR-long + pRK5-EGFR, and the level of EGFR expression was assessed by western blot. There was a dramatic decrease in EGFR expression in the presence of hRho expression (Figure 4.2 lane 4). This decrease was not attributable to a non-specific effect of co-transfection since co-transfected pRK7- β gal did not alter the level of EGFR expression (Figure 4.2 lane 3).

Decreased EGFR expression might explain (at least in part) the decrease in c-fos luciferase activity since the c-fos gene is a downstream target of a receptor mediated signaling pathway. However, this mechanism could not account for the observed decrease in β -galactosidase activity nor was there an obvious explanation for the decrease in EGFR expression upon co-expression of hRho. To further explore this phenomenon, CHO cells were co-transfected with a fixed amount of pRK7- β gal plasmid and an increasing amount of the pFHR-long plasmid, and the transfected cells were stained with X-gal. Where needed, vector DNA was added to assure that the same total amount of DNA was transfected for each condition. As shown in Figure 4.3, there was an hRho dose dependent decrease in the number of cells stained blue by the X-gal substrate. In addition, the cells that did stain were a lighter shade of blue than cells that stained in the absence of hRho expression.

Effect of hRho expression on EGFR phosphorylation

In addition to studying c-fos induction as a downstream readout of EGFR-MAPK activation, experiments were performed to address whether hRho might modulate this pathway at the level of the EGF receptor itself. Transient co-transfection experiments were performed both in CHO cells, which lack EGFR, and HEK-293 cells that express very low levels of endogenous EGFR. To assess possible effects of hRho on either the basal or ligand stimulated phosphorylation of EGFR, cells were transiently co-transfected with vector + pRK5-EGFR \pm pRK7-TGF α or pFHR-long + pRK5-EGFR \pm pRK7-TGF α and lysates were analyzed in parallel western blots for phosphorylated EGFR and total EGFR using anti-phosphotyrosine and anti-EGFR antibodies, respectively. Consistent with previous observations, the total EGFR expression level was lower in the presence of hRho compared to vector controls (Figure 4.4B lanes 3 and 4 vs. lanes 1 and 2). The TGF α level was also decreased in the presence of hRho although the decrease was more moderate than that seen for EGFR (Figure 4.4C lane 4 vs. lane 2). In contrast, the level of TGF α -stimulated EGFR phosphorylation was either the same or slightly increased in the presence of hRho (Figure 4.4A lane 4 vs. lane 2). Therefore, when considered as a ratio of phosphorylated receptor to total receptor, it appeared that hRho expression led to an increased proportion of EGF receptors in the active state.

To determine if the effect of hRho on EGFR was dose dependent, HEK-293 cells were transfected with a fixed amount of pRK5-EGFR and pRK7-TGF α and an increasing amount of pFHR-long. Where needed, vector DNA was added to the transfection in order to keep the total amount of DNA in each transfection constant. Cell lysates were

analyzed in parallel western blots as described above. A dose-dependent decrease in EGFR expression was observed while the level of phosphorylated EGFR remained constant (Figure 4.5). Thus, increasing hRho expression levels led to an apparent increase in the proportion of EGF receptors in the activated state.

STABLE TRANSFECTION EXPERIMENTS

Generation of a tetracycline regulatable cell line stably expressing hRho

In an effort to circumvent some of the problems encountered in the transient transfection experiments, stable cell lines were generated to permit the analysis of the effects of hRho on endogenous rather than co-transfected genes. N-terminally Flag tagged hRho was subcloned into the bidirectional expression vector pBi-5, which allows for tetracycline regulatable expression of both hRho and a luciferase reporter gene simultaneously. This construct (Figure 4.6) was co-transfected with the hygromycin resistance plasmid pRK7-Hygro into the HeLa tTA-1 cell line, and selection was performed with hygromycin. In addition, tetracycline was present in the culture medium to repress hRho expression during the selection.

Several single-cell clones were expanded, and a simple luciferase assay was used as a primary screen for tet regulated gene expression. Seven tet repressible, luciferase positive clones were identified and subjected to anti-Flag western blotting as a secondary screen for hRho expression. Three of the seven luciferase positive clones expressed the ~60 kd hRho protein (Figure 4.7). The three hRho positive clones were then tested to

determine if the hRho expression was tet repressible. For two of the clones, hRho expression was fully repressed by 1 ug/ml of tetracycline in the culture medium (Figure 4.8A #10 and #19). HRho expression in the third clone was only partially repressed by this concentration of tet (Figure 4.8A #26). Clone #19 was then grown with various concentrations of tet in the culture medium and cell lysates were analyzed by western blotting with anti-Flag. As shown in Figure 4.8B, the level of hRho expression was repressed in a tet dose-dependent fashion. The repression occurred over two orders of magnitude of tet concentration, ranging from unrepressed at 0.001 ug/ml to fully repressed at 0.1 ug/ml. Northern blot analysis confirmed the tet repressibility of clone #19. The mRNA corresponding to the exogenously introduced hRho cDNA was repressed in the presence of tetracycline and upregulated in its absence. Notably, no endogenous hRho was detected in the parental HeLa-tTA cells in either the presence or absence of tetracycline (data not shown).

Effect of stably expressed hRho on expression of endogenous EGFR

Since the transient transfection experiments designed to examine the effect of hRho on EGFR activation were complicated by the fact that hRho reduced the EGFR expression, it was important to assess whether this complication had been eliminated by stable integration of the hRho expression plasmid. Stable clone #19 was grown in the presence and absence of tetracycline and equal amounts of protein from the two cell lysates were analyzed by western blotting. Since the molecular weight of EGFR is ~170 kd and that of hRho is ~60 kd, they were easily resolved on SDS-PAGE. Therefore, the blotting membrane was cut horizontally, and the top was probed with anti-EGFR antibodies while

the bottom was probed with anti-Flag antibodies to detect hRho. As shown in Figure 4.9, the hRho protein was strongly expressed in the absence of tetracycline, yet this had no impact on the endogenous EGFR expression level.

Effect of stably expressed hRho on activation of endogenous EGFR

Having verified that hRho expression did not alter EGFR levels in this stable expression system, the effect of hRho expression on soluble TGF α ligand-stimulated EGFR activation was examined. An optimal ligand dose and duration were determined empirically. A dose of 2 ng/ml and timepoints ranging from 1 minute to 5 minutes resulted in approximately half maximal stimulation of the receptor such that either increases or decreases in stimulation due to hRho expression would be easily detected (data not shown). Stable clone #19 was grown for 24 hours in the presence or absence of tetracycline and then switched to serum free medium (again in the presence or absence tetracycline) for an additional 24 hours. The serum starvation served to reduce the background level of EGFR stimulation which might occur through EGFR ligands present in serum or through cross-talk from other serum growth factor stimulated signaling pathways. After starvation, the cells were either left untreated or stimulated with the 2 ng/ml TGF α for 1 minute or 5 minutes. Equal amounts of protein from cell lysates were immunoprecipitated with anti-EGFR antibody and western blotted with anti-phosphotyrosine antibody. Expression of hRho had no effect on the basal unstimulated level of endogenous EGFR phosphorylation (Figure 4.10 lanes 1 and 2). Furthermore, there was no effect of hRho overexpression on the ligand-stimulated level of EGFR

phosphorylation after 1 minute (Figure 4.10 lanes 3 and 4) or 5 minutes (Figure 4.10 lanes 5 and 6) of stimulation.

Given the physical interaction between hRho and transmembrane TGF α described in Chapter 3 and the hypothesis that hRho might influence processing of the transmembrane ligand, it was also important to test for an effect of hRho on EGFR activation mediated by this form of the ligand. Stable clone #19 was transiently transfected with either vector or pRK7-TGF α in the presence of tetracycline. The transfected cells were then cultured in normal growth medium with and without tetracycline for 24 hours followed by 24 hours in serum free medium with and without tetracycline. Equal amounts of protein from cell lysates were then immunoprecipitated with anti-EGFR and western blotted with anti-phosphotyrosine. Parallel western blots were performed on equal amounts of protein from the same lysates using anti-TGF α and anti-Flag antibodies. As in the previous experiment, expression of hRho had no effect on the basal unstimulated level of endogenous EGFR phosphorylation (Figure 4.11 lanes 1 and 3). Again, there was no convincing effect of hRho overexpression on the ligand-stimulated level of EGFR phosphorylation (Figure 4.11 lanes 2 and 4).

Effect of stably expressed hRho on MAPK activation

Despite the absence of an effect on EGFR activation, additional experiments were performed to explore whether hRho expression could modulate the activation of the two major MAP kinases p44 (ERK1) and p42 (ERK2). To assess the effect of hRho expression on soluble ligand-stimulated MAPK activation, a preliminary experiment was

performed using EGF. Stable clone #19 was grown for 24 hours in the presence or absence of tetracycline and then switched to serum free medium (again in the presence or absence tetracycline) for an additional 24 hours. After starvation, the cells were either left untreated or stimulated with 20 ng/ml EGF for 30 minutes. Equal amounts of protein from the cell lysates were western blotted with anti-Flag antibody to detect hRho or with phosphospecific anti-MAPK antibodies. Expression of hRho had no effect on the basal unstimulated level of endogenous MAPK phosphorylation (Figure 4.12 lanes 1 and 2). Furthermore, there was no effect of hRho overexpression on the ligand-stimulated level of MAPK activation (Figure 4.12 lanes 3 and 4) after 30 minutes of EGF stimulation.

Again, since the signal from the transmembrane TGF α ligand might be regulated or modulated differently from that of soluble TGF α , an experiment was conducted to examine the effect of hRho expression on endogenous MAP kinase activation resulting from TM-TGF α expression. Stable clone #19 was transiently transfected with either vector or pRK7-TGF α in the presence of tetracycline. The transfected cells were then cultured in normal growth medium with and without tetracycline for 24 hours followed by 24 hours in serum free medium with and without tetracycline. Parallel western blots were performed on equal amounts of protein from the same lysates using anti-TGF α and phosphospecific anti-MAPK antibodies. As in the previous experiment, expression of hRho had no effect on the basal unstimulated level of endogenous MAP kinase phosphorylation (Figure 4.13 lanes 1 and 3). Again, there was no effect of hRho overexpression on the ligand-stimulated level of MAP activation (Figure 4.13 lanes 2 and 4).

Effect of stably expressed hRho on DNA synthesis

Although it did not appear that hRho expression affected EGFR-MAPK signaling, it was possible that some other signaling pathway in the cell was modulated. As a general readout for possible affects of hRho expression on other cellular signaling pathways, the DNA synthesis of the hRho stable cell line was quantified by measuring the incorporation of tritiated thymidine. Stable clone #19 was grown in normal growth medium for 24 hours in the presence or absence of tetracycline. The cells were grown for an additional 24 hours in either normal growth medium or serum free medium with or without tetracycline. Next, the cells were pulse labeled with tritiated thymidine, and scintillation counting of cell lysates was used to measure the incorporation. Under serum free conditions, there was no significant difference in DNA synthesis in presence and absence of tetracycline (Figure 4.14, left), but in 10% serum there was a two-fold decrease in DNA synthesis in the absence of tetracycline (Figure 4.14, right). To control for the possibility that the tetracycline itself or some other component of the tet expression system might alter the level of DNA synthesis, three control clones stably transfected with the empty pBi5 vector were tested as described above. In 10% serum all three control clones showed a similar reduction in DNA synthesis in the absence of tetracycline (Figure 4.15).

TM-TGF α PROCESSING STUDIES

Effect of hRho expression on intracellular processing of TM-TGF α

To determine if hRho expression affected the intracellular processing of TM-TGF α , a “pulse-chase” experiment was performed. Transiently transfected COS cells were serum starved overnight, metabolically labeled for a short “pulse” and then “chased” with serum free medium for varying lengths of time. Cell lysates from each timepoint were immunoprecipitated with anti-TGF α antibodies and run on SDS-PAGE gels that were then dried and autoradiographed. From preliminary experiments, it was determined that hRho expression reduced the level of co-expressed TM-TGF α approximately two-fold (data not shown). Therefore, to compensate for this effect, twice as much pRK7-TGF α plasmid was co-transfected with pFHR-long in the experimental transfections than with vector in the control transfections.

The amounts of the core glycosylated proTM-TGF α precursor were approximately equal in the control and hRho expressing cells at the zero timepoint (Figure 4.16 middle arrowhead, lanes 1 and 6). By 30 minutes, a substantial quantity of fully glycosylated proTM-TGF α was generated in control cells, while significantly less was detected in hRho expressing cells (Figure 4.16 top arrowhead, lanes 3 and 8). In addition, the amount of the precursor had decreased more in the hRho expressing cells (Figure 4.16 middle arrowhead, lanes 3 and 8). By 100 minutes, a substantial quantity of the mature TM-TGF α lacking the pro-domain was generated in control cells while, significantly less was detected in hRho expressing cells (Figure 4.16 bottom arrowhead, lanes 5 and 10). Unlike in control cells, almost none of the fully glycosylated proTM-TGF α and very little

of the core glycosylated proTM-TGF α remained in the hRho expressing cells at this timepoint (Figure 4.16 top and middle arrowheads, lanes 5 and 10).

Effect of hRho expression on the processing of the TM-TGF α ectodomain

To examine possible effects of hRho expression on the shedding of the TM-TGF α ectodomain, CHO cells were used in a similar “pulse-chase” type of experiment. Again, more pRK7-TGF α was co-transfected with pFHR-long for the experimental cells than with vector for the control cells. Transiently transfected CHO cells were serum starved overnight, metabolically labeled for a short “pulse” and then “chased” with either serum free medium or medium supplemented with 20% serum for 30 minutes. To determine the levels of TGF α released, the culture medium was immunoprecipitated with anti-TGF α antibodies and the precipitated proteins were run on SDS-PAGE gels which were then dried and autoradiographed. At the zero timepoint, no secreted TGF α was detectable in the medium from control or hRho expressing cells (Figure 4.17 lanes 1 and 4). After a 30 minute chase in serum free medium, two forms of TGF α were detected in the medium from both control and transfected cells. The higher molecular weight form (Figure 4.17 upper arrow) results from the cleavage of the ectodomain of the fully glycosylated proTM-TGF α while the lower molecular weight form (Figure 4.17 lower arrow) results from the cleavage of the mature TM-TGF α lacking the pro-domain. There was slightly less of both forms present in the medium from the hRho expressing cells compared to the medium from the control cells (Figure 4.17 lanes 2 and 5). After a 30 minute chase in medium supplemented with 20% serum, the same two forms of TGF α were detected in the medium from both control and transfected cells. However, as a result of serum

stimulation, there was a significant increase in the amounts of both forms released from control cells, while no such increase was detected in medium of hRho expressing cells (Figure 4.17 lanes 3 and 6).

IN VIVO EXPERIMENTS – hRho TRANSGENIC FLIES

Through a collaboration with Dr. Ethan Bier's laboratory, genetic experiments were performed in *Drosophila* to determine what, if any, biological activity hRho had *in vivo*. It was of particular interest to determine the phenotype resulting from overexpression of hRho and to compare this with the dRho overexpression phenotype. To achieve this objective, the highly sensitive and well-defined wing vein assay described in Chapter 1 was utilized. The hRho cDNA was subcloned into the *Drosophila* expression vector pUAST behind an hsp70 minimal promoter preceded by a Gal4 upstream activating sequence (Figure 4.18). These constructs were microinjected into drosophila embryos to generate transgenic flies. To achieve tissue specific expression, the transformants were crossed to "driver" flies that expressed high levels of Gal4 protein in the wing (Brand and Perrimon 1993). The wing vein pattern of the progeny was analyzed. Compared to a normal wild-type wing (Figure 4.19 A), the dRho overexpression flies had extra and thicker veins. Since a strong driver line was used for this analysis, this resulted in a very strong dRho phenotype, such that most of the wing surface was converted to vein material and the two wing surfaces were partially separated (Figure 4.19 B). The hRho overexpression flies also had extra veins (to a lesser degree) and thicker L1, L3 and L5

veins (Figure 4.19 C). In addition, the hRho overexpression flies showed a reduced wing blade, a disrupted wing margin and an overall higher rate of lethality.

To assess whether the observed hRho phenotype was mediated by effects of the hRho transgene on the *Drosophila* EGF receptor (DER), a genetic interaction study was performed in a manner similar to those involving dRho flies described in Chapter 1 (Sturtevant *et al.* 1993). The hRho overexpression flies were crossed to a fly line carrying a dominant negative EGF receptor (dnDER), driven by the same wing-specific driver, and the progeny of this cross were analyzed. The phenotype of the progeny resembled that of dnDER alone in that fewer wing veins developed, particularly L3, the anterior cross-vein and the distal part of L5 (Figure 4.19 compare F to D and contrast with A).

A “rescue” type experiment was also conducted to establish whether hRho expression could complement a deficiency of dRho expression. The hRho overexpression flies were crossed to flies in which endogenous dRho was only weakly expressed in the wing, and the wing vein pattern of the progeny was analyzed. HRho overexpression was unable to compensate for the reduced dRho expression (data not shown).

DISCUSSION

While the preceding chapter focused on a descriptive characterization of hRho, the work presented in this chapter focused on elucidating the functional properties of this novel protein. Specifically, the physical interaction of hRho with TGF α and EGFR suggested a line of experimentation to pursue. Experiments were based on the hypothesized role of hRho in potentiating EGFR-MAPK signaling in analogy to the apparent role dRho plays in *Drosophila*. The basic approach taken was to overexpress the hRho protein in mammalian cell culture and measure the effect(s) on various components of this pathway.

The initial overexpression studies were performed by transient transfection of the epithelial cell lines CHO and HEK-293. Several properties of these cell lines made them ideal for these experiments. First, they are highly transfectable and express large amounts of protein from transfected plasmids. Second, it is well established that major mammalian signaling pathways can be reconstituted in these cell lines. Lastly, CHO cells lack EGFR and HEK-293 cells express very low levels of EGFR which are not detectable on western blot. This allowed for a greater signal-to-noise ratio, since only cells transfected with exogenous EGFR were capable of generating a significant response to ligand treatment.

The first set of transient transfection experiments examined transcriptional induction of the c-fos gene, a well-characterized downstream target of EGFR signaling (Marais *et al.* 1993, Hill *et al.* 1993, Muller *et al.* 1984). Experiments began here because of the relative simplicity of the assay and the quantitative nature of the readout. The

experiments utilized a c-fos luciferase reporter that had previously been demonstrated to respond to EGF stimulation in transient transfection assays (Chen *et al.* 1987). Transient transfection-luciferase assays commonly employ an internal control expression plasmid for β -galactosidase that allows for normalization of the luciferase value. This corrects for possible well-to-well variations in transfection efficiency or cell lysate preparation. For such a plasmid to serve as a proper internal control, it must meet certain criteria: The encoded protein must be detectable in the same sample that is measured for the primary readout, and its expression must not interfere with the primary readout. In addition, expression of the internal control protein must not be regulated by, or vary with, the biological process being studied. In the studies presented here the pRK7- β gal plasmid did not satisfy the last of these criteria. The β -gal expression, as measured both by activity assay (Figure 4.1C) and by colorimetric substrate staining (Figure 4.3), was decreased by co-expression of hRho in a dose dependent fashion. This downregulation was not CMV promoter specific, since pRSV- β gal was affected similarly (data not shown). This result was surprising because the β -gal gene was expressed under the control of the CMV or RSV promoter. Both are considered to be strong, constitutively active viral promoters and presumably should not have been subject to this kind of regulation.

The decreased number of blue cells observed in the staining experiment was not likely due to differences in transfection efficiency. The same total amount of plasmid DNA was used in each transfection, and the slight variations that occur under these conditions would not account for the dramatic differences observed in these experiments. In

addition, the cells that did stain blue appeared lighter in color than those which stained blue in the absence of hRho. Therefore, it is likely that the transfection efficiencies were relatively equal but that fewer cells expressed high enough levels of β -gal enzyme activity to cleave the colorimetric substrate and turn blue. Those that did express high enough activity to turn blue still expressed significantly lower levels than cells which did not express hRho, thus accounting for their lighter blue color. Apparently, hRho expression resulted in the general suppression of cellular transcription or translation by an as yet unidentified mechanism. This suppression was EGFR independent since CHO cells are EGFR negative, and the effect was observed when only the pFHR-long and pRK7- β gal plasmids were transfected. This is consistent with the fact that even the ligand independent luciferase and β -galactosidase activities (Figure 4.1 “-EGF”) were decreased in the presence of hRho expression.

Further studies demonstrated that β -gal was not the only gene that was “downregulated” in the presence of hRho expression. The EGFR gene, which was co-transfected into CHO cells to make them EGF responsive, was dramatically downregulated (Figure 4.2). This downregulation was most likely responsible for the decrease in c-fos luciferase activity observed in the hRho transfectants. The magnitude of the decrease in luciferase activity was less than that of the β -gal activity. Therefore, when the data were normalized, there was an *apparent* increase in the luciferase activity of the hRho transfectants relative to vector transfected controls.

Whether this represented a true induction of c-fos transcription by hRho was difficult to discern. The decreases in β -gal activity and EGFR expression might be interpreted as a decline in the general transcriptional activity or protein synthesis capacity of the cell. The argument could be made that since the c-fos luciferase activity did not decline as much, c-fos transcription was actually increased relative to the overall transcription in the cell. Alternatively, since the components of the system under study were changing, the experiment could be considered to have had multiple variables rather than the single variable of hRho expression. This would bring experimental control, and hence the validity of the data, into question.

Another approach was taken to examine the effect of hRho expression on EGFR-MAPK signaling. Experiments were performed to evaluate whether hRho modulated this pathway at the level of the EGF receptor itself. A direct activity of hRho on EGFR would have been consistent with the physical interaction between hRho and EGFR described in Chapter 3. EGFR signaling is activated by ligand binding which results in dimerization of the receptor and autophosphorylation of specific cytoplasmic tyrosine residues in trans (Lemmon and Schlessinger 1994). The “activated” receptor is then capable of interacting with a variety of downstream signaling molecules. Hence, the activation of the EGF receptor under various conditions can be monitored by analyzing its phosphorylation state using anti-phosphotyrosine antibodies for western blot analysis. Experiments were therefore performed to explore whether hRho could modulate the activation of EGFR.

The suppression phenomenon observed in the c-fos experiments also complicated these experiments. Examination of the effect of hRho expression on EGFR phosphorylation was confounded by the fact that the EGFR expression level declined in a dose dependent fashion with increased hRho expression (Figure 4.5 middle). Analogous to the luciferase and β -gal data described above, hRho expression caused the EGFR phosphorylation level to remain essentially unchanged, while the EGFR expression level decreased substantially (Figures 4.4 and 4.5). Again, when the data were normalized, there was an *apparent* increase in the EGFR phosphorylation in hRho transfectants relative to controls. The interpretation of these data is subject to the same caveats outlined above for the c-fos induction data.

While the data acquired from transient transfection experiments suggested a role for hRho in the amplification of signaling from the EGF receptor, the interpretation of the results was complicated by the fact that the expression level of the components being studied varied under the different experimental conditions. In addition, the transient approach did not allow for a direct examination of the activation of MAP kinases such as ERK1 and ERK2. Only a sub-population of cells is transfected in such experiments, yet the MAP kinases are endogenous to all cells and can be stimulated by multiple signaling pathways in addition to the EGFR pathway (reviewed in Robinson and Cobb 1997). For these reasons, a cell line stably expressing hRho was needed. HeLa cells were chosen because they express moderate levels of endogenous EGFR and also express low levels of endogenous TGF α (Derynck *et al.* 1987). Thus, they contained some of the key components of the signaling pathway being studied.

Due to the suppressive effects of hRho on genes which were co-expressed under strong CMV promoters, there was a concern that hRho might be toxic to cells. However, there was no apparent increase in the level of cell death in the transient transfection experiments in which hRho was overexpressed. Nonetheless, even mild toxicity might put transfected cells at a growth disadvantage during the antibiotic selection of stable clones. In addition, there was the possibility that hRho would suppress the expression of the co-transfected antibiotic resistance gene. As a consequence, very few clones expressing hRho would grow out.

To avoid these potential problems, the tetracycline or “tet” system (Gossen and Bujard 1992) was chosen to allow for regulated, rather than constitutive, expression of hRho in stable cell lines. Stable clones could then be selected in the presence of tetracycline to keep hRho expression “off” during the selection process. This strategy proved successful, and three hRho stable cell lines were established (Figure 4.7). All three lines demonstrated tetracycline regulatable hRho expression (Figure 4.8A). Clone #19 was chosen for use in subsequent functional studies because the expression of hRho could be tightly regulated in this cell line.

Before using this stable clone in the kinds of functional studies attempted in transient transfections, it was important to verify that overexpression of hRho in this system did not affect the endogenous level of EGFR expression. Indeed, the EGFR expression level was unchanged by overexpression of hRho protein (Figure 4.9 top). This could have been due to the stable integration of the hRho plasmid. Lower expression levels are

typically obtained in stable cell lines, due in part to the smaller number of expression plasmids in the cell compared to the large amounts present in transiently transfected cells. An additional explanation is that unlike the viral promoters used in the transient transfection experiments, expression of endogenous EGFR from its natural promoter was apparently not subject to the suppressive effects of hRho overexpression.

Given that EGFR levels were unchanged by hRho expression, if hRho potentiates EGFR signaling, it must do so by some mechanism other than increasing the level of receptor. Rather than increase the total *number* of receptors, hRho expression might increase the *activation level* of the existing receptors. This was evaluated by examining the level of phosphorylation of EGFR in the absence and presence of hRho expression. Variations on this experiment included comparisons between the basal EGFR phosphorylation levels (Figures 4.10 and 4.11), between soluble ligand-stimulated EGFR phosphorylation levels (Figure 4.10) and between transmembrane ligand-stimulated EGFR phosphorylation levels (Figure 4.11) in the absence and presence of hRho expression. These experiments were perfectly internally controlled, since the only variable was the presence or absence of tetracycline in culture medium. Theoretically this should have only directly affected the expression of hRho. In each of these experiments, the ligand increased the level of EGFR phosphorylation to the same extent regardless of whether or not hRho was expressed.

There are several possible explanations for why stably expressed hRho had no effect on endogenous EGFR phosphorylation. One possibility is that already high levels of

endogenous hRho in HeLa-tTA cells prevented stably expressed hRho from having any additional effects. This possibility was ruled out by the fact that no endogenous hRho message was detected on a Northern blot of RNA prepared from HeLa-tTA cells.

Another possibility is that hRho might modulate the *duration* of EGFR activation rather than the *level* of activation. Alternatively, hRho might bind to the receptor in order to modulate some downstream cytoplasmic process (see below) rather than the process by which the EGFR itself is activated. This explanation is more difficult to reconcile with the data that demonstrate a physical interaction between hRho and TM-TGF α , since such an interaction suggests that hRho acts either upstream or on the EGF receptor. Still, it is possible that the proteins form a complex on either the plasma membrane or some intracellular membrane and that this complex might then recruit or influence the activity of some cytoplasmic factor(s). Lastly, additional protein(s) might be required for hRho to mediate its effects on EGFR. The additional protein(s) might not be expressed by HeLa cells or might be present in substoichiometric levels. Recent evidence from studies in *Drosophila* support this latter explanation. As discussed in Chapter 1, experiments have demonstrated both a synergy and a co-dependence between dRho and the single transmembrane protein star (Guichard *et al.* 1999).

Despite the inability to detect an effect of hRho expression on EGFR phosphorylation, it was still possible that hRho might affect MAP kinase activation. For example, hRho might bind to EGFR not to assist in its activation, but rather to help recruit downstream signaling molecules to the activated receptor. As discussed in Chapter 1, ligand binding by EGFR and other growth factor receptors normally results in activation of the receptor.

This in turn results in recruitment of downstream signaling molecules to the activated receptors. Many such pathways converge upon the extracellular signal related kinases, or ERKs, of which the two most well characterized are ERK1 (p44 MAPK) and ERK2 (p42 MAPK). Recall that activation of these proteins is through dual phosphorylation of specific serine and threonine residues (Payne *et al.* 1991). Hence, the activation of these MAP kinases under various conditions can be monitored using phosphospecific antibodies for western blot analysis. Experiments were therefore performed to explore whether hRho could modulate the activation of the two major MAP kinases p44 (ERK1) and p42 (ERK2). Similar to the EGFR experiments described above, comparisons were made between the basal MAPK phosphorylation levels (Figures 4.12 and 4.13), between soluble ligand-stimulated MAPK phosphorylation levels (Figure 4.12), and between transmembrane ligand-stimulated MAPK phosphorylation levels (Figure 4.13) in the absence and presence of hRho expression. Again, in each of these experiments, the ligand increased the level of MAPK phosphorylation to the same extent regardless of whether or not hRho was expressed.

Explanations similar to those outlined above for EGFR activation apply to the absence of an effect of hRho expression on MAP kinase activation. The hRho protein might modulate the timing or duration of MAP kinase activation rather than the magnitude. Again, the absence of stoichiometric levels of additional factors such as star might have prevented an effect from being observed.

Although hRho overexpression alone apparently had no detectable effect on EGFR-MAPK signaling, an effect on other signaling pathways could not be excluded. There are certainly numerous other growth factor receptors and transcription factors in the cell, and although experiments in *Drosophila* have demonstrated a role for dRho in DER signaling, the biology is likely to be more complex in higher organisms. One mammalian homologue of dRho might indeed potentiate EGFR-MAPK signaling while another homologue of dRho might, for example, modulate TGF β -Smad signaling. As discussed in Chapter 2, at least two human homologues of dRho exist: rrp and hRho. Different rho's may provide the mammalian cell with a more complex yet more intricately regulated set of responses to stimuli such as growth factors. Since signaling from a variety of different pathways often results in changes in gene transcription which affect cell proliferation, it was important to test for this more general affect of hRho overexpression on the cell. DNA synthesis, as measured by the incorporation of tritiated thymidine, is a convenient surrogate for measuring cell proliferation directly. The assay was performed on hRho stable cells under both serum free and normal (10% serum) growth conditions. Under serum free conditions, there was no effect of hRho overexpression on the level of DNA synthesis. In serum containing medium, there was an apparent twofold reduction in the level of DNA synthesis in the presence of hRho (Figure 4.14). However, a subsequent experiment performed on control clones, which expressed tet regulatable luciferase but not hRho, revealed that this was a non-specific effect of the tet system itself, rather than a specific effect of hRho overexpression (Figure 4.15). This effect of the tet system on the DNA synthesis of HeLa-tTA cells has not been well-documented but might be explained by nonspecific binding of the tTA protein in the

absence of tetracycline to sites other than tet operator sequences in the genome. Such inappropriate binding might adversely affect the transcription of nearby host genes that normally regulate DNA synthesis.

Since hRho expression did not result in a detectable potentiation of EGFR-MAPK signaling at the level of the receptor or the major downstream MAP kinases, and since no specific effect was observed on DNA synthesis, the focus of experimentation shifted to the ligand TM-TGF α . It seemed feasible that hRho expression might affect transmembrane ligand synthesis, transport or processing in a manner that might have been difficult to detect using the standard signaling assays described in the preceding sections. Therefore, “pulse-chase” experiments were undertaken to follow the post-translational events that occur as TGF α traverses the secretory pathway of the cell and is released into the extracellular space. Recall from Chapter 1 that three major forms of TM-TGF α can typically be immunoprecipitated from cell lysates: the core glycosylated proTM-TGF α , the complex glycosylated proTM-TGF α , and the mature TM-TGF α which has undergone processing to remove the glycosylated pro-domain. In addition, under optimized conditions, two soluble forms of processed TGF α ligand can be immunoprecipitated from the culture medium: a major 6 kd form which derives from mature TM-TGF α and a minor larger form which derives from complex glycosylated proTM-TGF α .

Although HeLa cells have been shown to express low levels of TGF α as measured on Northern blots (Derynck *et al.* 1987), it was not detectable in stable clone #19 by western

blot, IP-western or metabolic labeling experiments (data not shown). For the pulse-chase assay to be sensitive enough to detect alterations in the processing events just described, a much higher level of expression of TGF α was needed. Therefore, hRho and TM-TGF α were transiently co-transfected into either COS or CHO cells rather than utilizing the stable clone #19. Recall that these types of co-transfection experiments presented certain difficulties due to the downregulation of co-expressed genes discussed previously. Thus, the results should be interpreted in this context.

The first experiment sought to measure the effects of hRho overexpression on post-translational intracellular events such as the complex glycosylation of the pro-domain and the removal of the pro-domain to generate the mature transmembrane form of the ligand. COS cells were transiently transfected with TGF α alone or with TGF α plus hRho, and pulse-chase experiments were performed to follow the processing of a metabolically labeled population of TGF α molecules. In order to compensate for the suppressive effect of hRho expression on co-transfected TGF α expression, twice as much TGF α was used in the hRho transfections as in the control transfections. This resulted in roughly equal amounts of core glycosylated proTGF α at time zero of the chase (Figure 4.16).

The effect of hRho expression on cell associated TM-TGF α processing was complex (Figure 4.16). There was a dramatic reduction in the amount of complex glycosylated proTM-TGF α generated at earlier timepoints. There was a similar reduction in the amount of unglycosylated mature TM-TGF α generated at later timepoints (presumably as a result of there being less of the complex glycosylated precursor). In addition, the

disappearance of the core glycosylated proTM-TGF α species seemed to occur more rapidly. These results suggested that hRho expression inhibited the glycosylation of proTM-TGF α and/or increased the turnover of the core glycosylated species. The difference in the level of transcription or translation of TM-TGF α under the two conditions, which required a compensatory increase in the amount of TM-TGF α co-transfected with hRho, was unlikely to account for the observed changes. The events being studied during the chase were *post*-translational modifications. Based on the amounts of the core glycosylated species present at time zero, an approximately equal number of metabolically labeled TM-TGF α molecules were being “followed” through the secretory pathway. Still, it is unclear whether the observed effects reflect specific functions of hRho. They may merely reflect a saturation of the secretory/glycosylation machinery of the cell by the combination of hRho and TM-TGF α protein expression.

A second experiment examined the effect of hRho on TM-TGF α ectodomain shedding. CHO cells were transiently transfected with TGF α alone or with TGF α plus hRho, and a pulse-chase experiment was performed to detect the shedding of a metabolically labeled population of TGF α molecules from the cell surface. CHO cells were used for this study for several important reasons. When transfected, they synthesize the very high levels of TGF α needed if it is to be easily detected in the culture medium. The basal level of cleavage is high enough that a reasonable quantity of TGF α is released into the medium, even in the absence of additional stimulation. Lastly, CHO cells lack EGFR, so the TGF α that is secreted remains in the medium rather than binding to cell surface receptors.

Again, more TGF α was used in the hRho transfections than in the control transfections to compensate for decreased expression. To allow a sufficient number of TGF α molecules to reach the cell surface, serum starved cells were pulsed for 2 hours. The chase was performed with either serum free medium or medium supplemented with 20% FBS (Figure 4.17). The serum free chase resulted in the release of both the major 6 kd soluble species, derived from the mature TM-TGF α and the minor higher molecular weight species derived from the complex glycosylated proTM-TGF α . There was less of this latter form released by the hRho transfected cells. This was consistent with the decreased formation of the complex glycosylated proTM-TGF α observed in the preceding experiment.

As shown in Figure 4.17, serum treatment resulted in an increased release of both the major 6 kd soluble species and also the glycosylated soluble species from control cells. This observation was consistent with previous reports demonstrating an increase in TGF α ectodomain shedding in response to serum (Fan and Derynck 1999, Pandiella and Massague 1991a, Pandiella and Massague 1991b). This increase has been shown to be independent of new protein synthesis and to be mediated by the ERK MAP kinases (Fan and Derynck 1999). No such serum induced increase in TGF α release was observed from hRho transfected cells. A role for hRho in modulating TGF α ectodomain processing would be consistent with the cell surface biotinylation and immunofluorescence data presented in Chapter 3, which demonstrated that some of the hRho protein localized to the plasma membrane. However, it remained unclear as to whether this blockage of

serum induced ectodomain cleavage was a specific effect of hRho or just another manifestation of its suppressive effects in co-transfection experiments.

When the results of both processing studies are considered together, it appears that hRho expression tends to skew the relative abundance of the various forms of TM-TGF α away from the complex glycosylated form. The complex N-glycosylation that occurs on the pro-domain has been shown to be dispensible for proper TGF α secretion and is not a prerequisite for pro-domain removal (Bringman *et al.* 1987 and Teixido *et al.* 1990). However, it is possible that signaling by the transmembrane ligand might be negatively regulated by this glycosylation. For example, the bulky sugar might prevent the ligand from properly engaging the EGF receptor. Removal of the pro-domain might serve to “activate” the ligand by reducing its size or changing its conformation so that it is able to bind to the receptor. Following this line of reasoning and given the processing data described above, it is tempting to speculate that hRho may contribute to ligand activation by allowing proTM-TGF α to bypass the complex glycosylation step and proceed directly to the processing step which removes the pro-domain. Complex glycosylation of proteins typically occurs in the late ER and Golgi apparatus. A role for hRho on the TGF α processing which occurs in these locations would be consistent with the immunofluoresence data presented in Chapter 3 which demonstrated that some of the hRho protein co-localized with an ER marker (Figure 3.3). One aspect of the processing data that did not support this hypothesis was the fact that the reduced complex glycosylation that occurred as a result of hRho expression did not translate into a corresponding increase in the amount of mature TM-TGF α . This might be explained,

however, by the apparent increase in the rate of turnover of the core glycosylated species. Again, any reasonable interpretation of these data needs to take into account the fact that these experiments were not perfectly controlled since different amounts of TGF α were transfected in the two conditions being compared.

In parallel and as a complement to the biochemical experiments performed in mammalian cell culture, transgenic flies were generated to study the function of hRho genetically (Figure 4.19). Overexpression of hRho in the wing resulted in a range of phenotypes. Ectopic vein material was often present in hRho flies, although to a lesser degree than is typically seen in dRho flies. In addition, the veins (particularly L3 and L5) appeared thicker than normal. These phenotypes were consistent with an increased level of DER signaling in the wing and resembled a weak to moderate dRho phenotype. The hRho fly wings also had disrupted margins, reduced blade size, and occasionally even showed a loss of vein material. These latter phenotypes were consistent with a reduction of DER signaling in the wing and resembled the effects of dnDER or other DER loss of function alleles.

When hRho was co-expressed with dnDER in the wing, the ectopic veins induced by hRho were completely suppressed, consistent with the possibility that hRho produces ectopic veins by enhancing DER signaling. Moreover, the loss-of-vein phenotype caused by dnDER alone, was somewhat enhanced by hRho, suggesting that hRho also has a dnDER-like activity. Finally, preliminary evidence suggested that hRho overexpression could not rescue a deficiency of dRho expression in the wing. This was not all that

surprising given that the hRho phenotype was considerable weaker than the dRho phenotype.

Overall, hRho appeared to have *partial* functional homology with dRho. Furthermore, it was suggested that hRho acted upstream, through, or at the level of the EGF receptor. One interpretation, consistent with both the agonistic and antagonistic effects of hRho on DER, was that hRho bound to DER *in vivo* but only weakly activated it.

The goal of the studies presented in this chapter was to elucidate the function(s) of hRho. Specifically the hypotheses that hRho potentiates EGFR-MAPK signaling and/or regulates TM-TGF α processing were tested. While some suggestive results supporting both of these hypotheses were obtained, the majority of the experiments yielded negative results. The notable exceptions were the experiments performed *in vivo* through the generation and use of hRho transgenic flies. These experiments clearly demonstrated that hRho shared at least some functional homology with dRho and that the actions of hRho require the presence of functional EGF receptors. The apparent discrepancy between the *Drosophila* data and the mammalian cell culture data most likely stems from both the increased complexity of mammalian cell signaling and the inevitable oversimplification which occurs when cells in culture are used as a model for complex biological processes which occur *in vivo*.

CHO Cells
c-fos induction
 (0.5 ug EGFR, 0.5 ug p2FTL, 0.25 ug RKBgal, 0.1 ug other)

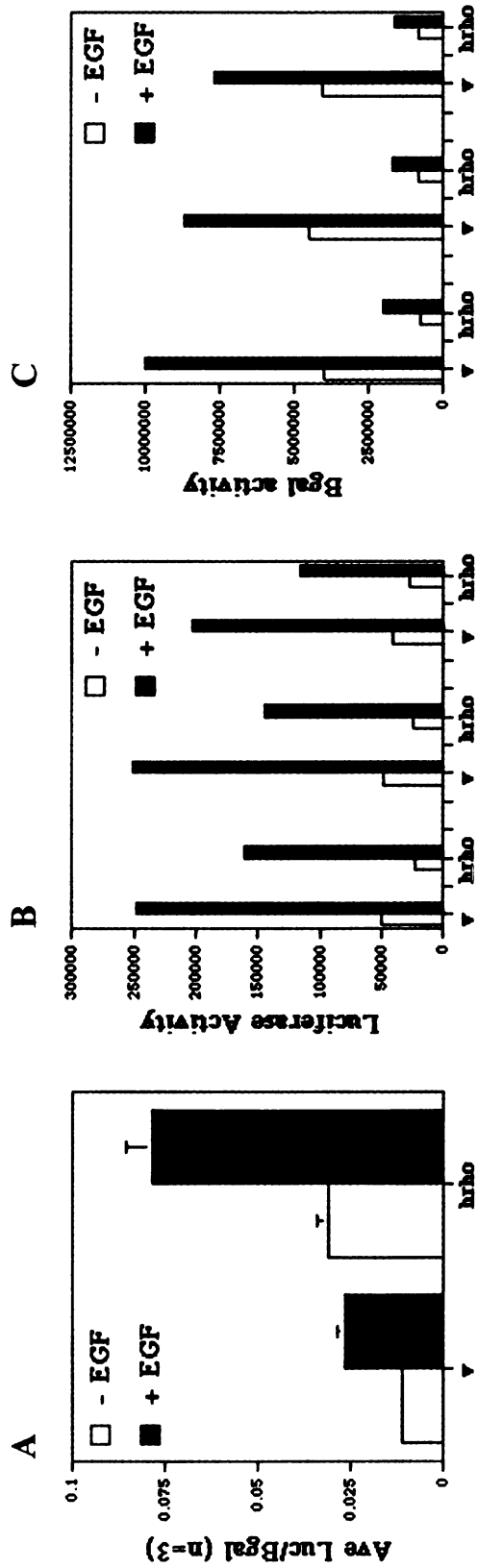


Figure 4.1 Apparent c-fos induction by hrho. CHO cells were transiently transfected as indicated, and each cell lysate was assayed independently for luciferase and β -galactosidase activity. When the data were analyzed as luciferase activity normalized to β -gal activity (A), there was an apparent stimulation due to hrho expression. However, when the data were analyzed separately, hrho expression actually resulted in a decrease in luciferase activity (B) and an even larger decrease in β -gal activity (C).

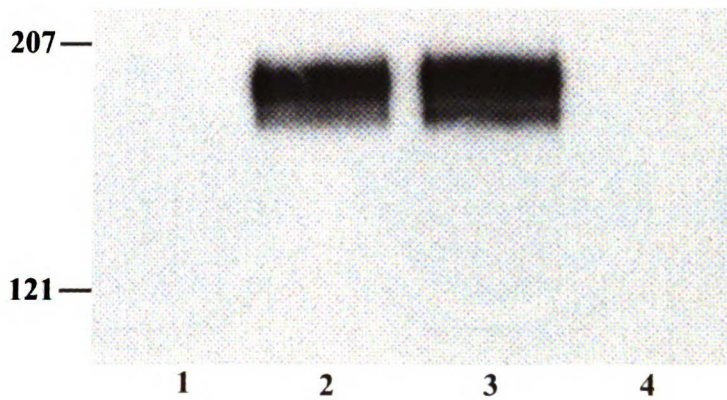


Figure 4.2 "Downregulation" of co-expressed EGFR in the presence of hrho expression. CHO cells were transiently transfected with vector (lane 1), pRK5-EGFR (lane 2), pRK7-βgal + pRK5-EGFR (lane 3) or pFHR-long + pRK5-EGFR (lane 4). The same amount of pRK5-EGFR plasmid and the same total amount of DNA was used in each transfection. Cell lysates were analyzed by western blotting with an anti-EGFR antibody.

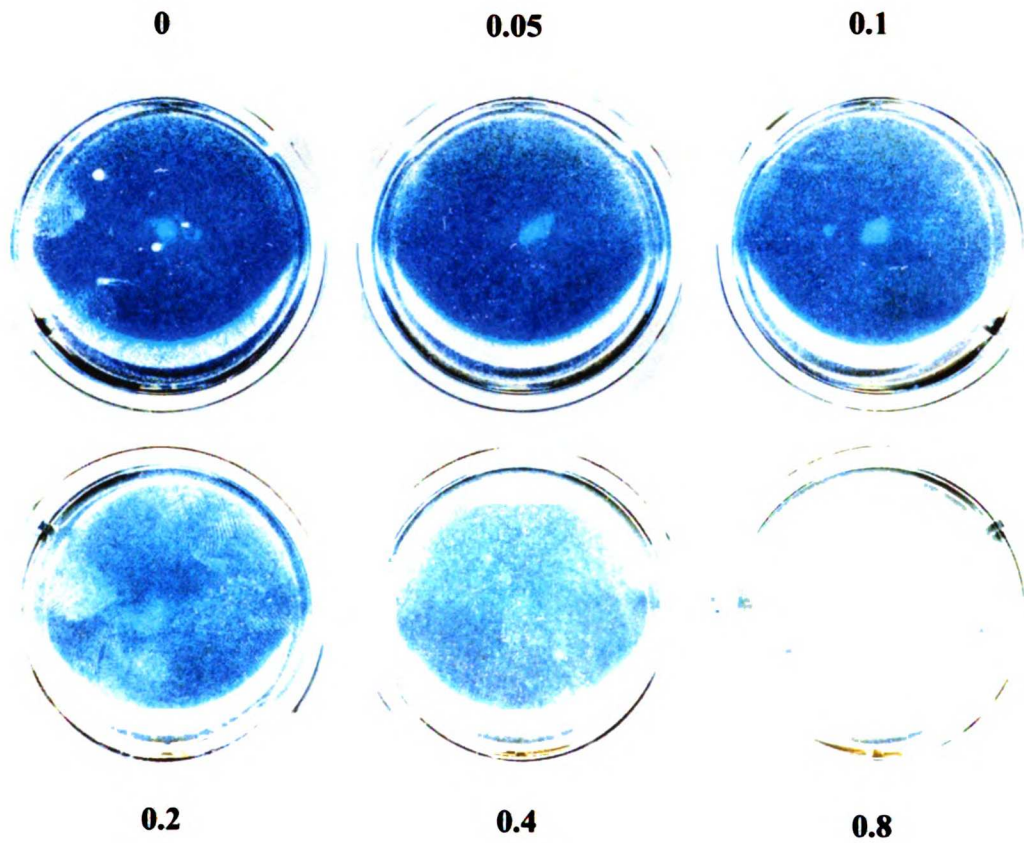


Figure 4.3 "Downregulation" of co-transfected genes in the presence of hrho expression. A fixed amount of pRK7-βgal plasmid was co-transfected with an increasing amount of pFHR-long plasmid (amount in micrograms shown) into CHO cells and the cells were stained with the X-gal substrate.

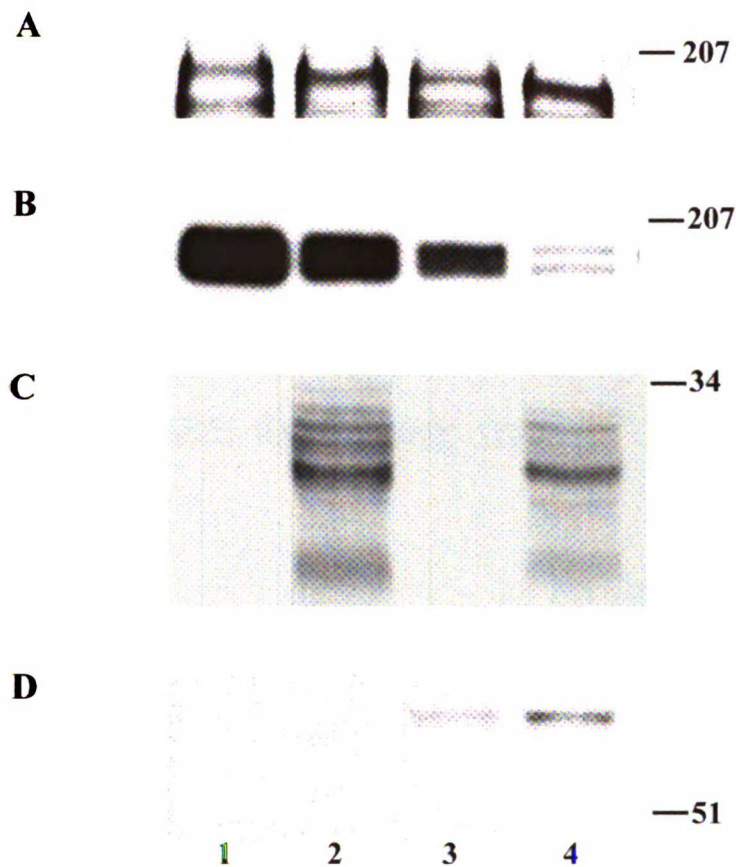


Figure 4.4 Apparent increase in EGFR phosphorylation due to hrho expression. HEK-293 cells were transiently transfected with vector + pRK5-EGFR (lane 1), vector + pRK5-EGFR + pRK7-TGF α (lane 2), pFHR-long + pRK5-EGFR (lane 3) or pFHR-long + pRK5-EGFR + pRK7-TGF α (lane 4). Cell lysates were analyzed in parallel western blots probed with anti-phosphotyrosine (A), anti-EGFR (B), anti-TGF α (C) or anti-Flag (D) antibodies. Note that the level of EGFR expression declines but the ratio of EGFR-P to EGFR increases in the presence of hrho expression.

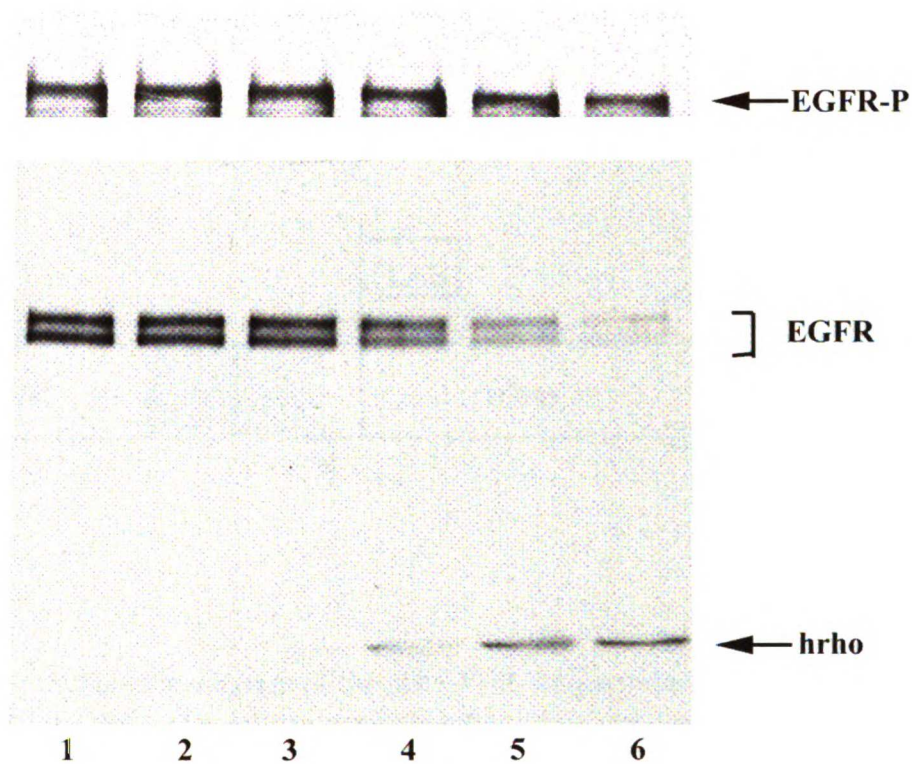


Figure 4.5 Apparent increase in EGFR phosphorylation with increasing levels of hrho expression. Cell lysates from HEK-293 cells transiently transfected with 2.1 ug of pRK5-EGFR + 2.1 ug of pRK7-TGF α + 0 ng (lane 1), 25 ng (lane 2), 50 ng (lane 3), 100 ng (lane 4), 200 ng (lane 5) and 400 ng (lane 6) of pFHR-long were analyzed by western blotting with anti-phosphotyrosine (top) and in parallel with anti-EGFR (middle) and anti-Flag (bottom). Note that the level of EGFR expression declines but the ratio of EGFR-P to EGFR increases with increasing amounts of hrho transfected.

pBi5-FHR-long

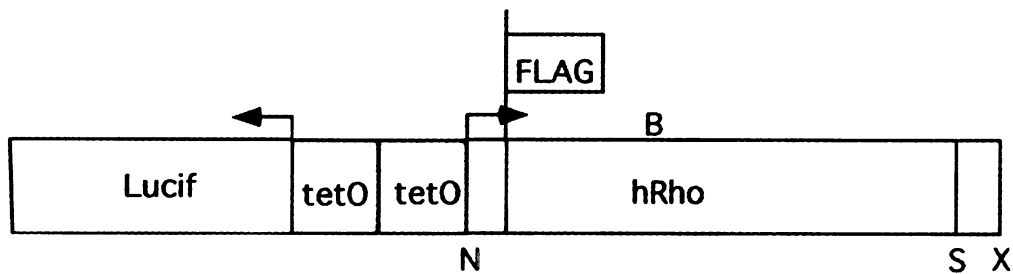


Figure 4.6 Schematic diagram of the pBi5-FHR-long construct stably transfected into HeLa-tTA cells to generate tetracycline regulatable hrho stable cell lines. In the absence of tetracycline, tTA proteins bind to the bi-directional tet operators to drive simultaneous expression of hrho and the luciferase reporter gene. In the presence of tetracycline, the tTA proteins are rendered incapable of binding to the tet operators, and transcription of both genes is turned off.

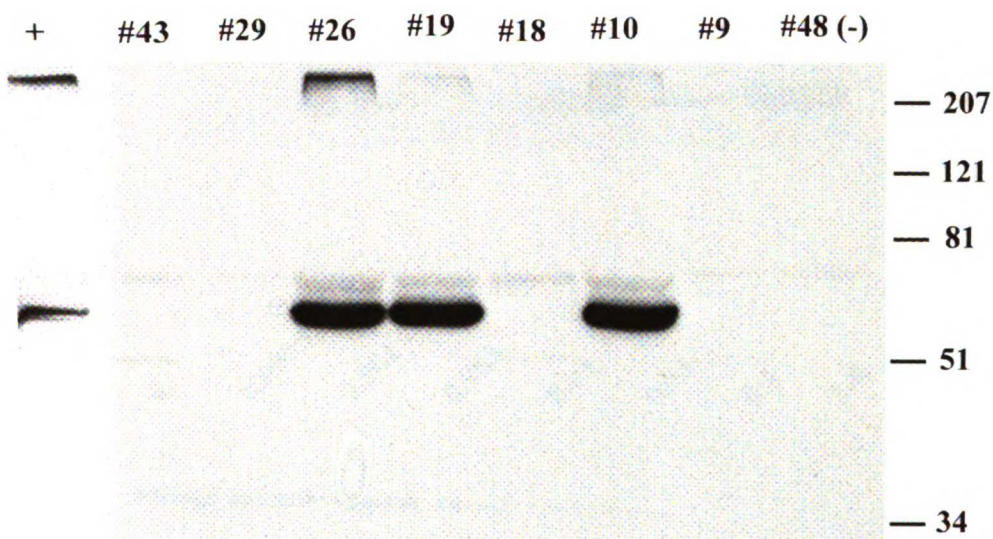


Figure 4.7 Screen of pBi5-FHR-long stable HeLa-tTA clones for hrho expression. Luciferase positive clones were grown in the absence of tetracycline for 48 hours, and equal amounts of cell lysate were analyzed by western blotting with anti-Flag. A lysate from HeLa-tTA cells transiently transfected with pFHR-long was used as a positive control (+), and a lysate from a luciferase negative clone was used as a negative control (#48 -). Three hrho positive clones (#10, #19 and #26) were detected.

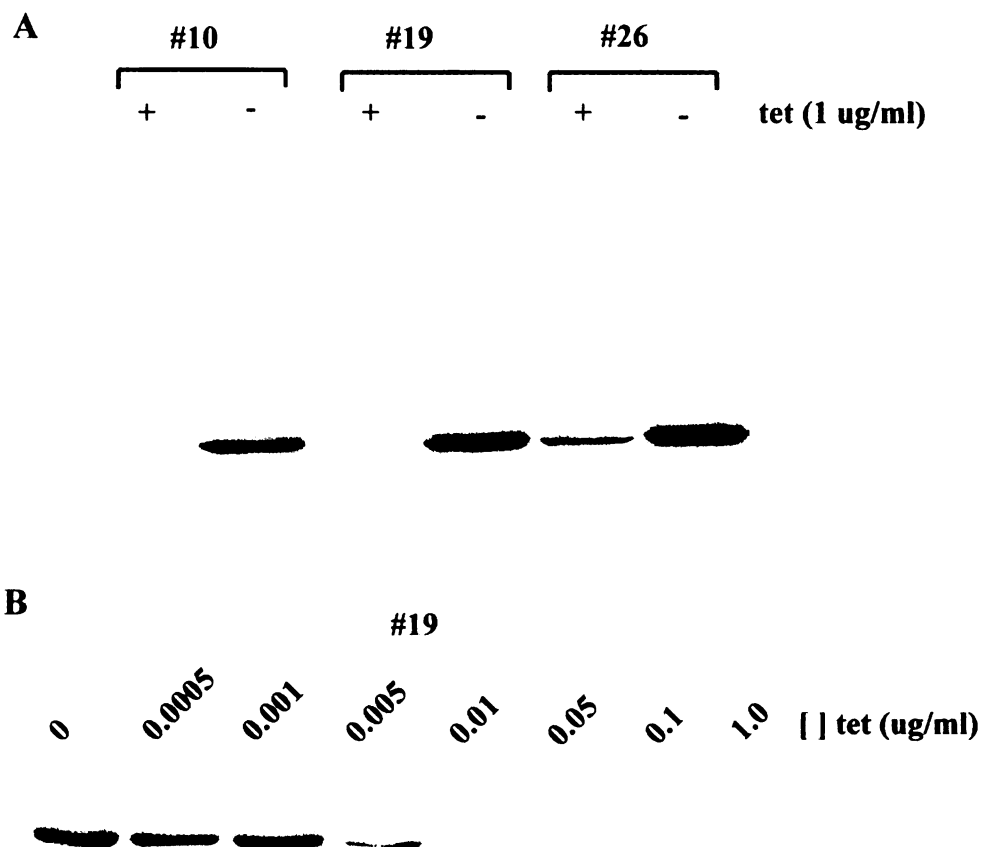


Figure 4.8 Tetracycline repressibility of pBi5-FHR-long stable HeLa-tTA clones. **A.**The three hrho positive clones were grown for 48 hours in the presence (+) or absence (-) of 1 ug/ml tetracycline in the culture medium. Cell lysates were analyzed by western blotting with anti-Flag. Clones #10 and #19 were completely repressible while clone #26 showed only partial repression at this tetracycline concentration. **B.**Clone #19 was grown for 48 hours with the indicated concentrations of tetracycline in the culture medium. Cell lysates were analyzed by western blotting with anti-Flag. This clone was repressible over two orders of magnitude of tetracycline concentration from unrepressed at 0.001 ug/ml to fully repressed at 0.1 ug/ml.

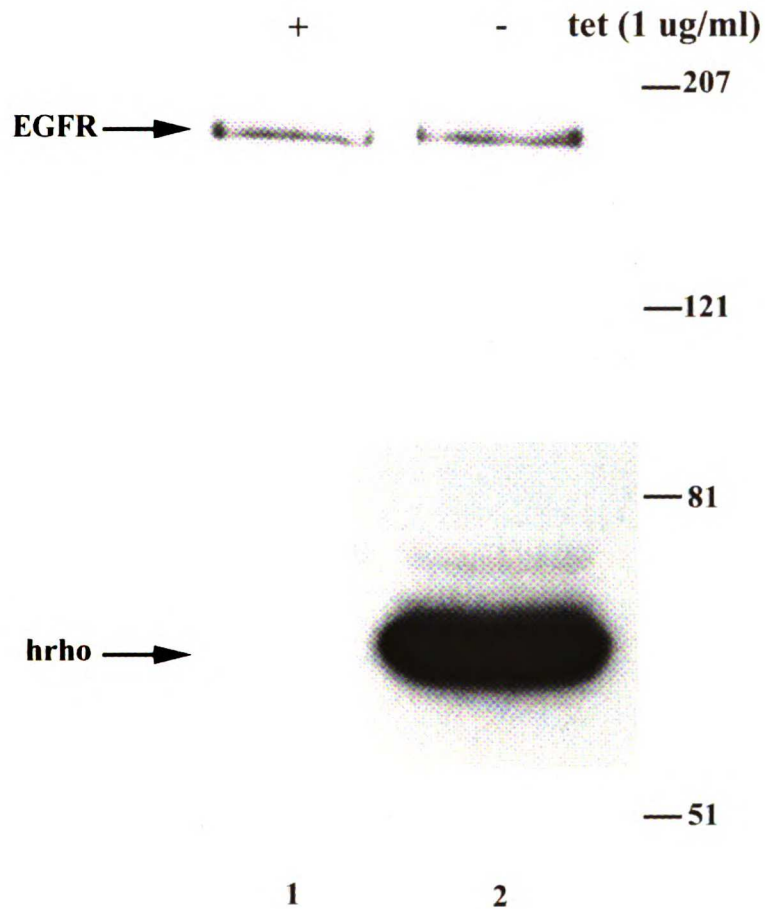


Figure 4.9 Stable expression of hrho does not alter the level of endogenous EGFR expression. Stable clone #19 was grown for 48 hours in the presence (+) or absence (-) of 1 ug/ml tetracycline in the culture medium. Equal amounts of protein from cell lysates were analyzed by western blotting with anti-EGFR (top) and anti-Flag (bottom).

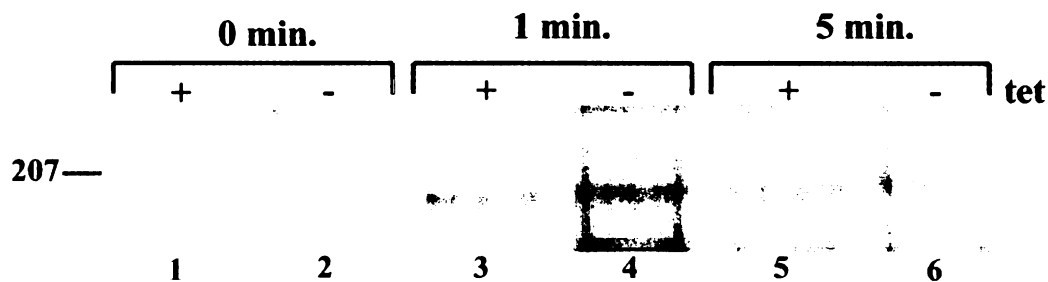


Figure 4.10 Stable expression of hrho does not affect the level of soluble TGF α mediated phosphorylation of endogenous EGFR. Stable clone #19 was grown for 24 hours in normal growth medium in the presence (+) or absence (-) of 1 μ g/ml tetracycline in the culture medium. The cells were grown for an additional 24 hours in serum free medium with or without tetracycline and then stimulated for the indicated amounts of time with 2 ng/ml TGF α . Equal amounts of protein from cell lysates were immunoprecipitated with anti-EGFR and western blotted with anti-phosphotyrosine. The higher than normal background in lane 4 is likely due to inadequate washing of the immunoprecipitate.

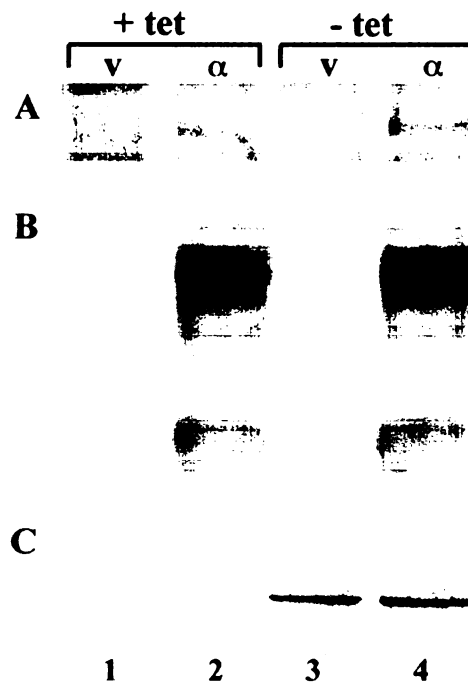


Figure 4.11 Stable expression of hrho does not affect the level of TM-TGF α mediated phosphorylation of endogenous EGFR. Stable clone #19 was transiently transfected with vector (lanes 1 and 3) or pRK7-TGF α (lanes 2 and 4) in the presence of tetracycline. The cells were then grown for 24 hours in normal growth medium in the presence (lanes 1 and 2) or absence (lanes 3 and 4) of 1 μ g/ml tetracycline. The cells were grown for an additional 24 hours in serum free medium with or without tetracycline, and equal amounts of protein were either immunoprecipitated with anti-EGFR and western blotted with anti-phosphotyrosine (A), western blotted with anti-TGF α (B) or western blotted with anti-Flag (C).

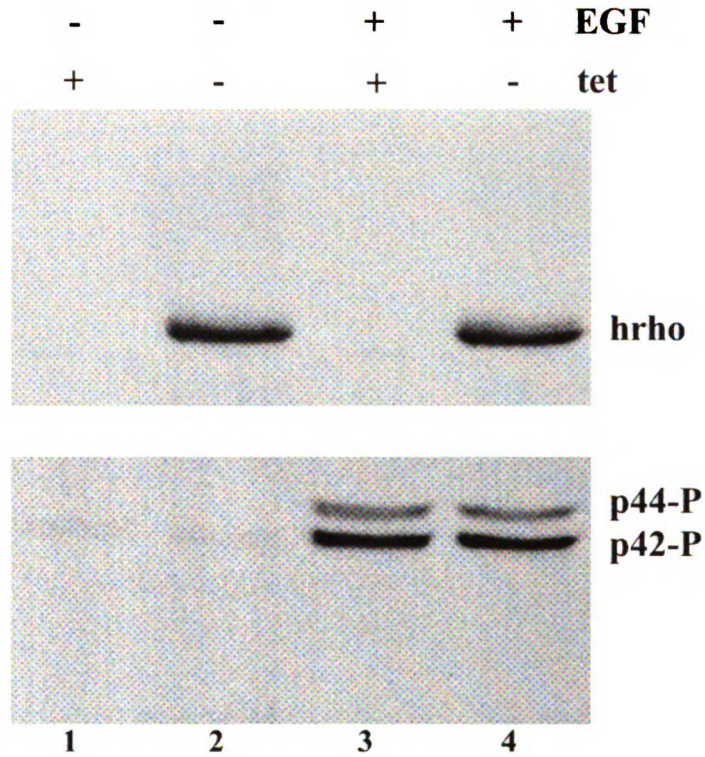


Figure 4.12 Stable expression of hrho does not affect the basal or EGF stimulated phosphorylation of endogenous p42 or p44 MAP kinase. Stable clone #19 was grown for 24 hours in normal growth medium in the presence (+, lanes 1 and 3) or absence (-, lanes 2 and 4) of 1 ug/ml tetracycline in the culture medium. The cells were grown for an additional 24 hours in serum free medium with or without tetracycline and then either left unstimulated (-, lanes 1 and 2) or stimulated for 30 minutes with 20 ng/ml EGF (+, lanes 3 and 4). Equal amounts of protein from cell lysates were western blotted with anti-Flag (top) or phosphospecific anti-MAPK (bottom).

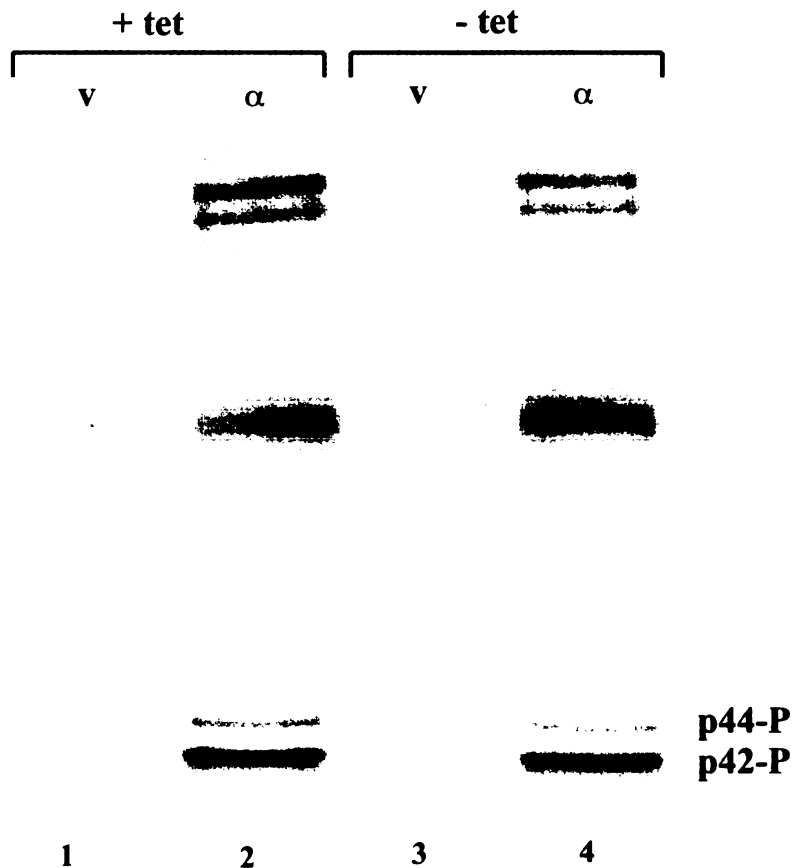


Figure 4.13 Stable expression of hrho does not affect the basal or TM-TGF α stimulated phosphorylation of endogenous p42 or p44 MAP kinase. Stable clone #19 was transiently transfected with vector (lanes 1 and 3) or pRK7-TGF α (lanes 2 and 4) in the presence of tetracycline. The cells were then grown for 24 hours in normal growth medium in the presence (lanes 1 and 2) or absence (lanes 3 and 4) of 1 μ g/ml tetracycline. The cells were grown for an additional 24 hours in serum free medium with or without tetracycline, and equal amounts of protein were western blotted in parallel with anti-TGF α (top) or phosphospecific anti-MAPK (bottom).

Stable Clone #19 ³H-Thymidine Incorporation

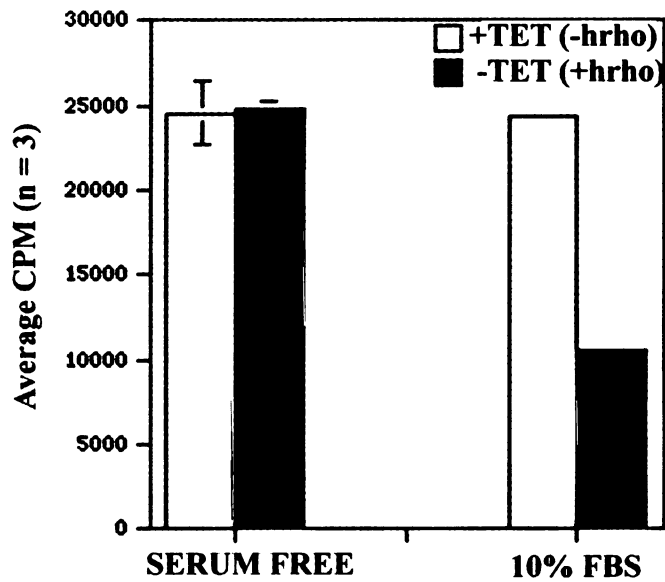


Figure 4.14 Apparent effect of stable hrho expression on DNA synthesis. Stable clone #19 was grown in normal growth medium for 24 hours in the presence (+tet, white bars) or absence (-tet, black bars) of 1 ug/ml tetracycline. The cells were grown for an additional 24 hours in either serum free medium or normal growth medium (10% FBS) with or without tetracycline and then pulse labeled with tritiated thymidine. Each bar represents the average counts per minute from triplicate samples, and error bars indicate the standard error of the mean.

Control Clones ³H-Thymidine Incorporation

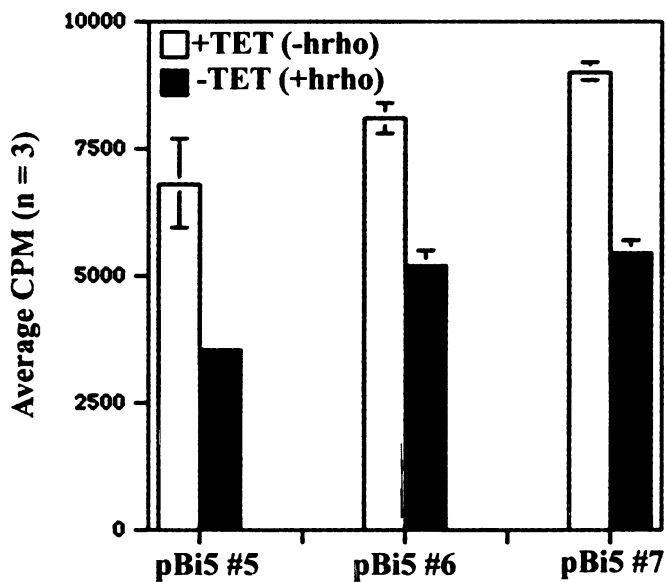


Figure 4.15 Effect of tetracycline on DNA synthesis of control clones stably transfected with empty pBi5 vector. Luciferase positive stable control clones #5, #6 and #7 were grown in normal growth medium for 24 hours in the presence (+tet, white bars) or absence (-tet, black bars) of 1 ug/ml tetracycline. The cells were grown for an additional 24 hours in normal growth medium (10% FBS) with or without tetracycline and then pulse labeled with tritiated thymidine. Each bar represents the average counts per minute from triplicate samples, and error bars indicate the standard error of the mean.

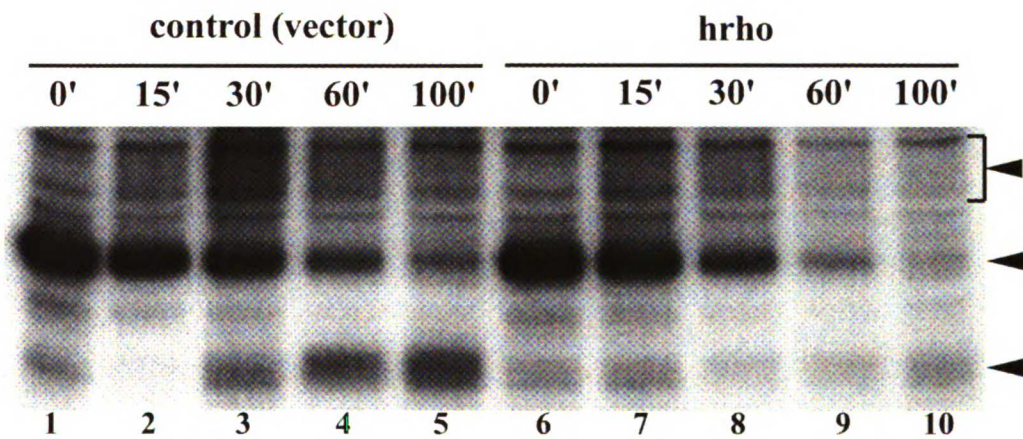


Figure 4.16 Expression of hrho reduces the conversion of the proTM-TGF α precursor to the complex glycosylated proTM-TGF α and the mature TM-TGF α . The half-life of the precursor form is also decreased. COS cells were transiently transfected with vector + pRK7-TGF α (lanes 1-5) or pFHR-long + pRK7-TGF α (lanes 6-10). After serum starvation, the cells were metabolically labeled for a 20 minute pulse and then chased for the indicated times in serum free medium. Cell lysates were immunoprecipitated with anti-TGF α . The middle arrowhead indicates the precursor proTM-TGF α , the upper arrowhead indicates the fully glycosylated proTM-TGF α , and the lower arrowhead indicates the mature TM-TGF α .

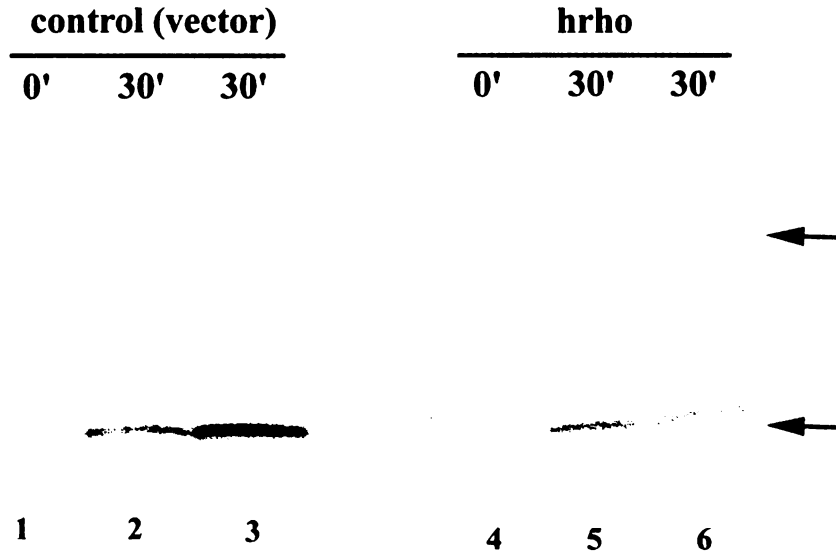


Figure 4.17 Expression of hrho inhibits the serum induced proteolysis of TM-TGF α . CHO cells were transiently transfected with vector + pRK7-TGF α (lanes 1-3) or pFHR-long + pRK7-TGF α (lanes 4-6). After serum starvation, the cells were metabolically labeled for a 20 minute pulse and then chased for the indicated times in either serum free medium (lanes 1-2 and 4-5) or medium supplemented with 20% serum (lanes 3 and 6). The chase medium was then immunoprecipitated with anti-TGF α . The arrows indicate the two major forms of TGF α released into the medium during the 30 minute chase. The upper form derives from the fully glycosylated proTM-TGF α , while the more abundant lower form derives from the mature TM-TGF α which lacks the pro-domain.

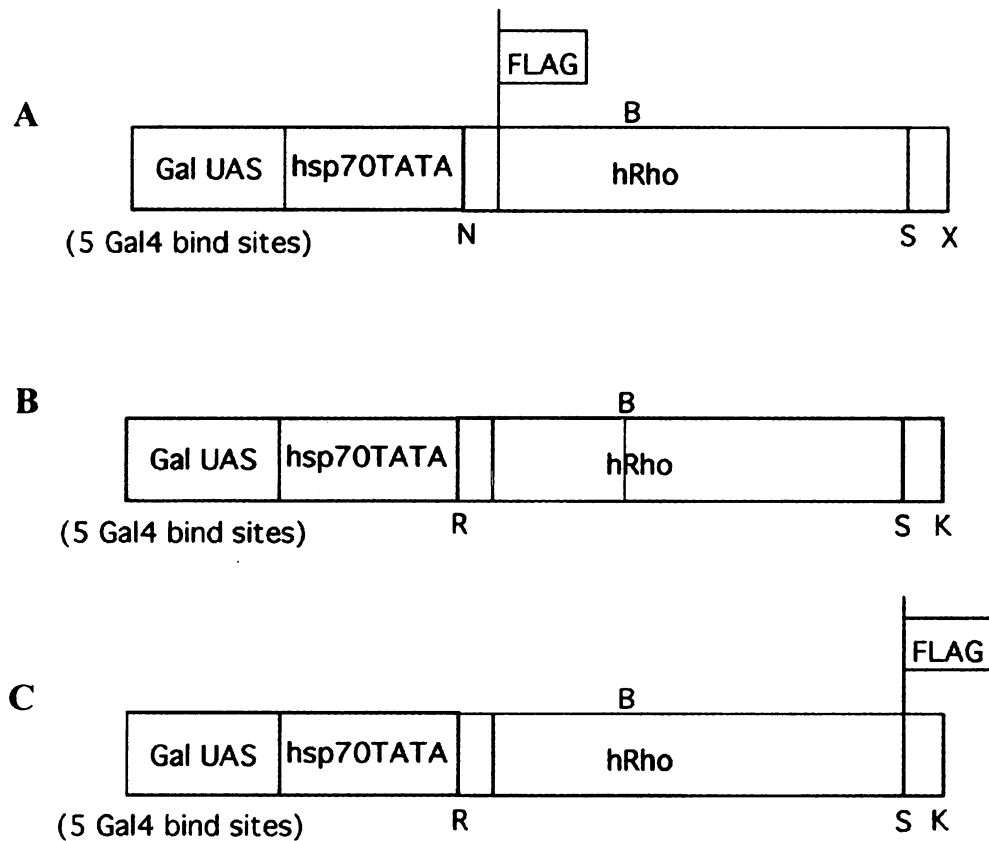


Figure 4.18 Schematic diagrams of constructs used to generate *hrho* transgenic flies. The *hrho* cDNA was subcloned behind an *hsp70* minimal promoter preceded by a Gal4 upstream activating sequence. N-terminally Flag tagged (pUAST-FHR-long,**A**), untagged (pUAST-HR-long,**B**) and C-terminally Flag tagged (pUAST-HRF-long,**C**) constructs were made. To overexpress *hrho* in a tissue-specific fashion, the flies generated with these constructs were crossed to a "driver" line that expressed high levels of Gal4 protein in the wing.

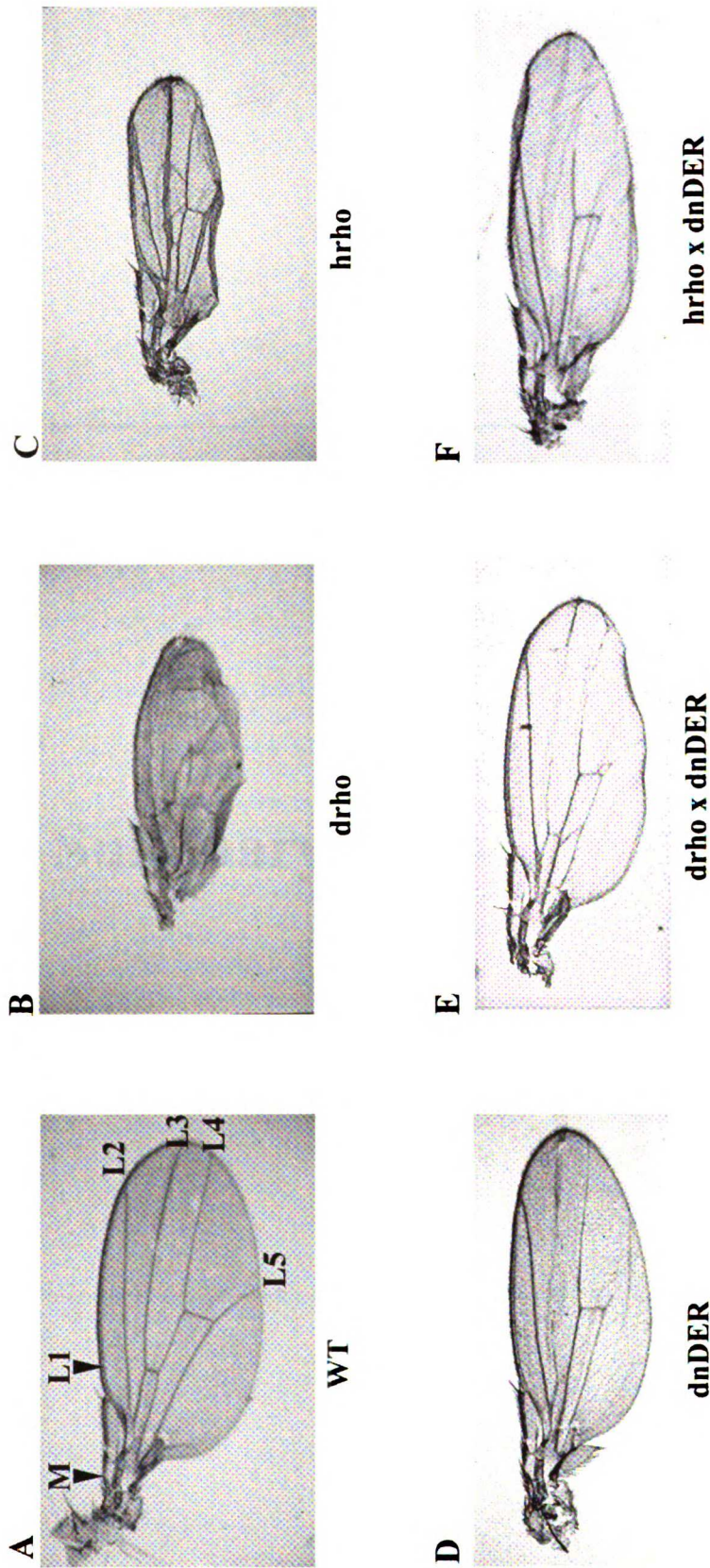


Figure 4.19 Analysis of hrho transgenic flies. The hrho cDNA was subcloned behind an hsp70 minimal promoter preceded by a Gal4 upstream activating sequence. This construct was used to transform flies. These flies were then crossed to "driver" flies expressing high levels of Gal4 in the wing. The wing vein pattern of the progeny is shown in (C). The pattern from a cross of these progeny with dnDER flies generated in a similar manner is shown in (F). For comparison, a wing from a wild-type fly (A), a wing from a drho fly (B), a wing from a dnDER fly (D) and a wing from the progeny of a cross between drho and dnDER (E) are shown.

Chapter 5

Summary and Future Directions

This thesis described the successful cloning of hRho, a human homologue of *Drosophila rhomboid*, and the first generation of experiments designed to characterize the protein product of this gene both physically and functionally.

The hRho gene was cloned out of a human placental cDNA library constructed in lambda phage. A human expressed sequence tag homologous to dRho was identified through database searches and used to generate PCR primers for use in PCR based screening of the human cDNA library. After several rounds of dilution and replating of the phage library, a partial hRho cDNA was isolated from a single plaque. DNA sequencing and amino acid alignment confirmed that the isolated sequence was in fact a homologue of dRho. However, when this cDNA was expressed in mammalian cells, no protein product could be detected by either immunofluorescence or western blotting. These findings, in addition to ambiguity about the 5' start site of the gene, suggested that the isolated cDNA was a partial cDNA. Using available human genomic sequence which was found to contain the isolated cDNA, PCR primers were designed to amplify additional 5' sequence. This sequence, when added to the cloned cDNA, constituted the full-length hRho cDNA as verified by the ability to detect the protein by both immunofluorescence and western blotting.

The focus of the experiments then turned to a physical characterization of the hRho protein. Sequence analysis was performed, with a particular emphasis on comparisons to dRho. In addition to moderate sequence identity and similarity, the protein was found to be structurally similar to dRho. Features common to both proteins included the absence

of an N-terminal signal sequence, the prediction of multiple transmembrane domains and the presence of a putative PEST domain. Through a combination of immunofluorescence and cell surface biotinylation studies, it was determined that the majority of hRho localized to what appeared to be intracellular membrane structures, with a smaller amount appearing at the plasma membrane. Co-localization with an ER marker suggested that the intracellular membranes to which much of the hRho localized were in fact ER membranes. This localization was consistent with a role for hRho in either intracellular transmembrane ligand processing or in ligand processing or signal reception occurring at the cell surface. At the tissue level, RT-PCR analysis of various mouse tissues found that hRho was expressed ubiquitously in all tissues tested. This was similar to the expression patterns of TGF α and EGFR, consistent with a hypothesized role for hRho in modulating the interaction between this ligand-receptor pair. Finally, co-immunoprecipitation experiments detected specific physical interactions between hRho, EGFR and TM-TGF α . The interaction between hRho and EGFR was found to require the cytoplasmic portion of the receptor which contains the kinase domain. The interaction between hRho and TM-TGF α was found to require the extracellular 50 amino acid core TGF α domain of the transmembrane ligand. Preliminary evidence also suggested the possibility that the three proteins can form a tripartite complex. These physical interactions were again consistent with a role for hRho in mediating TGF α stimulated EGFR signaling.

A combination of *Drosophila* genetic data regarding dRho and results from the physical characterization of hRho guided the subsequent functional analysis of hRho. Mammalian cell culture systems were used in an attempt to establish a biochemical basis for the

contribution of hRho to EGFR signaling. Transient transfection studies suggested that hRho expression might result in increased c-fos induction and EGFR phosphorylation, two hallmarks of EGFR signaling. However, these studies were plagued by the fact that hRho expression itself nonspecifically reduced the levels of co-expressed proteins under study.

In an attempt to circumvent this problem and to allow additional components of the EGFR signaling pathway to be analyzed, stable cell lines were established. A tetracycline regulatable system was chosen to allow tight control of hRho expression in case similar problems were encountered. HeLa cells were chosen because they expressed easily detectable levels of endogenous EGFR. Using one of the stable cell lines, studies were performed to analyze the effect of hRho expression EGFR signaling.

Unfortunately, overexpressed hRho had no detectable effect on either soluble or transmembrane ligand stimulation of EGFR or MAP kinase in this cell system. In addition, a more general effect on cell proliferation was not detected.

Because of the inability to detect an effect of hRho expression on EGFR and downstream signaling, focus then shifted to analyzing the effects of hRho on an upstream component of the pathway, namely the ligand. Again, this was motivated by both the *Drosophila* genetic studies which suggested a role for *rhomboid* in ligand processing and the characterization studies which demonstrated a physical interaction between hRho and TM-TGF α . In particular, the effect of hRho overexpression on both intracellular processing and ectodomain cleavage of TM-TGF α were analyzed. For technical reasons,

these studies required a return to transient transfection systems. Complex effects of hRho expression on these processes were observed, however they were difficult to quantify and interpret due to the aforementioned technical problems associated with transient co-transfection experiments involving hRho.

In parallel with the transient and stable mammalian cell culture experiments summarized above, the hRho cDNA was used to generate transgenic flies. The effects of hRho overexpression were compared to the known effects of dRho overexpression on *Drosophila* wing vein development. Like dRho, hRho resulted in the generation of extra and thickened vein material. Although the phenotype was significantly weaker than the dRho phenotype, it nonetheless suggested that hRho expression might result in enhanced DER signaling in the fly wing. The complete suppression of the hRho phenotype by dnDER demonstrated that the effects of hRho on the wing veins were in fact mediated through DER.

The relative success of the *in vivo* experiments in flies compared to the mammalian cell culture experiments demonstrates the difficulties of modeling complex biological properties *in vitro*. While fly genetic experiments alone cannot establish the biochemical mechanism(s) underlying hRho function, they might nonetheless continue to reveal clues about hRho which could then potentially be tested biochemically. The wing vein phenotype of the hRho fly, while similar to the dRho fly, even more closely resembles that of a recently generated C-terminally truncated dRho fly (dRho Δ C). Therefore an

experiment is underway to generate a transgenic fly expressing a chimeric hRho/dRho gene consisting of the hRho cDNA sequence with its 3' end replaced by the 3' end of the dRho cDNA. If the resulting chimeric protein more closely reproduces the dRho wing-vein phenotype, it would suggest that the C-terminus constitutes an important functional domain of rhomboid-like proteins. Other planned fly experiments include additional genetic interaction studies, for example of hRho with *star*. That such an interaction exists might be predicted from the subcellular localization of both the hRho and *star* proteins to intracellular membrane structures such as the ER membrane. The idea would be to see if hRho can synergize with *star* in a manner similar to that previously observed with dRho.

A completely different line of future genetic experimentation on hRho would be to clone and subsequently either overexpress or knockout the *mrho* gene in mice. The cloning of *mrho* might be a relatively straightforward task now that hRho has been cloned. Recall that a portion of the hRho cDNA was found to be >90% identical at the base pair level to a mouse sequence which is most likely part of the *mrho* gene. This was exploited in this thesis to characterize the *mrho* tissue expression pattern by RT-PCR as a surrogate for the hRho tissue expression pattern. Due to the unusually high level of sequence conservation, PCR primers could be designed directly from the hRho sequence and used to amplify the *mrho* coding sequence from a mouse cDNA library. Mice could then be generated which either overexpress *mrho* or which have a targeted deletion of the *mrho* gene. Genetic interaction studies analogous to those performed in flies might be envisioned. For example, *mrho* overexpressing or knockout mice could be crossed with mice which either overexpress or are deficient in mTGF α or mEGFR. Through these

types of experiments, overexpression of *mrho* or its elimination from the mouse genome might provide unique insights into the role of rhomboid-like proteins in mammalian development and physiology.

Besides the genetic studies in flies and mice proposed above, additional physical and functional characterization of hRho could be undertaken in a second generation of cell culture experiments. Immunofluorescence studies might be performed on the hRho stable cells to determine if hRho expression alters the subcellular localization of EGFR in either the absence or presence of soluble or transmembrane ligands. For example, hRho might modulate receptor internalization and/or recycling to the plasma membrane in response to ligand stimulation. Additional experiments such as immunofluorescent co-localization studies with hRho and TGF α might provide insights into the observed effects of hRho on the processing of TM-TGF α .

In this thesis, functional studies focused on potential effects of hRho expression on the EGFR-MAP kinase signaling pathway. The focus on the MAP kinase pathway was reasonable given the genetic evidence from *Drosophila* studies demonstrating that dRho contributes to DER mediated MAP kinase activation. However, these data do not rule out possible effects dRho (hRho) on other DER (EGFR) mediated pathways. As discussed in Chapter 1, multiple signaling pathways emanate from EGFR, including the PLC- γ and PI-3 kinase pathways. While it is possible that hRho expression modulates one of these other pathways, the likelihood seems low given that hRho expression had no detectable impact on the initiating event, the activation of EGFR. Alternatively, future

studies might examine the effect of hRho expression on the activation of other EGFR family members. As discussed previously, in humans EGFR is one of several members of a family of related receptors which also includes ERBB2, ERBB3 and ERBB4. This is quite different from *Drosophila* where only DER has been identified. Given this added level of complexity, it is possible that hRho modulates the activation of, or signaling from, one of these other receptors. This hypothesis could be tested using methods similar to those used in this thesis to study EGFR.

Along the same lines, multiple EGF-like ligands exist both in flies and humans. It is certainly possible that in humans hRho modulates the presentation, processing or signaling of one of these other ligands. For example, there is some evidence that the effects of *rhomboid* on wing vein development might be mediated by *vein* in addition to or instead of *spitz* (Guichard *et al.* 1999, Simcox 1997, Simcox *et al.* 1996). Perhaps by analogy the functions of hRho are mediated by, for example, HB-EGF or neuregulin. Again, this hypothesis could be tested using methods similar to those used in this thesis to study TGF α .

The concept of cell autonomous versus cell non-autonomous *rhomboid* function was discussed in Chapter 1 in the context of the various mechanisms of dRho function in flies. This issue might be addressed with hRho *in vitro* using a more complex cell culture system than the stable cell culture system employed in this thesis. Recall that in the cell line used here (described in Chapter 4) hRho was stably expressed in HeLa cells which themselves express moderately high levels of endogenous EGFR. Transient transfection

of TM-TGF α into these cells and subsequent analysis of the effects on EGFR and MAP kinase activation could therefore be considered an examination of the effects of hRho on *autocrine* TGF α -EGFR signaling. Alternatively, the effects of hRho expression on *paracrine* signaling might be studied by establishing a more complex co-culture system. For example CHO cells which lack EGFRs or CHO α cells which stably express TM-TGF α could be co-cultured with haemopoietic 32D cells which lack EGFRs or 32D-EGFR cells which stably express EGFR (Pierce *et al.* 1988). The effects of hRho expression on TGF α processing and/or EGFR and MAP kinase activation could then be studied in this system by transiently or stably expressing hRho in either the CHO component or 32D component of the co-culture system. Such a system might more closely mimic the *in vivo* events that occur, for example, at the *Drosophila* midline during development. This type of co-culture system has recently been used to study the effects of the tetraspan plasma membrane protein CD9 on TGF α mediated EGFR signaling (Shi *et al.* 1999).

Other types of cell culture systems might also prove useful for studying hRho function. *Drosophila* Schneider S2 cells or S2:DER cells might be used to perform experiments with hRho similar to those previously described for dRho (Schweitzer 1995). For example, hRho could be transiently or stably expressed in these cells using a *Drosophila* expression vector. Additional *Drosophila* components, such as cDNAs for *spitz* or *star*, could be used to reconstitute DER signaling in these cells. Reagents similar to those used to study EGFR signaling in the HeLa stable system could then be used to study DER signaling in this cell culture system. It is noteworthy that previous experiments in

Schneider cells failed to demonstrate an effect of *rhomboid* or *star* on *spitz* mediated DER signaling (Schweitzer 1995). However, in these experiments, conditioned medium containing secreted *spitz* was applied to *rhomboid* and *star* expressing cells, rather than co-transfecting transmembrane *spitz* with *star* and/or *rhomboid*.

Finally, some additional experiments might add to our understanding of hRho. For example, it would be interesting to purify and identify of the ~36 kd protein which co-immunoprecipitated with hRho in two different metabolically labeled human cell lines (described in Chapter 3). One intriguing possibility is that this protein is p38 MAP kinase, whose function was recently demonstrated to be responsible for most of the basal TGF α cleavage activity exhibited by CHO cells transiently transfected with TM-TGF α (Fan and Derynck 1999). To assist in the purification of the ~36 kd protein, a 6-histidine tagged version of hRho was generated and could be used as part of a metal affinity column purification scheme. This scheme might also identify additional hRho interacting proteins that were not previously identified in the metabolic immunoprecipitation experiments.

Additional reagents have been generated which might prove useful in further characterization of hRho. Approximately 9 kb of human genomic sequence upstream of the hRho gene was available in the GenBank database. This sequence was used to design PCR primers that were then used to amplify the first 1 kb of this upstream sequence from HeLa genomic DNA. This sequence contains a putative minimal promoter (TATA box) sequence upstream of the in frame stop codon which immediately precedes the full-length

hRho translation initiation site. The amplified 1 kb hRho promoter sequence was subcloned into a luciferase reporter vector. This construct could be used as a starting point to begin to study the regulation of hRho gene expression. Longer and shorter promoter constructs could be generated and “promoter-bashing” could be used to identify key regulatory elements and potentially the transcription factors that bind to them. For example, *Drosophila* studies have shown that the transcription factor *dorsal* positively regulates *rhomboid* transcription (Ip *et al.* 1992). A binding site for the transcription factor NF- κ B, a mammalian homologue of *dorsal*, is present in the 1 kb hRho promoter described above. Analysis of the regulation of hRho gene expression using tools such as these may provide additional clues about the function of the hRho protein.

Another reagent recently generated to assist in the future characterization of hRho is a mutant version of the hRho cDNA designated hRho- Δ PEST. This is an hRho cDNA sequence from which sequence encoding the 12 amino acid putative PEST domain was deleted. Presumably the hRho- Δ PEST protein represents a more biochemically stable version of hRho, since PEST domains typically target proteins for degradation. This could be tested experimentally by stably expressing hRho- Δ PEST and comparing its half-life to wild-type hRho in a pulse-chase experiment. If it is indeed found to be more stable, hRho- Δ PEST could be used to repeat some of the functional experiments performed with wild-type hRho in the hope of revealing some previously unidentified function. This mutant hRho might also be used to study the regulation of hRho turnover, which could be an important component of hRho regulation and a determinant of how hRho regulates the function of other proteins. Finally, hRho- Δ PEST could also be used

to generate transgenic flies which might have a more pronounced wing-vein phenotype (i.e. more like dRho) than wild-type hRho flies.

Certainly, further descriptive and functional characterization will be necessary to fully understand the hRho protein and its connection to TGF α mediated EGFR signaling. The work presented in this thesis has established a foundation upon which future experiments such as those described above can be designed and conducted. The ultimate result of this and future work will be a more complete knowledge of the role of hRho in human cell biology.

Bibliography

Angeletti PU, Salvi ML, Chesnow RL, Cohen S. 1964. Action of the "epidermal growth factor" on nucleic acid and protein synthesis in cutaneous epithelium. *Experientia* 20:146-148.

Argetsinger LS, Campbell GS, Yang X, Witthuhn BA, Silvennoinen O, Ihle JN, Carter-Su C. 1993. Identification of JAK2 as a growth hormone receptor-associated tyrosine kinase. *Cell* 74:237-244.

Arribas J and Massague J. 1995. Transforming growth factor-alpha and beta-amyloid precursor protein share a secretory mechanism. *J. Cell. Biol.* 128:433-441.

Arribas J, Coodly L, Vollmer P, Kishimoto TK, Rose-John S, Massague J. 1996. Diverse cell surface protein ectodomains are shed by a system sensitive to metalloprotease inhibitors. *J. Biol. Chem.* 271:11376-11382.

Auger KR, Serunian LA, Soltoff SP, Libby P, Cantley LC. 1989. PDGF-dependent tyrosine phosphorylation stimulates production of novel polyphosphoinositides in intact cells. *Cell* 57:167-175.

Ausubel F, Brent R, Kingston RE, Moore DD, Seidman JG, Smith JA, Struhl K. 1998. *Current Protocols in Molecular Biology* Vol. 1: Pages 9.1.1 – 9.1.11.

Baron U, Freundlieb S, Gossen M, Bujard H. 1995. Co-regulation of two gene activities by tetracycline via a bidirectional promoter. *Nucleic Acids Res.* 23:3605-3506.

Barrandon Y and Green H. 1987. Cell migration is essential for sustained growth of keratinocyte colonies: the roles of transforming growth factor-alpha and epidermal growth factor. *Cell* 50:1131-1137.

Beato, M; Herrlich, P; Schütz, G. 1995. Steroid hormone receptors: many actors in search of a plot. *Cell* 83:851-857.

Berridge MJ. 1993. Inositol trisphosphate and calcium signalling. *Nature* 361:315-325.

Bertics PJ, Weber W, Cochet C, Gill GN. 1985. Regulation of the epidermal growth factor receptor by phosphorylation. *J. Cell. Biochem.* 29:195-208.

Bier E, Jan LY, Jan YN. 1990. Rhomboid, a gene required for dorsoventral axis establishment and peripheral nervous system development in *Drosophila melanogaster*. *Genes. Dev.* 4:190-203.

Bier E. 1998. Localized activation of RTK/MAPK pathways during *Drosophila* development. *Bioessays* 20:189-194.

Bjorge JD, Chan TO, Antczak M, Kung HJ, Fujita DJ. 1990. Activated type I phosphatidylinositol kinase is associated with the epidermal growth factor (EGF) receptor following EGF stimulation. *Proc. Natl. Acad. Sci.* 87:3816-3820.

Black RA, Rauch CT, Kozlosky CJ, Peschon JJ, Slack JL, Wolfson MF, Castner BJ, Stocking KL, Reddy P, Srinivasan S, Nelson N, Boiani N, Schooley KA, Gerhart M, Davis R, Fitzner JN, Johnson RS, Paxton RJ, March CJ, Cerretti DP. 1997. A metalloproteinase disintegrin that releases tumour-necrosis factor-alpha from cells. *Nature* 385:729-733.

Boguski MS and McCormick F. 1993. Proteins regulating Ras and its relatives. *Nature* 366:643-654.

Bosenberg MW, Pandiella A, Massague J. 1993. Activated release of membrane-anchored TGF-alpha in the absence of cytosol. *J. Cell. Biol.* 122:95-101.

Bosenberg MW and Massague J. 1993. Juxtacrine cell signaling molecules. *Curr. Opin. Cell. Biol.* 5:832-838.

Bourne HR. 1997. How receptors talk to trimeric G proteins. *Curr. Opin. Cell. Biol.* 9:134-142.

Bourne HR, Sanders DA, McCormick F. 1991. The GTPase superfamily: conserved structure and molecular mechanism. *Nature* 349:117-127.

Brachmann R, Lindquist PB, Nagashima M, Kohr W, Lipari T, Napier M, Derynck R. 1989. Transmembrane TGF-alpha precursors activate EGF/TGF-alpha receptors. *Cell* 56:691-700.

Brendel V, Bucher P, Nourbakhsh IR, Blaisdell BE, Karlin S. 1992. Methods and algorithms for statistical analysis of protein sequences. *Proc. Natl. Acad. Sci.* 89:2002-2006.

Bridges CB and Morgan TH. 1919. Contributions to the genetics of *Drosophila melanogaster*. *Carnegie Institute Washington Publication* 278:123-304.

Briley GP, Hissong MA, Chiu ML, Lee DC. 1997. The carboxyl-terminal valine residues of proTGF alpha are required for its efficient maturation and intracellular routing. *Mol. Biol. Cell.* 8:1619-1631.

Bringman TS, Lindquist PB, Derynck R. 1987. Different transforming growth factor-alpha species are derived from a glycosylated and palmitoylated transmembrane precursor. *Cell* 48:429-440.

- Brunet A, Roux D, Lenormand P, Dowd S, Keyse S, Pouyssegur J. 1999. Nuclear translocation of p42/p44 mitogen-activated protein kinase is required for growth factor-induced gene expression and cell cycle entry. *EMBO J.* 18:664-674.
- Buday L and Downward J. 1993. Epidermal growth factor regulates p21ras through the formation of a complex of receptor, Grb2 adapter protein, and Sos nucleotide exchange factor. *Cell* 73:611-620.
- Bustin SA, Nie XF, Barnard RC, Kumar V, Pascall JC, Brown KD, Leigh IM, Williams NS, McKay IA. 1994. Cloning and characterization of ERF-1, a human member of the Tis11 family of early-response genes. *DNA Cell Biol* 13:449-459.
- Campbell SL, Khosravi-Far R, Rossman KL, Clark GJ, Der CJ. 1998. Increasing complexity of Ras signaling. *Oncogene* 17:1395-1413.
- Carpenter CL, Auger KR, Duckworth BC, Hou WM, Schaffhausen B, Cantley LC. 1993. A tightly associated serine/threonine protein kinase regulates phosphoinositide 3-kinase activity. *Mol. Cell. Biol.* 13:1657-1665.
- Carpenter G and Cohen S. 1976. 125I-labeled human epidermal growth factor. Binding, internalization, and degradation in human fibroblasts. *J. Cell. Biol.* 71:159-171.
- Carpenter G, Stoscheck CM, Preston YA, DeLarco JE. 1983. Antibodies to the epidermal growth factor receptor block the biological activities of sarcoma growth factor. *Proc. Natl. Acad. Sci.* 80:5627-5630.
- Carter-Su C and Smit LS. Signaling via JAK tyrosine kinases: growth hormone receptor as a model system. 1998. *Recent. Prog. Horm. Res.* 53:61-82; discussion 82-83.
- Cartlidge SA and Elder JB. 1989. Transforming growth factor alpha and epidermal growth factor levels in normal human gastrointestinal mucosa. *Br. J. Cancer* 60:657-660.
- Chardin P, Camonis JH, Gale NW, van Aelst L, Schlessinger J, Wigler MH, Bar-Sagi D. 1993. Human Sos1: a guanine nucleotide exchange factor for Ras that binds to GRB2. *Science* 260:1338-1343.
- Chen RH and Derynck R. 1994. Homomeric interactions between type II transforming growth factor-beta receptors. *J. Biol. Chem.* 269:22868-22874.
- Chen RH, Sarnecki C, Blenis J. 1992. Nuclear localization and regulation of erk- and rsk-encoded protein kinases. *Mol. Cell. Biol.* 12:915-927.
- Clapham DE. 1995. Calcium signaling. *Cell* 80:259-268.
- Chen WS, Lazar CS, Poenie M, Tsien RY, Gill GN, Rosenfeld MG. 1987. Requirement for intrinsic protein tyrosine kinase in the immediate and late actions of the EGF receptor. *Nature* 328:820-823.

- Clifford R and Schupbach T. 1992. The torpedo (DER) receptor tyrosine kinase is required at multiple times during *Drosophila* embryogenesis. *Development* 115:853-872.
- Coffey RJ Jr, Derynck R, Wilcox JN, Bringman TS, Goustin AS, Moses HL, Pittelkow MR. 1987. Production and auto-induction of transforming growth factor-alpha in human keratinocytes. *Nature* 328:817-820.
- Cohen S. 1962. Isolation of a mouse submaxillary gland protein accelerating incisor eruption and eyelid opening in the newborn animal. *J. Biol. Chem.* 237:1555-1562.
- Cohen S and Elliot GA. 1963. The stimulation of epidermal keratinization by a protein isolated from the submaxillary gland of mice. *J Invest. Dermatol.* 40:1-5.
- Cohen S. 1965. The stimulation of epidermal proliferation by a specific protein (EGF). *Dev. Biol.* 12:394-407
- Countaway JL, Northwood IC, Davis RJ. 1989. Mechanism of phosphorylation of the epidermal growth factor receptor at threonine 669. *J. Biol. Chem.* 264:10828-10835.
- Crews CM, Alessandrini A, Erikson RL. 1992. The primary structure of MEK, a protein kinase that phosphorylates the ERK gene product. *Science* 258:478-480.
- Crews CM and Erikson RL. 1993. Extracellular signals and reversible protein phosphorylation: what to Mek of it all. *Cell* 74:215-217.
- de Larco JE and Todaro GJ. 1978. Growth factors from murine sarcoma virus-transformed cells. *Proc. Natl. Acad. Sci.* 75:4001-4005.
- Dempsey PJ and Coffey RJ. 1994. Basolateral targeting and efficient consumption of transforming growth factor-alpha when expressed in Madin-Darby canine kidney cells. *J. Biol. Chem.* 269:16878-16889.
- Denhardt DT. 1996. Signal-transducing protein phosphorylation cascades mediated by Ras/Rho proteins in the mammalian cell: the potential for multiplex signalling. *Biochem J.* 318:729-747.
- Dent P, Haser W, Haystead TA, Vincent LA, Roberts TM, Sturgill TW. 1992. Activation of mitogen-activated protein kinase kinase by v-Raf in NIH 3T3 cells and in vitro. *Science* 257:1404-1407.
- Derynck R, Roberts AB, Winkler ME, Chen EY, Goeddel DV. 1984. Human transforming growth factor-alpha: precursor structure and expression in *E. coli*. *Cell* 38:287-297.

Derynck R, Goeddel DV, Ullrich A, Gutterman JU, Williams RD, Bringman TS, Berger WH. 1987. Synthesis of messenger RNAs for transforming growth factors alpha and beta and the epidermal growth factor receptor by human tumors. *Cancer Res.* 47:707-712.

Derynck R. 1992. The physiology of transforming growth factor-alpha. *Adv. Cancer Res.* 58:27-52.

Dhand R, Hiles I, Panayotou G, Roche S, Fry MJ, Gout I, Totty NF, Truong O, Vicendo P, Yonezawa K, *et al.* 1994. PI 3-kinase is a dual specificity enzyme: autoregulation by an intrinsic protein-serine kinase activity. *EMBO J* 13:522-533.

Di Fiore PP, Pierce JH, Fleming TP, Hazan R, Ullrich A, King CR, Schlessinger J, Aaronson SA. 1987. Overexpression of the human EGF receptor confers an EGF-dependent transformed phenotype to NIH 3T3 cells. *Cell* 51:1063-1070.

Di Marco E, Pierce JH, Fleming TP, Kraus MH, Molloy CJ, Aaronson SA, Di Fiore PP. 1989. Autocrine interaction between TGF alpha and the EGF-receptor: quantitative requirements for induction of the malignant phenotype. *Oncogene* 4:831-838.

Diaz-Benjumea FJ and Garcia-Bellido A. 1990. Genetic analysis of the wing vein pattern of *Drosophila*. *Wilhelm Roux's Arch. Dev. Biol.* 198:336-354.

Diaz-Benjumea FJ and Hafen E. 1994. The sevenless signalling cassette mediates *Drosophila* EGF receptor function during epidermal development. *Development* 120:569-578.

Dobashi Y and Stern DF. 1991. Membrane-anchored forms of EGF stimulate focus formation and intercellular communication. *Oncogene* 6:1151-1159.

Dong J, Opresko LK, Dempsey PJ, Lauffenburger DA, Coffey RJ, Wiley HS. 1999. Metalloprotease-mediated ligand release regulates autocrine signaling through the epidermal growth factor receptor. *Proc. Natl. Acad. Sci.* 96:6235-6240.

Downward J, Waterfield MD, Parker PJ. 1985. Autophosphorylation and protein kinase C phosphorylation of the epidermal growth factor receptor. Effect on tyrosine kinase activity and ligand binding affinity. *J. Biol. Chem.* 260:14538-14546.

Egan SE, Giddings BW, Brooks MW, Buday L, Sizeland AM, Weinberg RA. 1993. Association of Sos Ras exchange protein with Grb2 is implicated in tyrosine kinase signal transduction and transformation. *Nature* 363:45-51

Egan SE and Weinberg RA. 1993. The pathway to signal achievement. *Nature* 365:781-783.

Earp HS, Dawson TL, Li X, Yu H. 1995. Heterodimerization and functional interaction between EGF receptor family members: a new signaling paradigm with implications for breast cancer research. *Breast Cancer Research Treat.* 35:115-132.

Evans RM. 1988. The steroid and thyroid hormone receptor superfamily. *Science* 240:889-895.

Fan HZ and Derynck R. 1999. Ectodomain shedding regulated by distinct MAP kinase signaling cascades. *EMBO J.* submitted.

Fantl WJ, Johnson DE, Williams LT. 1993. Signaling by receptor tyrosine kinases. *Annu. Rev. Biochem.* 62:453-481.

Feehan C, Darlak K, Kahn J, Walcheck B, Spatola AF, Kishimoto TK. 1996. Shedding of the lymphocyte L-selectin adhesion molecule is inhibited by a hydroxamic acid-based protease inhibitor. Identification with an L-selectin-alkaline phosphatase reporter. *J. Biol. Chem.* 271:7019-7024.

Freeman M, Kimmel BE, Rubin GM. 1992. Identifying targets of the rough homeobox gene of *Drosophila*: evidence that rhomboid functions in eye development. *Development* 116:335-346.

Freeman M. 1994. The spitz gene is required for photoreceptor determination in the *Drosophila* eye where it interacts with the EGF receptor. *Mech. Dev.* 48:25-33.

Freeman M. 1996. Reiterative use of the EGF receptor triggers differentiation of all cell types in the *Drosophila* eye. *Cell* 87:651-660.

Gabay L, Seger R, Shilo BZ. 1997. In situ activation pattern of *Drosophila* EGF receptor pathway during development. *Science* 277:1103-1106.

Gether U and Kobilka BK. 1998. G protein-coupled receptors. II. Mechanism of agonist activation. *J. Biol. Chem.* 273:17979-17982.

Gill GN. 1990. Regulation of EGF receptor expression and function. *Mol. Reprod. Dev.* 27:46-53

Gilman AG. 1987. G proteins: transducers of receptor-generated signals. *Annu. Rev. Biochem.* 56:615-649.

Golembo M, Raz E, Shilo BZ. 1996. The *Drosophila* embryonic midline is the site of Spitz processing, and induces activation of the EGF receptor in the ventral ectoderm. *Development* 122:3363-3370.

- Gomperts M, Pascall JC, Brown KD. 1990. The nucleotide sequence of a cDNA encoding an EGF-inducible gene indicates the existence of a new family of mitogen-induced genes. *Oncogene* 5:1081-1083.
- Gonzalez-Reyes A, Elliott H, St Johnston D. 1995. Polarization of both major body axes in *Drosophila* by gurken-torpedo signalling. *Nature* 375:654-658.
- Gossen M and Bujard H. 1992. Tight control of gene expression in mammalian cells by tetracycline-responsive promoters. *Proc. Natl. Acad. Sci.* 89:5547-5551.
- Gregory H. 1975. Isolation and structure of urogastrone and its relationship to epidermal growth factor. *Nature* 257:325-327.
- Guichard A, Biehs B, Sturtevant MA, Wickline L, Chacko J, Howard K, Bier E. 1999. Rhomboid and Star interact synergistically to promote EGFR/MAPK signaling during *Drosophila* wing vein development. *Development* 126:2663-2676.
- Hammacher A, Mellstrom K, Heldin CH, Westermark B. 1989. Isoform-specific induction of actin reorganization by platelet-derived growth factor suggests that the functionally active receptor is a dimer. *EMBO J.* 8:2489-2495.
- Hawkins PT, Jackson TR, Stephens LR. 1992. Platelet-derived growth factor stimulates synthesis of PtdIns(3,4,5)P3 by activating a PtdIns(4,5)P2 3-OH kinase. *Nature* 358:157-159.
- Heberlein U and Rubin GM. 1991. Star is required in a subset of photoreceptor cells in the developing *Drosophila* retina and displays dosage sensitive interactions with rough. *Dev. Biol.* 144:353-361.
- Heberlein U, Hariharan IK, Rubin GM. 1993. Star is required for neuronal differentiation in the *Drosophila* retina and displays dosage-sensitive interactions with Ras1. *Dev. Biol.* 160:51-63.
- Heldin CH. 1995. Dimerization of cell surface receptors in signal transduction. *Cell* 80:213-223.
- Hepler JR and Gilman AG. 1992. G proteins. *Trends Biochem. Sci.* 17:383-387.
- Higashiyama S, Iwamoto R, Goishi K, Raab G, Taniguchi N, Klagsbrun M, Mekada E. 1995. The membrane protein CD9/DRAP 27 potentiates the juxtacrine growth factor activity of the membrane-anchored heparin-binding EGF-like growth factor. *J. Cell. Biol.* 128:929-938.
- Hill CS, Marais R, John S, Wynne J, Dalton S, Treisman R. 1993. Functional analysis of a growth factor-responsive transcription factor complex. *Cell* 73:395-406.

- Hock RA, Nexø E, Hollenberg MD. 1979. Isolation of the human placenta receptor for epidermal growth factor-urogastrone. *Nature* 277:403-405.
- Hoffmann P, Zeeh JM, Lakshmanan J, Wu VS, Procaccino F, Reinshagen M, McRoberts JA, Eysselein VE. 1997. Increased expression of transforming growth factor alpha precursors in acute experimental colitis in rats. *Gut* 41:195-202.
- Hofmann K and Stoffel W. 1993. TMbase - A database of membrane spanning proteins segments. *Biol. Chem. Hoppe-Seyler* 347:166-170.
- Hoover JK and Cohen S. 1967. Epidermal growth factor. I. The stimulation of protein and ribonucleic acid synthesis in chick embryo epidermis. *Biochim. Biophys. Acta* 138:347-356
- Howe LR, Leever SJ, Gomez N, Nakielny S, Cohen P, Marshall CJ. 1992. Activation of the MAP kinase pathway by the protein kinase raf. *Cell* 71:335-342.
- Hu P, Margolis B, Skolnik EY, Lammers R, Ullrich A, Schlessinger J. 1992. Interaction of phosphatidylinositol 3-kinase-associated p85 with epidermal growth factor and platelet-derived growth factor receptors. *Mol. Cell. Biol.* 12:981-990.
- Hunter T. 1995. When is a lipid kinase not a lipid kinase? When it is a protein kinase. *Cell* 83:1-4.
- Ip YT, Park RE, Kosman D, Bier E, Levine M. 1992. The dorsal gradient morphogen regulates stripes of rhomboid expression in the presumptive neuroectoderm of the *Drosophila* embryo. *Genes Dev.* 6:1728-1739.
- Jhappan C, Stahle C, Harkins RN, Fausto N, Smith GH, Merlino GT. 1990. TGF alpha overexpression in transgenic mice induces liver neoplasia and abnormal development of the mammary gland and pancreas. *Cell* 61:1137-1146.
- Ji TH, Grossmann M, Ji I. 1998. G protein-coupled receptors. I. Diversity of receptor-ligand interactions. *J. Biol. Chem.* 273:17299-17302.
- Jurgens G, Wieschaus E, Nusslein-Volhard C, Kluding H. 1984. Mutations affecting the pattern of the larval cuticle in *Drosophila melanogaster*. II. Zygotic loci on the third chromosome. *Wilhelm Roux's Arch. Dev. Biol.* 193:283-295.
- Kammermeyer KL and Wadsworth SC. 1987. Expression of *Drosophila* epidermal growth factor receptor homologue in mitotic cell populations. *Development* 100:201-210.
- Kanashiro CA and Khalil RA. 1998. Signal transduction by protein kinase C in mammalian cells. *Clin. Exp. Pharmacol. Physiol.* 25:974-985.

Katzen AL, Kornberg T, Bishop JM. 1991. Expression during *Drosophila* development of DER, a gene related to erbB-1 and neu: correlations with mutant phenotypes. *Dev. Biol.* 145:287-301.

Kielman MF, Smits R, Devi TS, Fodde R, Bernini LF. 1993. Homology of a 130-kb region enclosing the alpha-globin gene cluster, the alpha-locus controlling region, and two non-globin genes in human and mouse. *Mamm. Genome* 4:314-323.

Kiessling LL and Gordon EJ. 1998. Transforming the cell surface through proteolysis. *Chem. Biol.* 5:R49-R62.

Kim SH and Crews ST. 1993. Influence of *Drosophila* ventral epidermal development by the CNS midline cells and spitz class genes. *Development* 118:893-901.

King AJ, Sun H, Diaz B, Barnard D, Miao W, Bagrodia S, Marshall MS. 1998. The protein kinase Pak3 positively regulates Raf-1 activity through phosphorylation of serine 338. *Nature* 396:180-183.

Kolodkin AL, Pickup AT, Lin DM, Goodman CS, Banerjee U. 1994. Characterization of Star and its interactions with sevenless and EGF receptor during photoreceptor cell development in *Drosophila*. *Development* 120:1731-1745.

Kotani K, Yonezawa K, Hara K, Ueda H, Kitamura Y, Sakaue H, Ando A, Chavanieu A, Calas B, Grigorescu F, *et al.* 1994. Involvement of phosphoinositide 3-kinase in insulin- or IGF-1-induced membrane ruffling. *EMBO J.* 13:2313-2321.

Kozak M. 1987. At least six nucleotides preceding the AUG initiator codon enhance translation in mammalian cells. *J. Mol. Biol.* 196:947-950.

Kuo, AC. 1999. Identification and characterization of proteins that associate with transmembrane transforming growth factor alpha. *Doctoral Thesis, UCSF.*

Kyriakis JM, App H, Zhang XF, Banerjee P, Brautigan DL, Rapp UR, Avruch J. 1992. Raf-1 activates MAP kinase-kinase. *Nature* 358:417-421.

Laird AD, Brown PI, Fausto N. 1994. Inhibition of tumor growth in liver epithelial cells transfected with a transforming growth factor alpha antisense gene. *Cancer Res.* 54:4224-4432.

Lavoie JN, L'Allemain G, Brunet A, Muller R, Pouyssegur J. 1996. Cyclin D1 expression is regulated positively by the p42/p44MAPK and negatively by the p38/HOGMAPK pathway. *J. Biol. Chem.* 271:20608-20616.

Lee DC, Rose TM, Webb NR, Todaro GJ. 1985. Cloning and sequence analysis of a cDNA for rat transforming growth factor-alpha. *Nature* 313:489-491.

- Lemmon MA and Schlessinger J. 1994. Regulation of signal transduction and signal diversity by receptor oligomerization. *Trends Biochem. Sci.* 19:459-464.
- Lenormand P, Sardet C, Pages G, L'Allemain G, Brunet A, Pouyssegur J. 1993. Growth factors induce nuclear translocation of MAP kinases (p42mapk and p44mapk) but not of their activator MAP kinase kinase (p45mapkk) in fibroblasts. *J. Cell. Biol.* 122:1079-1088.
- Li N, Batzer A, Daly R, Yajnik V, Skolnik E, Chardin P, Bar-Sagi D, Margolis B, Schlessinger J. 1993. Guanine-nucleotide-releasing factor hSos1 binds to Grb2 and links receptor tyrosine kinases to Ras signalling. *Nature* 363:85-88.
- Livneh E, Glazer L, Segal D, Schlessinger J, Shilo BZ. 1985. The Drosophila EGF receptor gene homolog: conservation of both hormone binding and kinase domains. *Cell* 40:599-607.
- Lowenstein EJ, Daly RJ, Batzer AG, Li W, Margolis B, Lammers R, Ullrich A, Skolnik EY, Bar-Sagi D, Schlessinger J. 1992. The SH2 and SH3 domain-containing protein GRB2 links receptor tyrosine kinases to ras signaling. *Cell* 70:431-442.
- Lowy DR and Willumsen BM. 1993. Function and regulation of ras. *Annu. Rev. Biochem.* 62:851-891.
- Luetke NC, Qiu TH, Peiffer RL, Oliver P, Smithies O, Lee DC. 1993. TGF alpha deficiency results in hair follicle and eye abnormalities in targeted and waved-1 mice. *Cell* 73:263-278.
- Madtes DK, Raines EW, Sakariassen KS, Assoian RK, Sporn MB, Bell GI, Ross R. 1988. Induction of transforming growth factor-alpha in activated human alveolar macrophages. *Cell* 53:285-293.
- Mann GB, Fowler KJ, Gabriel A, Nice EC, Williams RL, Dunn AR. 1993. Mice with a null mutation of the TGF alpha gene have abnormal skin architecture, wavy hair, and curly whiskers and often develop corneal inflammation. *Cell* 73:249-261.
- Marais R, Wynne J, Treisman R. 1993. The SRF accessory protein Elk-1 contains a growth factor-regulated transcriptional activation domain. *Cell* 73:381-393.
- Marais R, Light Y, Paterson HF, Marshall CJ. 1995. Ras recruits Raf-1 to the plasma membrane for activation by tyrosine phosphorylation. *EMBO J.* 14:3136-3145.
- Margolis B, Rhee SG, Felder S, Mervic M, Lyall R, Levitzki A, Ullrich A, Zilberstein A, Schlessinger J. 1989. EGF induces tyrosine phosphorylation of phospholipase C-II: a potential mechanism for EGF receptor signaling. *Cell* 57:1101-1107.

- Margolis B, Bellot F, Honegger AM, Ullrich A, Schlessinger J, Zilberstein A. 1990. Tyrosine kinase activity is essential for the association of phospholipase C-gamma with the epidermal growth factor receptor. *Mol. Cell. Biol.* 10:435-441.
- Marquardt H, Hunkapiller MW, Hood LE, Todaro GJ. 1984. Rat transforming growth factor type 1: structure and relation to epidermal growth factor. *Science* 223:1079-1082.
- Martin P, Hopkinson-Woolley J, McCluskey J. 1992. Growth factors and cutaneous wound repair. *Prog. Growth. Factor. Res.* 4:25-44.
- Massague J. 1983. Epidermal growth factor-like transforming growth factor I. Isolation, chemical characterization, and potentiation by other transforming factors from feline sarcoma virus-transformed rat cells. *J. Biol. Chem.* 258:13606-13613.
- Massague J and Pandiella A. 1993. Membrane-anchored growth factors. *Annu. Rev. Biochem.* 62:515-541.
- Matsui Y, Halter SA, Holt JT, Hogan BL, Coffey RJ. 1990. Development of mammary hyperplasia and neoplasia in MMTV-TGF alpha transgenic mice. *Cell* 61:1147-1155.
- Mayer U and Nusslein-Volhard C. 1988. A group of genes required for pattern formation in the ventral ectoderm of the Drosophila embryo. *Genes Dev.* 2:1496-1511.
- McCormick F. 1995. Ras-related proteins in signal transduction and growth control. *Mol. Reprod. Dev.* 42:500-506.
- Merlos-Suarez A and Arribas J. 1999. Mechanisms controlling the shedding of transmembrane molecules. *Biochem. Soc. Trans.* 27:243-246.
- Miettinen PJ, Berger JE, Meneses J, Phung Y, Pedersen RA, Werb Z, Derynck R. 1995. Epithelial immaturity and multiorgan failure in mice lacking epidermal growth factor receptor. *Nature* 376:337-341.
- Miettinen PJ, Chin JR, Shum L, Slavkin HC, Shuler CF, Derynck R, Werb Z. 1999. Epidermal growth factor receptor function is necessary for normal craniofacial development and palate closure. *Nature Genetics* 22:69-73.
- Moghal N and Sternberg PW. 1999. Multiple positive and negative regulators of signaling by the EGF-receptor. *Curr. Op. Cell. Biol.* 11:190-196.
- Moodie SA, Willumsen BM, Weber MJ, Wolfman A. 1993. Complexes of Ras.GTP with Raf-1 and mitogen-activated protein kinase kinase. *Science* 260:1658-1661.

Moss ML, Jin SL, Milla ME, Bickett DM, Burkhart W, Carter HL, Chen WJ, Clay WC, Didsbury JR, Hassler D, Hoffman CR, Kost TA, Lambert MH, Leesnitzer MA, McCauley P, McGeehan G, Mitchell J, Moyer M, Pahel G, Rocque W, Overton LK, Schoenen F, Seaton T, Su JL, Becherer JD, et al. 1997. Cloning of a disintegrin metalloproteinase that processes precursor tumour-necrosis factor-alpha. *Nature* 385:733-736.

Muller R, Bravo R, Burckhardt J, Curran T. 1984. Induction of c-fos gene and protein by growth factors precedes activation of c-myc. *Nature* 312:716-720.

Naglich JG, Metherall JE, Russell DW, Eidels L. 1992. Expression cloning of a diphtheria toxin receptor: identity with a heparin-binding EGF-like growth factor precursor. *Cell* 69:1051-1061.

Nakagawa T, Higashiyama S, Mitamura T, Mekada E, Taniguchi N. 1996. Amino-terminal processing of cell surface heparin-binding epidermal growth factor-like growth factor up-regulates its juxtacrine but not its paracrine growth factor activity. *J. Biol. Chem.* 271:30858-30863.

Neuman-Silberberg FS and Schupbach T. 1993. The *Drosophila* dorsoventral patterning gene *gurken* produces a dorsally localized RNA and encodes a TGF alpha-like protein. *Cell* 75:165-174.

Neuman-Silberberg FS and Schupbach T. 1996. The *Drosophila* TGF-alpha-like protein *Gurken*: expression and cellular localization during *Drosophila* oogenesis. *Mech. Dev.* 59:105-113.

Newton AC. 1997. Regulation of protein kinase C. *Curr. Opin. Cell. Biol.* 9:161-167.

Nobes CD and Hall A. 1995. Rho, rac, and cdc42 GTPases regulate the assembly of multimolecular focal complexes associated with actin stress fibers, lamellipodia, and filopodia. *Cell* 81:53-62.

Nusslein-Volhard C, Wieschaus E, Kluding H. 1984. Mutations affecting the pattern of the larval cuticle in *Drosophila melanogaster*. I. Zygotic loci on the second chromosome. *Wilhelm Roux's Arch. Dev. Biol.* 183:267-282.

Ono M, Raab G, Lau K, Abraham JA, Klagsbrun M. 1994. Purification and characterization of transmembrane forms of heparin-binding EGF-like growth factor. *J. Biol. Chem.* 269:31315-31321.

Pandiella A and Massague J. 1991a. Cleavage of the membrane precursor for transforming growth factor alpha is a regulated process. *Proc. Natl. Acad. Sci.* 88:1726-1730.

Pandiella A and Massague J. 1991b. Multiple signals activate cleavage of the membrane transforming growth factor-alpha precursor. *J. Biol. Chem.* 266:5769-5773.

Pandiella A, Bosenberg MW, Huang EJ, Besmer P, Massague J. 1992. Cleavage of membrane-anchored growth factors involves distinct protease activities regulated through common mechanisms. *J. Biol. Chem.* 267:24028-24033.

Paria BC, Das SK, Andrews GK, Dey SK. 1993. Expression of the epidermal growth factor receptor gene is regulated in mouse blastocysts during delayed implantation. *Proc. Nat. Acad. Sci.* 90:55-59

Pascall JC and Brown KD. 1998. Characterization of a mammalian cDNA encoding a protein with high sequence similarity to the Drosophila regulatory protein Rhomboid. *FEBS Lett.* 429:337-340.

Payne DM, Rossomando AJ, Martino P, Erickson AK, Her JH, Shabanowitz J, Hunt DF, Weber MJ, Sturgill TW. 1991. Identification of the regulatory phosphorylation sites in pp42/mitogen-activated protein kinase (MAP kinase). *EMBO J.* 10:885-892.

Perez C, Albert I, DeFay K, Zachariades N, Gooding L, Kriegler M. 1990. A nonsecretable cell surface mutant of tumor necrosis factor (TNF) kills by cell-to-cell contact. *Cell* 63:251-258.

Perrimon N. 1993. The torso receptor protein-tyrosine kinase signaling pathway: an endless story. *Cell* 74:219-222.

Perrimon N and Perkins LA. 1997. There must be 50 ways to rule the signal: the case of the Drosophila EGF receptor. *Cell* 89:13-16.

Peschon JJ, Slack JL, Reddy P, Stocking KL, Sunnarborg SW, Lee DC, Russell WE, Castner BJ, Johnson RS, Fitzner JN, Boyce RW, Nelson N, Kozlosky CJ, Wolfson MF, Rauch CT, Cerretti DP, Paxton RJ, March CJ, Black RA. 1998. An essential role for ectodomain shedding in mammalian development. *Science* 282:1281-1284.

Pickup AT and Banerjee U. 1999. The role of star in the production of an activated ligand for the EGF receptor signaling pathway. *Dev. Biol.* 205:254-259.

Pierce JH, Ruggiero M, Fleming TP, Di Fiore PP, Greenberger JS, Varticovski L, Schlessinger J, Rovera G, Aaronson SA. 1988. Signal transduction through the EGF receptor transfected in IL-3-dependent hematopoietic cells. *Science* 239:628-631.

Price JV, Clifford RJ, Schupbach T. 1989. The maternal ventralizing locus torpedo is allelic to faint little ball, an embryonic lethal, and encodes the Drosophila EGF receptor homolog. *Cell* 56:1085-1092.

- Raffioni S and Bradshaw RA. 1992. Activation of phosphatidylinositol 3-kinase by epidermal growth factor, basic fibroblast growth factor, and nerve growth factor in PC12 pheochromocytoma cells. *Proc. Natl. Acad. Sci.* 89:9121-9125.
- Rappolee DA, Brenner CA, Schultz R, Mark D, Werb Z. 1988a. Developmental expression of PDGF, TGF-alpha, and TGF-beta genes in preimplantation mouse embryos. *Science* 241:1823-1825.
- Rappolee DA, Mark D, Banda MJ, Werb Z. 1988b. Wound macrophages express TGF-alpha and other growth factors in vivo: analysis by mRNA phenotyping. *Science* 241:708-712.
- Raz E and Shilo BZ. 1992. Dissection of the faint little ball (flb) phenotype: determination of the development of the Drosophila central nervous system by early interactions in the ectoderm. *Development* 114:113-123.
- Raz E and Shilo BZ. 1993. Establishment of ventral cell fates in the Drosophila embryonic ectoderm requires DER, the EGF receptor homolog. *Genes Dev.* 7:1937-1948.
- Rechsteiner M and Rogers SW. 1996. PEST sequences and regulation by proteolysis. *Trends Biochem. Sci.* 21:267-271.
- Reszka AA, Seger R, Diltz CD, Krebs EG, Fischer EH. 1995. Association of mitogen-activated protein kinase with the microtubule cytoskeleton. *Proc. Natl. Acad. Sci.* 92:8881-8885.
- Rhee SG, Bae YS. 1997. Regulation of phosphoinositide-specific phospholipase C isozymes. *J. Biol. Chem.* 272:15045-15048.
- Riese DJ and Stern DF. 1998. Specificity within the EGF family/ErbB receptor family signaling network. *Bioessays* 20:41-48.
- Robinson MJ and Cobb MH. 1997. Mitogen-activated protein kinase pathways. *Curr. Opin. Cell. Biol.* 9:180-186.
- Rogers S, Wells R, Rechsteiner M. 1986. Amino acid sequences common to rapidly degraded proteins: the PEST hypothesis. *Science* 234:364-368.
- Rozakis-Adcock M, Fernley R, Wade J, Pawson T, Bowtell D. 1993. The SH2 and SH3 domains of mammalian Grb2 couple the EGF receptor to the Ras activator mSos1. *Nature* 363:83-85.
- Ruohola-Baker H, Grell E, Chou TB, Baker D, Jan LY, Jan YN. 1993. Spatially localized rhomboid is required for establishment of the dorsal-ventral axis in Drosophila oogenesis. *Cell* 73:953-965.

Russell WE, Dempsey PJ, Sitaric S, Peck AJ, Coffey RJ Jr. 1993. Transforming growth factor-alpha (TGF alpha) concentrations increase in regenerating rat liver: evidence for a delayed accumulation of mature TGF alpha. *Endocrinology* 133:1731-1738.

Rutledge BJ, Zhang K, Bier E, Jan YN, Perrimon N. 1992. The *Drosophila* spitz gene encodes a putative EGF-like growth factor involved in dorsal-ventral axis formation and neurogenesis. *Genes Dev.* 6:1503-1517.

Salomon DS, Brandt R, Ciardiello F, Normanno N. 1995. Epidermal growth factor-related peptides and their receptors in human malignancies. *Crit. Rev. Oncol. Hematol.* 19:183-232.

Sandgren EP, Luetkeke NC, Palmiter RD, Brinster RL, Lee DC. 1990. Overexpression of TGF alpha in transgenic mice: induction of epithelial hyperplasia, pancreatic metaplasia, and carcinoma of the breast. *Cell* 61:1121-1135.

Savage CR Jr, Hash JH, Cohen S. 1973. Epidermal growth factor. Location of disulfide bonds. *J. Biol. Chem.* 248:7669-7672.

Schejter ED, Segal D, Glazer L, Shilo BZ. 1986. Alternative 5' exons and tissue-specific expression of the *Drosophila* EGF receptor homolog transcripts. *Cell* 46:1091-1101.

Schejter ED and Shilo BZ. 1989. The *Drosophila* EGF receptor homolog (DER) gene is allelic to faint little ball, a locus essential for embryonic development. *Cell* 56:1093-1104.

Schlessinger J. 1988. Signal transduction by allosteric receptor oligomerization. *Trends Biochem. Sci.* 13:443-447.

Schlessinger J. 1993. How receptor tyrosine kinases activate Ras. *Trends. Biochem. Sci.* 18:273-275.

Schnepf B, Grumblin G, Donaldson T, Simcox A. 1996. Vein is a novel component in the *Drosophila* epidermal growth factor receptor pathway with similarity to the neuregulins. *Genes Dev.* 10:2302-2313.

Schreiber AB, Winkler ME, Derynck R. 1986. Transforming growth factor-alpha: a more potent angiogenic mediator than epidermal growth factor. *Science* 232:1250-1253.

Schultz GS, White M, Mitchell R, Brown G, Lynch J, Twardzik DR, Todaro GJ. 1987. Epithelial wound healing enhanced by transforming growth factor-alpha and vaccinia growth factor. *Science* 235:350-352.

Schultz G, Rotatori DS, Clark W. 1991. EGF and TGF-alpha in wound healing and repair. *J. Cell. Biochem.* 45:346-352.

- Schupbach T. 1987. Germ line and soma cooperate during oogenesis to establish the dorsoventral pattern of egg shell and embryo in *Drosophila melanogaster*. *Cell* 49:699-707
- Schweitzer R, Shaharabany M, Seger R, Shilo BZ. 1995. Secreted Spitz triggers the DER signaling pathway and is a limiting component in embryonic ventral ectoderm determination. *Genes Dev.* 9:1518-1529.
- Schweitzer R and Shilo BZ. 1997. A thousand and one roles for the *Drosophila* EGF receptor. *Trends Genet.* 13:191-196.
- Seger R and Krebs EG. 1995. The MAPK signaling cascade. *FASEB J.* 9:726-735.
- Seki S, Sakai Y, Kitada T, Kawakita N, Yanai A, Tsutsui H, Sakaguchi H, Kuroki T, Monna T. 1997. Induction of apoptosis in a human hepatocellular carcinoma cell line by a neutralizing antibody to transforming growth factor- α . *Virchows Arch.* 430:29-35.
- Shi W, Fan H-Z, Shum L, Derynck R. 1999. The tetraspannin CD9 associates with transmembrane TGF α and regulates EGFR stimulation . *J. Cell. Biol.* Submitted
- Shum L, Reeves SA, Kuo AC, Fromer ES, Derynck R. 1994. Association of the transmembrane TGF- α precursor with a protein kinase complex. *J. Cell. Biol.* 125:903-916.
- Shum L, Turck CW, Derynck R. 1996. Cysteines 153 and 154 of transmembrane transforming growth factor- α are palmitoylated and mediate cytoplasmic protein association. *J. Biol. Chem.* 271:28502-28508.
- Sibilia M and Wagner EF. 1995. Strain-dependent epithelial defects in mice lacking the EGF receptor. *Science* 269:234-238.
- Simcox AA, Grumblin G, Schnepf B, Bennington-Mathias C, Hersperger E, Shearn A. 1996. Molecular, phenotypic, and expression analysis of vein, a gene required for growth of the *Drosophila* wing disc. *Dev. Biol.* 177:475-489.
- Simcox A. 1997. Differential requirement for EGF-like ligands in *Drosophila* wing development. *Mech. Dev.* 62:41-50
- Skolnik EY, Margolis B, Mohammadi M, Lowenstein E, Fischer R, Drepps A, Ullrich A, Schlessinger J. 1991. Cloning of PI3 kinase-associated p85 utilizing a novel method for expression/cloning of target proteins for receptor tyrosine kinases. *Cell* 65:83-90
- Snedeker SM, Brown CF, DiAugustine RP. 1991. Expression and functional properties of transforming growth factor α and epidermal growth factor during mouse mammary gland ductal morphogenesis. *Proc. Natl. Acad. Sci.* 88:276-280.

Soderquist AM and Carpenter G. 1984. Glycosylation of the epidermal growth factor receptor in A-431 cells. The contribution of carbohydrate to receptor function. *J. Biol. Chem.* 259:12586-12594.

Solomon KA, Covington MB, DeCicco CP, Newton RC. 1997. The fate of pro-TNF-alpha following inhibition of metalloprotease-dependent processing to soluble TNF-alpha in human monocytes. *J. Immunol.* 159:4524-4531.

Sorkin A. 1998. Endocytosis and intracellular sorting of receptor tyrosine kinases. *Front. Biosci.* 3:D729-D738.

Spiess M and Lodish HF. 1986. An internal signal sequence: the asialoglycoprotein receptor membrane anchor. *Cell* 44:177-185.

Sporn MB and Todaro GJ. 1980. Autocrine secretion and malignant transformation of cells. *N. Engl. J. Med.* 303:878-880.

Sturtevant MA, Roark M, Bier E. 1993. The Drosophila rhomboid gene mediates the localized formation of wing veins and interacts genetically with components of the EGF-R signaling pathway. *Genes Dev.* 7:961-973.

Sturtevant MA, Roark M, O'Neill JW, Biehs B, Colley N, Bier E. 1996. The Drosophila rhomboid protein is concentrated in patches at the apical cell surface. *Dev. Biol.* 174:298-309.

Tajima S, Lauffer L, Rath VL, Walter P. 1986. The signal recognition particle receptor is a complex that contains two distinct polypeptide chains. *J. Cell. Biol.* 103:1167-1178.

Tapon N and Hall A. 1997. Rho, Rac and Cdc42 GTPases regulate the organization of the actin cytoskeleton. *Curr. Opin. Cell. Biol.* 9:86-92.

Teixido J, Gilmore R, Lee DC, Massague J. 1987. Integral membrane glycoprotein properties of the prohormone pro-transforming growth factor-alpha. *Nature* 326:883-885.

Teixido J and Massague J. 1988. Structural properties of a soluble bioactive precursor for transforming growth factor-alpha. *J. Biol. Chem.* 263:3924-3929.

Teixido J, Wong ST, Lee DC, Massague J. 1990. Generation of transforming growth factor-alpha from the cell surface by an O-glycosylation-independent multistep process. *J. Biol. Chem.* 265:6410-6415.

Therrien M, Wong AM, Rubin GM. 1998. CNK, a RAF-binding multidomain protein required for RAS signaling. *Cell* 95:343-353.

Therrien M, Chang HC, Solomon NM, Karim FD, Wassarman DA, Rubin GM. 1995. KSR, a novel protein kinase required for RAS signal transduction. *Cell* 83:879-888.

Threadgill DW, Dlugosz AA, Hansen LA, Tennenbaum T, Lichti U, Yee D, LaMantia C, Mourton T, Herrup K, Harris RC, et al. 1995. Targeted disruption of mouse EGF receptor: effect of genetic background on mutant phenotype. *Science* 269:230-234.

Tio M, Ma C, Moses K. 1994. Spitz, a Drosophila homolog of transforming growth factor-alpha, is required in the founding photoreceptor cells of the compound eye facets. *Mech. Dev.* 48:13-23.

Todaro GJ, Fryling C, De Larco JE. 1980. Transforming growth factors produced by certain human tumor cells: polypeptides that interact with epidermal growth factor receptors. *Proc. Natl. Acad. Sci.* 77:5258-5262.

Toker A. 1998. Signaling through protein kinase C. *Frontiers Biosci.* 3:D1134-D1147.

Tzahar E, Waterman H, Chen X, Levkowitz G, Karunakaran D, Lavi S, Ratzkin B and Yarden Y. 1996. A hierarchical network of interreceptor interactions determines signal transduction by Neu differentiation factor/Neuregulin and epidermal growth factor. *Mol. Cell. Biol.* 16:5276-5287.

Tzivion G, Luo Z, Avruch J. 1998. A dimeric 14-3-3 protein is an essential cofactor for Raf kinase activity. *Nature* 394:88-92.

Ullrich A, Coussens L, Hayflick JS, Dull TJ, Gray A, Tam AW, Lee J, Yarden Y, Libermann TA, Schlessinger J *et al.* 1984. Human epidermal growth factor receptor cDNA sequence and aberrant expression of the amplified gene in A431 epidermoid carcinoma cells. *Nature* 309:418-425.

van der Geer P, Hunter T, Lindberg RA. 1994. Receptor protein-tyrosine kinases and their signal transduction pathways. *Annu. Rev. Cell. Biol.* 10:251-337.

Vojtek AB, Hollenberg SM, Cooper JA. 1993. Mammalian Ras interacts directly with the serine/threonine kinase Raf. *Cell* 74:205-214.

Wadsworth SC, Vincent WS 3d, Bilodeau-Wentworth D. 1985. A Drosophila genomic sequence with homology to human epidermal growth factor receptor. *Nature* 314:178-180.

Wagner AC and Williams JA. 1994. Low molecular weight GTP-binding proteins: molecular switches regulating diverse cellular functions. *Am. J. Physiol.* 266:G1-14.

Walker C, Everitt J, Ferriola PC, Stewart W, Mangum J, Bermudez E. 1995. Autocrine growth stimulation by transforming growth factor alpha in asbestos-transformed rat mesothelial cells. *Cancer Res.* 55:530-536.

- Wappner P, Gabay L, Shilo BZ. 1997. Interactions between the EGF receptor and DPP pathways establish distinct cell fates in the tracheal placodes. *Development* 124:4707-4716.
- Warne PH, Viciano PR, Downward J. 1993. Direct interaction of Ras and the amino-terminal region of Raf-1 in vitro. *Nature* 364:352-355.
- Wasserman JD and Freeman M. 1998. An autoregulatory cascade of EGF receptor signaling patterns the Drosophila egg. *Cell* 95:355-364.
- Wennstrom S, Hawkins P, Cooke F, Hara K, Yonezawa K, Kasuga M, Jackson T, Claesson-Welsh L, Stephens L. 1994. Activation of phosphoinositide 3-kinase is required for PDGF-stimulated membrane ruffling. *Curr. Biol.* 4:385-393.
- Werb Z and Yan Y. 1998. A cellular striptease act. *Science* 282:1279-1280.
- Whiteley B and Glaser L. 1986. Epidermal growth factor (EGF) promotes phosphorylation at threonine-654 of the EGF receptor: possible role of protein kinase C in homologous regulation of the EGF receptor. *J. Cell. Biol.* 103:1355-1362.
- Widmann C, Gibson S, Jarpe MB, Johnson GL. 1999. Mitogen-activated protein kinase: conservation of a three-kinase module from yeast to human. *Physiol. Rev.* 79:143-180.
- Wilcox JN and Derynck R. 1988a. Developmental expression of transforming growth factors alpha and beta in mouse fetus. *Mol. Cell. Biol.* 8:3415-3422.
- Wilcox JN and Derynck R. 1988b. Localization of cells synthesizing transforming growth factor-alpha mRNA in the mouse brain. *J. Neurosci.* 8:1901-1904.
- Wiley HS, Woolf MF, Opresko LK, Burke PM, Will B, Morgan JR, Lauffenburger DA. 1998. Removal of the membrane-anchoring domain of epidermal growth factor leads to intracrine signaling and disruption of mammary epithelial cell organization. *J. Cell. Biol.* 43:1317-1328.
- Williams GR, Franklyn JA. 1994. Physiology of the steroid-thyroid hormone nuclear receptor superfamily. *Baillieres Clinical Endocrinology and Metabolism* 8:241-266.
- Wong ST, Winchell LF, McCune BK, Earp HS, Teixido J, Massague J, Herman B, Lee DC. 1989. The TGF-alpha precursor expressed on the cell surface binds to the EGF receptor on adjacent cells, leading to signal transduction. *Cell* 56:495-506.
- Yamamoto KR. 1985. Steroid receptor regulated transcription of specific genes and gene networks. *Annu. Rev. Genet.* 19:209-252.

Yarden Y and Schlessinger J. 1987. Self-phosphorylation of epidermal growth factor receptor: evidence for a model of intermolecular allosteric activation. *Biochemistry* 26:1434-1442.

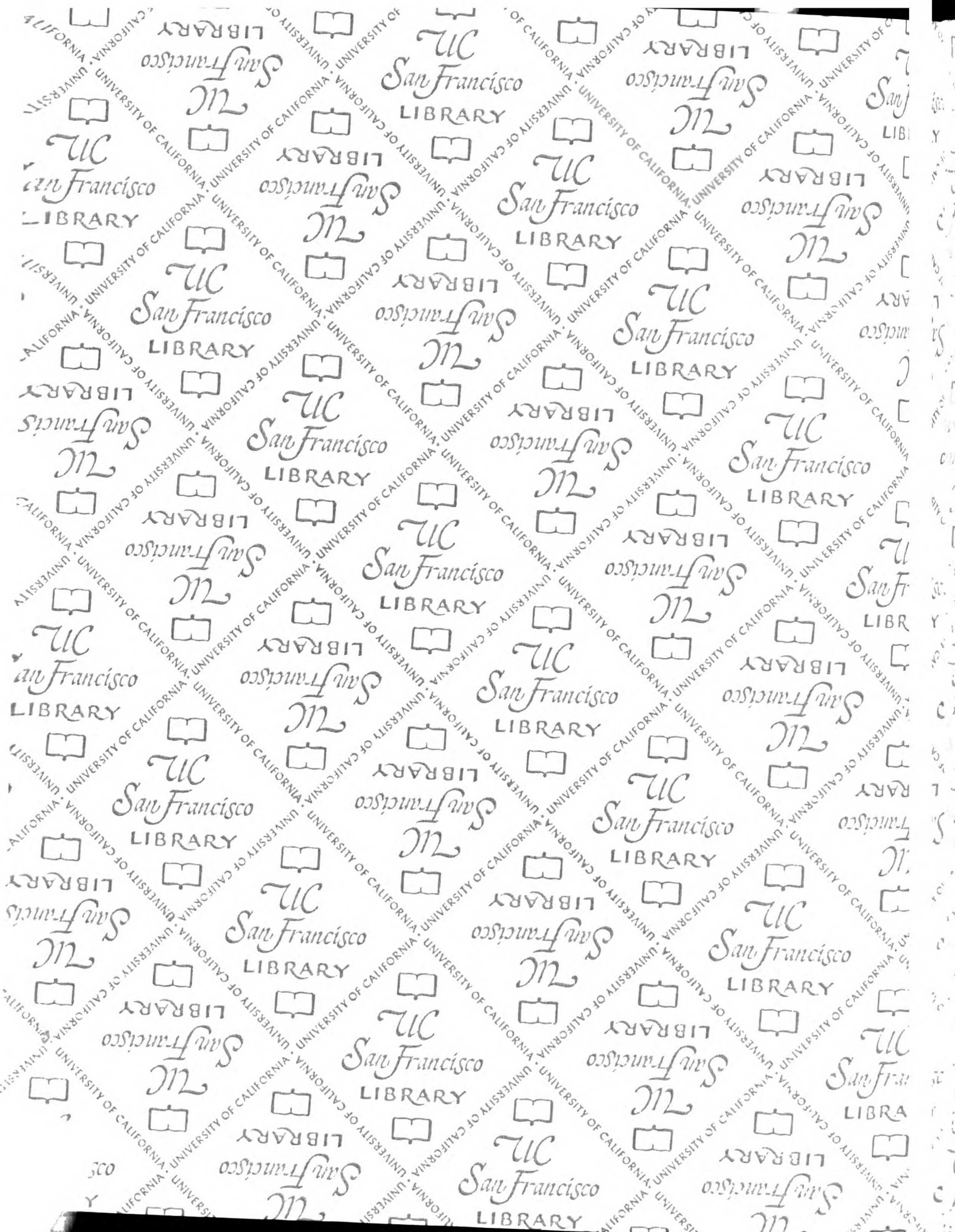
Yarden Y and Ullrich A. 1988. Growth factor receptor tyrosine kinases. *Annu. Rev. Biochem.* 57:443-478.

Zak NB, Wides RJ, Schejter ED, Raz E, Shilo BZ. 1990. Localization of the DER/flb protein in embryos: implications on the faint little ball lethal phenotype. *Development* 109:865-874.

Zhang XF, Settleman J, Kyriakis JM, Takeuchi-Suzuki E, Elledge SJ, Marshall MS, Bruder JT, Rapp UR, Avruch J. 1993. Normal and oncogenic p21ras proteins bind to the amino-terminal regulatory domain of c-Raf-1. *Nature* 364:308-313.

Zheng CF and Guan KL. 1993a. Cloning and characterization of two distinct human extracellular signal-regulated kinase activator kinases, MEK1 and MEK2. *J. Biol. Chem.* 268:11435-11439.

Zheng CF and Guan KL. 1993b. Properties of MEKs, the kinases that phosphorylate and activate the extracellular signal-regulated kinases. *J. Biol. Chem.* 268:23933-23939.



For reference

Not to be taken
from the room.



